Transport and Dispersion of Labeled Bed Material North Loup River, Nebraska

GEOLOGICAL SURVEY PROFESSIONAL PAPER 433-C

Prepared in cooperation with the U.S. Atomic Energy Commission

Transport and Dispersion of Labeled Bed Material North Loup River, Nebraska

By W. W. SAYRE *and* D. W. HUBBELL

TRANSPORT OF RADIONUCLIDES BY STREAMS

GEOLOGICAL SURVEY PROFESSIONAL PAPER 433-C

Prepared in cooperation with the U.S. Atomic Energy Commission

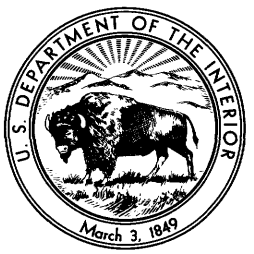

UNITED STATES GOVERNMENT PRINTING OFFICE, WASHINGTON : 1965

UNITED STATES DEPARTMENT OF THE INTERIOR

STEWART L. UDALL, *Secretary*

GEOLOGICAL SURVEY

Thomas B. Nolan, *Director*

For sale by the Superintendent of Documents, U.S. Government Printing Office
Washington, D.C. 20402 - Price 45 cents (paper cover)

CONTENTS

ILLUSTRATIONS

TABLES

SYMBOLS

Symbol	Definition	Dimensions	Units
a	Vertical distance from surface of sand to center of the detector crystal ($a=1$ in. for a 2×2-in. crystal).	L	in.
A	Area under concentration-distribution curve.	F/L^2	g per sq ft
A'	An event.	----------	----------
B	Width of streambed.	L	ft
B'	An event.	----------	----------
$C/\sqrt{g}$	Resistance coefficient—ratio of Chezy coefficient to square root of acceleration of gravity.	----------	----------
C_1, C_2	Constants.	----------	cpm per μc
d	Average depth beneath the surface of the bed through which tracer particles are distributed; also the average depth of the zone in which particle movement occurs.	L	ft
d_i	Mean distance between the bed surface and the corresponding line of length l_i (see fig. 41).	L	ft
E	An event—the movement of a tracer particle.	----------	----------
$f(\ )$	Probability-density function	L^{-1} or T^{-1}	----------
$f(r)$	Counting rate per μc from a point source located in submerged sand a distance r from the center of the detector crystal.	----------	cpm per μc
$F(\ )$	Distribution function (cumulative probability-distribution function).	----------	----------
h	Horizontal distance between point source and centerline of detector.	L	in.
i	Number of occurrences of the event E (or number of steps or waiting periods that are associated with E).	----------	----------
i_b	Fraction, by weight, of bed material particles within the approximate size range of the tracer particles.	----------	----------
$I_0(\ ), I_1(\ ), I_2(\ )$	Modified Bessel functions of the first kind of orders 0, 1, and 2.	----------	----------
k_1	Proportionality constant in concentration-distribution and related functions; may also be interpreted as the mean number of steps per unit of longitudinal distance.	L^{-1}	ft^{-1}
k_2	Proportionality constant in concentration-distribution and related functions; may also be interpreted as the mean number of waiting periods per unit of time.	T^{-1}	hr^{-1}
l_i	Length of a section (see fig. 41) defined by the lowest line that can be drawn in such a way that it is parallel to the mean bed surface and is tangent to the bottom of a trough at its upstream end.	L	ft
L	Total length of reach.	L	ft
m	Specific activity in the bed material.	----------	μc per cu in.
M	Amount of radioactivity.	----------	mc
n	Particular number of occurrences of the event E (or number of steps or waiting periods that are associated with E).	----------	----------
N	Mean number of tracer particles in a given volume of bed material.	----------	----------
$p(\ )$	Probability mass function.	----------	----------
$P[\ ]$	Probability.	----------	----------
Q_s	Bed-material discharge.	F/T	tons per day
r	Radial distance from center of detector crystal to a point source of radioactivity.	L	in.
r_0	Radial distance from the center of the detector crystal within which a radioactive source is uniformly distributed.	L	in.
R_a	Adjusted counting rate.	----------	cpm
R_b	Background counting rate.	----------	cpm
R_o	Observed counting rate.	----------	cpm
(R_o-R_b)	Minimum net counting rate over background that is required during an experiment for statistical significance.	----------	cpm
R_{r_o}	Counting rate of a particular detection system due to a source that is uniformly distributed throughout a volume of submerged sand within the radius r_0.	----------	cpm
R_∞	Counting rate due to a source uniformly distributed throughout an infinite volume.	----------	cpm

Symbol	Definition	Dimensions	Units
s	Length, in the direction of flow, of a source of contaminated particles.	L	----------
S	Sensitivity of radiation-detection system.	----------	cpm per mc per cu ft
$S(\xi)$	Function that describes the variation in strength with respect to distance from the origin of a longitudinally distributed source released instantaneously at $t=0$.	F/L	----------
$S(\tau)$	Function that describes the variation in strength with respect to time of a source discharging continuously at the origin.	F/T	----------
$S(\xi, \tau)$	Function that describes the variation in strength with respect to both distance from the origin and time of a continuously discharging longitudinally distributed source.	F/LT	----------
t	Time.	T	min, hr, or days
t_1	Length of time during which a continuous source discharges.	T	----------
T	Half-life of radionuclide.	T	days
v	Vertical distance between point source and surface of sand.	L	in.
V	Volume.	L^3	cu ft or cu in.
W	Weight of tracer particles released from source.	F	g
x	Distance downstream from source.	L	ft
x'	Dummy variable of integration.	L	----------
x_m	Distance that mode of concentration-distribution curve is downstream from source.	L	ft
$\bar{x}$	Distance that mean of concentration-distribution curve is downstream from source.	L	ft
$\bar{x}_n$	Mean distance over which a particle would be transported during n repeated occurrences of E.	L	----------
α_1, α_2	Constants.	L^{-1}	in.$^{-1}$
γ_s	Bulk specific weight of bed material.	F/L^3	lbs per cu ft
ξ	Distance from the origin ($x=0$) to a point in a longitudinally distributed source.	L	ft
σ_x^2	Variance of concentration-distribution curve.	L^2	sq ft
τ	Time after $t=0$ during which a continuous source is discharging.	T	----------
ϕ	Observed concentration of tracer particles in the bed material.	F/L^3	g per cu ft
ϕ_{max}	Observed peak concentration of tracer particles in the bed material.	F/L^3	g per cu ft
$\phi(x, t)$	Theoretical concentration of tracer particles in the bed material.	F/L^3	----------
$\psi(t, x)$	Theoretical discharge of tracer particles through a unit cross section.	F/T	----------

TRANSPORT AND DISPERSION OF LABELED BED MATERIAL NORTH LOUP RIVER, NEBRASKA

By W. W. Sayre and D. W. Hubbell

ABSTRACT

One significant facet of the disposal of radioactive wastes in alluvial streams pertains to the influence that natural sediments have on the transport and dispersion of radioactive wastes. The sorption of radioactive wastes by clay, silt, and sand (particularly clay-coated sand) is a common phenomenon; hence, the transport and dispersion of waste can be affected to a significant extent by the transport and dispersion of the individual sediment particles.

To study the transport and dispersion of bed-material particles (sand), an experiment was conducted in the North Loup River near Purdum, Nebr. In the experiment, sand labeled with radioactive iridium 192 was released from a line source on the bed of the river. After release, the movement of the tracer particles downstream was observed by monitoring the streambed with a sled-mounted scintillation detector. In addition, the vertical distribution of the tracer particles in the bed was observed by monitoring core samples of the bed material. The amount of activity and the number of tracer particles used in the experiment were determined from detailed calibrations in which field conditions were simulated. The tracer particles varied within a fairly narrow range about a median fall diameter of 0.305 mm. The size of the tracer particles was selected so that they would be slightly coarser than the dominant size range of the bed material. Longitudinal traverses with the radiation-detection equipment at approximately daily intervals and extending over a 13-day period defined the dispersion of tracer particles along the channel. The traverses also indicated that some of the tracer particles were buried as a concentrated deposit for about 7 days. Presumably, these tracer particles were deposited in an unusually deep dune trough and were not reexposed until a similarly deep trough passed by. The temporary burial of the tracer particles demonstrates that deposits of contaminated particles in an alluvial stream can remain undisturbed for relatively long periods of time and then suddenly be released.

A concentration-distribution function, which is based on probability theory, was derived to characterize the dispersion process. The parameters of the function are related to the dispersion time and distance. Significant characteristics of the function are that the variance and the mean of the distribution are proportional to time and that for large times the maximum concentration varies inversely with the square root of time. Comparable observed and theoretical distributions agreed well except near the origin and at the downstream tail. The explanation for the differences is based on certain discrepancies between physical features of the experiment and the corresponding assumptions on which the theoretical distribution function is based. The major discrepancy is that the theory applies only to a group of tracer particles having identical transport characteristics, whereas the tracer particles did not all have the same characteristics.

In addition to defining the dispersion of particles, the observed distribution curves provided information for computing the bed-material discharge. The computation of discharge was made with a continuity-type equation, which states simply that the discharge is the product of the mean velocity of the particles and the cross-sectional area through which they move. Although a direct comparison of the computed discharge and a measured discharge could not be made, the computed discharge compared favorably with the discharge computed by the modified Einstein procedure.

Although the concentration-distribution function was derived for the initial conditions of a vertical-plane source, it can be extended to more complex conditions by performing appropriate mathematical operations. In addition, the function can be applied to real situations if the constants in the concentration-distribution function and the depth of the zone of particle movement in the bed are known. When the bed configuration consists of dunes or ripples, the depth of the zone of particle movement can be estimated from longitudinal profiles of the bed surface. However, until the relations between hydraulic and sediment parameters and the constants in the theoretical distribution function are defined, the constants can be evaluated only by experiment.

INTRODUCTION AND ACKNOWLEDGMENTS

The potential benefits of nuclear industries to mankind depend on the extent to which safe, reliable, and economically feasible means are found to dispose of radioactive wastes. Radioactive wastes present a unique disposal problem because, unlike most other industrial wastes, they cannot be rendered biologically harmless by any of the conventional treatment techniques. One current disposal practice is to release wastes into the environment. The U.S. Geological Survey, in cooperation with the Division of Reactor Development of the Atomic Energy Commission, is engaged in investigations related to the management of radioactive

wastes that are released into natural streams. One of these investigations deals with aspects of the influence of fluvial sediment in the disposal process. The study reported herein is one facet of that investigation.

At the present time (1962), about 95 percent of the low-level, short-lived liquid waste that is released into the environment is disposed of in waterways such as streams, lakes, and reservoirs (Nace, 1959). If a waterway is used for the disposal of radioactive wastes, the possibility exists for the activity to exceed safe levels in and along the waterway. The concentration of activity in a waterway at any time and place depends on a variety of factors which often operate in conjunction with one another. For instance, radionuclides initially dispersed by turbulent diffusion to concentrations far below the maximum permissible concentration may be taken up and concentrated to many thousand times the ambient water concentration (Robeck and others, 1954) by aquatic biota or fluvial sediment. Unfortunately the various factors and processes that tend to concentrate and disperse activity are neither understood well nor easily evaluated. Additional complications are introduced by the exchange of radionuclides between the various transporting media. The exchange processes are usually complex and depend on chemical and physical factors related to the radioactive waste effluent, the transporting media, and the flow.

One of the major transporting media in natural waterways is sediment (Sayre and others, 1963). Abundant evidence indicates that the uptake of radioactive waste products by sediment is a common phenomenon. Fine sediment (clay and silt) tends to have a much higher sorption capacity per unit weight than does sand; however, Kennedy (1963) has shown that some stream sands, particularly those containing clay-impregnated rock fragments, may have relatively high sorption capacities. According to Kennedy, most of the sorption capacity of suspended sediment is due to the clay fraction, but most of the sorption capacity of the bed material may be due to sand and silt, because those components constitute a very high percentage of the bed material.

Because of the potential for high amounts of exchange, the distribution of activity in the waterway may be governed to a significant extent by the rates at which the individual contaminated sediment particles are transported and dispersed. If flow conditions induce high concentrations of contaminated sediment, the level of activity within the body of the flow could exceed a safe level. If flow conditions induce low transport rates or deposition of contaminated sediment, activity could build up in and along the channel to an unsafe level. Deposits might consist of sand particles, flocculated fine materials, organic sediments, or unflocculated fine materials that have penetrated into the bed. Hazardous conditions can also arise as a result of exposure of contaminated sediment through flooding and fluctuating water levels.

To evaluate the various potential sediment-induced hazards in waterways, the characteristics of the sediment and the rates of transport and dispersion of the different fractions of the sediment load must be considered. Ordinarily, the total sediment load is divided according to the size and source of the sediment into the bed-material load and the fine-material load. The bed-material load is that part of the total sediment load derived from the bed material; consequently, it is composed of particles whose sizes are similar to those of bed-material particles. The bed-material load also includes some suspended sediment in addition to all the bedload. The fine-material load is that part of the total sediment load composed of particles whose sizes are finer than those of particles present in the bed material. Generally, particles of the fine material are in suspension almost continuously and are transported at almost the same velocities as the fluid particles; however, the average velocities of bed-material particles, because of a process of alternate movement and temporary storage in the bed, are much lower than those of fluid particles. Because the transport mechanisms associated with the two kinds of sediment loads are different, the ways in which they are dispersed are also different.

This report describes a field experiment, conducted in the North Loup River near Purdum, Nebr., in which the dispersion and transport of bed-material particles were studied by means of radioactive-tracer techniques. In the experiment, sand particles that were labeled with a radioactive nuclide were released on the riverbed. As the tracer particles moved and dispersed downstream with the natural bed-material load, their distribution along the channel was determined with radiation-detection equipment. Because the application of radioactive-tracer techniques in sediment studies is relatively new, part of the report is devoted to the design, techniques, and equipment that were used in the experiment. The discussion of the experiment is followed by derivation of a theoretical concentration-distribution function based on probability theory and of a bed-material transport formula. The experimental results are compared with predictions based on the derived functions, and the applicability of the combined results to practical situations is discussed.

Permission to conduct the experiment, which involved the release of radioactive materials into the North Loup River, was given by Dr. E. A. Rogers, Director of Health, State of Nebraska, and by the Licensing and Regulation Branch of the Atomic Energy Commission.

Prior to the field investigations, meetings were held in Lincoln, Nebr., on September 14, 1960, and in Thedford, Nebr., on September 20, 1960, to inform representatives of various State and local agencies of the nature of the experiment. In all, representatives from the Nebraska State Health Department, the Nebraska Water Resources Department, the Conservation and Survey Division of the University of Nebraska, the Water Resources Division of the U.S. Geological Survey, and a board of local ranchers were present at the meetings. D. M. Culbertson, district engineer of the U.S. Geological Survey, assisted with the arrangements for the meeting in Lincoln, Nebr., and furnished valuable information on the characteristics of the North Loup River. Dale Langford, County Extension Agent, arranged for the local-level meeting in Thedford, Nebr. Kyle Cox, a local rancher, not only allowed work to be carried out on his property adjacent to the test reach but also furnished information on the history of the reach and on the condition of the stream. Aspects of the experimental program relating to radiation safety were carried out in accordance with the advice of Dr. W. D. Carlson, Radiation Safety Officer, Colorado State University. W. L. Haushild of the U.S. Geological Survey assisted materially with many aspects of the field operations and participated in the data collection, as did A. A. El Darwish, Colorado State University graduate student. F. C. Ames and C. L. Scott of the Geological Survey also assisted in the field during the first few days of data collection. Dr. D. L. Bentley, Assistant Professor of Mathematics, and E. J. Plate, Assistant Civil Engineer at Colorado State University, contributed several fundamental ideas that aided substantially in the development of the final form of the concentration-distribution function. Robert McDowell, Colorado State University graduate student, assisted with the analysis of data and the preparation of this report.

THE EXPERIMENT

The radioactive-tracer technique was selected as the most feasible method for studying the transport and dispersion of sediment particles along the channel because, with suitable instrumentation, the distribution of the particles at any time could be measured in place. With the radioactive-tracer technique, the accuracy of the measurements increases as the level of radioactivity increases. However, as the level of radioactivity increases, so does the possibility for harmful contamination to the stream environment. Hence, the experiment had to be designed to maintain satisfactory accuracy in the measurements and at the same time to limit the radioactivity to a safe level. To achieve a satisfactory balance, careful consideration had to be given to the nature and location of the test reach, the labeling and detecting of the tracer particles, and the operational procedures. These general topics are discussed in the following sections.

THE TEST REACH

The study was conducted on the North Loup River near Purdum, Blaine County, Nebr. (see fig. 1), in a

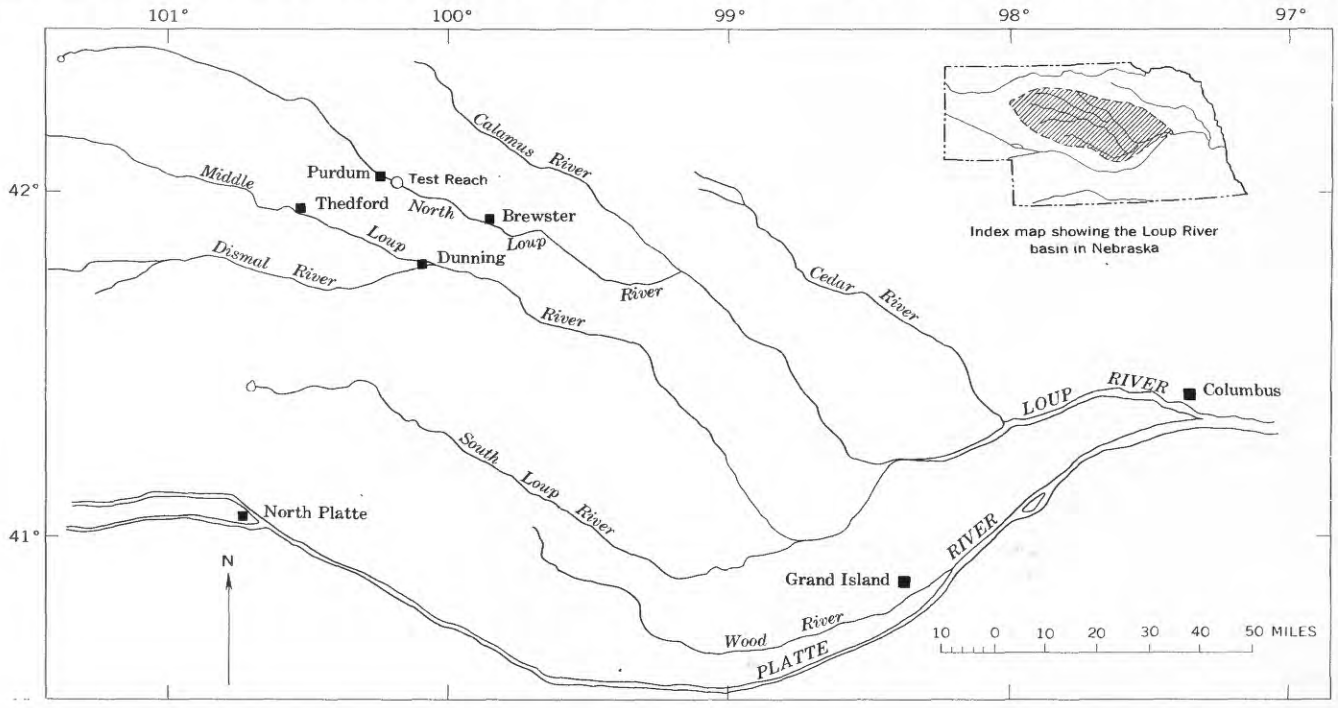

FIGURE 1.—Location of the Loup River basin.

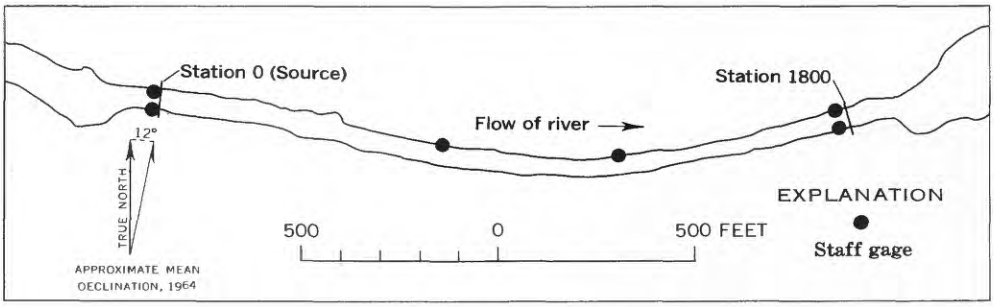

FIGURE 2.—Sketch of the test reach.

reach (see fig. 2) in sec. 10, T. 24 N., R. 25 W. The site was selected because it was particularly suitable for the experiment from both a hydraulic and a radiological-health standpoint. Specifically, the North Loup River maintains a relatively constant water discharge for weeks at a time; ground-water flow adjacent to the river is toward rather than away from the stream; the bed form is normally one of large dunes; the bed material is sand having a median diameter of about 0.29 mm; the test reach is fairly straight and has stable banks; the channel width is narrow, and the depth is such that a small boat carrying radiation-detection equipment can be navigated; the reach is isolated from any community; and very few people live near the river.

The North Loup River flows southeastward across the sandhills region of north-central Nebraska. The topography of the region is formed by northwest-trending sand dunes that are stabilized by grass cover. The dune sand extends to a depth of 100 feet in some places and is underlain by the Ogallala Formation of Tertiary age. The valley floor along the North Loup River is composed mostly of alluvial sand. Meanders are not well developed, although bank erosion is prevalent and is the source of most of the sediment load. The flow is mainly derived from ground-water accretion along the entire channel and is about 250 cfs (cubic feet per second) at the test reach.

The test reach (figs. 3, 4), a manmade cutoff constructed about 1950, is bordered on the north side by a hay meadow and on the south side by a swamp having heavy brush growth. The alinement of the channel is straight except for two minor bends that are approximately 700 and 1,300 feet downstream from the beginning of the reach. The reach varies in width from about 40 to 55 feet and is approximately 1,800 feet long.

THE RADIOACTIVE LABEL AND THE DETECTION SYSTEM

Although no other investigations have been made in which the radioactive-tracer technique has been applied specifically to the study of the dispersion of contaminated bed-material particles in alluvial channels, the technique has been applied successfully in other kinds of sediment and hydraulic studies. Lean and Crickmore (1960) studied sand transport in a laboratory flume, using experimental techniques which were very similar to those described in this report; however, their research was directed primarily toward developing a method for measuring the bed-material discharge. Other, less closely related studies have been reviewed by Krone (1957) and by Hours and Jaffry (1959).

In nearly all the sediment studies, the radionuclide either has been incorporated into glass particles that simulated the sediment or has been plated, by an adsorption process, on the surface of natural sediment.

FIGURE 3.—Downstream view of the test reach. Station 0 is indicated by the dashed line.

FIGURE 4.—Upstream view of test reach from about station 1000.

Lean and Crickmore (1960), however, used natural sand that had been irradiated in a nuclear reactor. A characteristic of the glass-particle and irradiation methods is that the radioactivity is proportional to the weight of the particles rather than to their surface area. This characteristic, however, is not significant if the tracer particles are uniform in size. In this experiment, Ottawa sand plated with a radionuclide was used because such particles of the proper size could be purchased.

In many of the sediment investigations, the radiation-detection equipment has been adapted for underwater detection. However, in some studies, samples of sediment have been collected and subsequently analyzed for radioactivity. The use of underwater-detection apparatus virtually dictates that the tracer particles be labeled with a gamma-emitting radionuclide, because the penetration range of alpha and beta radiation in water is limited to about 1 cm or less. In this experiment, both the underwater and sample-collection detection methods were used, and, therefore, a gamma-emitting radionuclide was most suitable. Iridium 192 was selected because (1) the gamma rays it emits have energies from 0.14 to 0.90 mev (million electron volts) and are readily detectable under water; (2) it has a half-life of 74 days and, hence, would decay slowly enough to be readily detectable during the entire experiment but rapidly enough to preclude long-term contamination of the stream; and (3) sand particles already plated with iridium 192 by a high-temperature oxidizing process were available for purchase.

Both scintillation detectors and Geiger-Mueller (G-M) tubes are used for detecting radiation. G-M tubes generally are relatively rugged and inexpensive; however, scintillation detectors are more sensitive to gamma radiation and are usable over a much wider range of counting rates. In addition, scintillation detectors, when used in conjunction with a pulse-height analyzer, enable differentiation of the emission energies of gamma rays thus permitting the identification of different radionuclides. Because of its versatility and inherently high sensitivity, a scintillation-detection system was selected for this experiment. In addition to the scintillation detector, the system included a pulse-height analyzer, count-rate meter, a strip-chart recorder, and, for some operations, a scaler.

AMOUNT OF RADIOACTIVITY

The amount of radioactivity required for the experiment depended on (1) the level of the background radiation, (2) the volume of sand throughout which the tracer particles would be dispersed, (3) the decay rate of the radionuclide, (4) the radiation-absorption characteristics of the media between the detector and the tracer particles, (5) the efficiency of the radiation-detection system, and (6) the geometrical orientation of the detector to the tracer particles. Items 4–6 were evaluated together by determining an overall sensitivity from calibration measurements with the equipment under conditions that simulated the experimental environment. A method for determining overall sensitivity with license-exempt quantities of the tracer radionuclide is presented on p. C44.

If the sensitivity is determined, the amount of radioactivity, M (in millicuries), required for the experiment can be computed from

$$M=\frac{(R_o-R_b)Ve^{0.693\frac{t}{T}}}{S}$$

where

R_o-R_b = the minimum net counting rate over background, in counts per minute, that is required during the experiment for statistical significance

V = the estimated volume, in cubic feet, through which the tracer particles will be dispersed at the end of the experiment. If this volume is estimated to be the product of the length and width of the test reach and the depth to which the particles will penetrate into the bed material, the tracer particles can disperse within the reach to the maximum possible extent and counting rates will still be statistically significant

S = the overall sensitivity, in counts per minute divided by millicuries per cubic foot, for the conditions simulating the experimental environment (see p. C47 for S values)

$e^{0.693\frac{t}{T}}$ = a correction factor for radioactive decay

t = the duration of the experiment, in days

T = the half-life of the radionuclide, in days.

In the design of this experiment, a minimum net counting rate equal to one-half the background rate was considered acceptable for the condition of a uniform distribution of tracer particles throughout the test reach. The volume through which the tracer particles would be dispersed was estimated to be $1{,}800\times50\times1.5=135{,}000$ cubic feet. Furthermore, it was estimated that the experiment would last for 1 month. By using the sensitivity determined with cesium 137 (S had not been determined for iridium 192 prior to the design of the experiment), the 74-day half-life of iridium 192, and a background counting rate of 200 cpm (counts per minute), the required amount of activity was computed to be 39.4 mc (millicuries). This amount was rounded off to 40 mc, which was the amount used in the experiment.

After the sensitivity with iridium 192 had been determined, calculations showed that with comparable assumptions, only 30.6 mc would have been required.

NUMBER OF TRACER PARTICLES

In the determination of the required amount of radioactivity, a uniformly distributed source was assumed. Actually, each particle is a separate source, and the counting rate recorded by the detection system depends not only on the amount of radioactivity within detection range of the scintillation crystal but also on the distribution of the tracer particles.

If the distribution of tracer particles throughout the bed is random, as the concentration of tracer particles increases, the relative distribution of the tracer particles tends to become more even and random variations in the number of tracer particles per unit volume of bed material tend to have less effect on the counting rate. In statistical terms, the random variations in the number of particles in a given volume can be characterized by the coefficient of variation, or relative standard deviation. Because the variation in the number of tracer particles in a given volume follows the Poisson distribution, the coefficient reduces to $100/\sqrt{N}$, where N is the mean number of tracer particles in the given volume of bed material.

The number of tracer particles required for a particular experiment can be determined by setting limits on the coefficient of variation and by precisely defining the given volume. Intuitively, the volume can be defined by the practical range of the detector, and N can be defined as the required number of tracer particles within the volume at the end of the experiment when the tracer particles are distributed over the entire test reach. Inasmuch as the maximum range of the detector approaches infinity asymptotically and therefore is not defined, the practical range of the detector can be considered as the radial distance from the center of the detector crystal to the loci of points in the bed within which 50 percent of the counts originate when the sand bed contains a uniformly distributed source of infinite extent. The practical range of the detection system used in this experiment, as determined from figure 46, is 4.4 inches for iridium 192, 4.8 inches for gold 198, and 6.8 inches for cesium 137.

Because the counting rate varies with the source-to-detector distance and because the spatial distribution of the tracer particles is not always precisely the same, the coefficient of variation, when defined in terms of the number of tracer particles within the practical range of the detector, provides only an index to the expected variation in counting rate attributable to random variations in the number of tracer particles. However, if a relatively long ratemeter time constant is used and the detector is moved along the bed, the fluctuations in the counting rate due to local variations in the distribution of tracer particles are damped appreciably. As a result, the required number of tracer particles near the detector need not be determined precisely, and the measure provided by the coefficient of variation is adequate for the purpose of experimental design.

Because the practical range of the detector for iridium 192 had not been determined at the time the experiment was designed, the method described in the preceding paragraphs was not used, and the required number of tracer particles was estimated on the basis of information reported by Krone. According to Krone (1957), a distribution of three tracer particles per square centimeter on the surface of the bed would provide an adequate number of tracer particles near the detector. The number of particles required for this experiment was calculated on the assumption that the tracer particles would be evenly distributed over the entire test reach at the end of the experiment and that one-half of the particles would be either lost or buried beyond the range of the detector. The calculation showed that about 5.0×10^8 particles were needed.

A post-experimental analysis showed that if the number of particles that were actually used in the experiment (approximately 4.6×10^8) were uniformly distributed throughout the test reach to a depth of 1.5 feet, the particle population density would be 1.98 particles per cubic inch. Because the volume within the practical range of the detector (4.4 in. for iridium 192) is 116 cubic inches, about 230 particles would be within the practical range. Thus, the coefficient of variation would be ±6.6 percent.

SIZE OF TRACER PARTICLES

Another critical consideration in the design of the experiment was the optimum size range of tracer particles to use for simulating the transport and dispersion of the bed-material particles. To insure that the tracer particles would not be in suspension any significant part of the time but that the most dominant particle-size fraction would be represented, a narrow particle-size range slightly coarser than the dominant size range of the bed material was selected. Figure 5 shows the size distribution of the tracer particles along with those of the bed material and the measured suspended sediment.

The median size of the tracer particles (0.305 mm) and the assumption that the tracer particles were spherical and had a specific gravity of 2.65 were used to calculate the weight of the required number of tracer particles (43.5 lb). For the experiment, the quantity of particles was rounded off to 40 pounds.

EXPERIMENTAL EQUIPMENT

The field investigation consisted of four principal operations: placing the tracer particles on the stream-

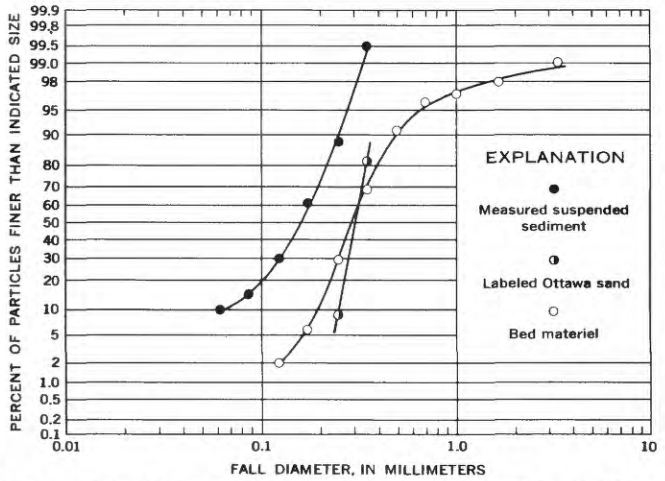

FIGURE 5.—Size distributions of measured suspended sediment, labeled Ottawa sand, and bed material.

FIGURE 6.—The dosing apparatus. Note the tongs used for handling the cans of labeled sand and the adjustable mount with parallelogram linkage, which permits the funnel tube to be raised and lowered vertically.

bed (dosing), tracing the particles, sampling the bed material, and collecting hydraulic and sediment data. Each of these operations, except the last, required special equipment that could be transported in and operated from a small boat.

Placement of the labeled sand on the streambed was accomplished by means of the apparatus shown in figure 6. This apparatus, which consists chiefly of an electric can opener and a movable funnel tube, was connected to the stern of the boat. In the dosing operation, the funnel tube was lowered until the bell at the bottom rested on the streambed, the storage cans containing the tracer particles were introduced into the can opener by means of tongs and opened, and the particles were poured down the funnel and deposited on the streambed (see fig. 7). During the dosing, the boat was attached to a cable that extended accross the width of the stream.

Tracing of the labeled particles was accomplished wih a scintillation-detection system that consisted of a scintillation detector, a pulse-height analyzer, and a count-rate meter with an output to a strip-chart recorder. The scintillation detector was housed in a watertight aluminum casing and mounted to a sled that was dragged along the streambed (see fig. 8). To assure that the detector remained in continuous contact with the streambed, it was mounted to the sled by a four-bar parallelogram linkage and supported

FIGURE 7.—The dosing operation.

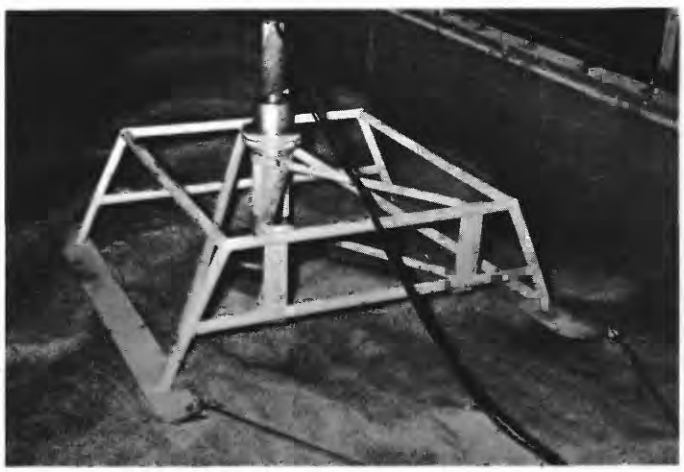

FIGURE 8.—Sled and scintillation detector. Note the parallelogram linkage, which allows the detector to move independently from the sled, and the wooden dish-shaped piece that supports the detector on the bed.

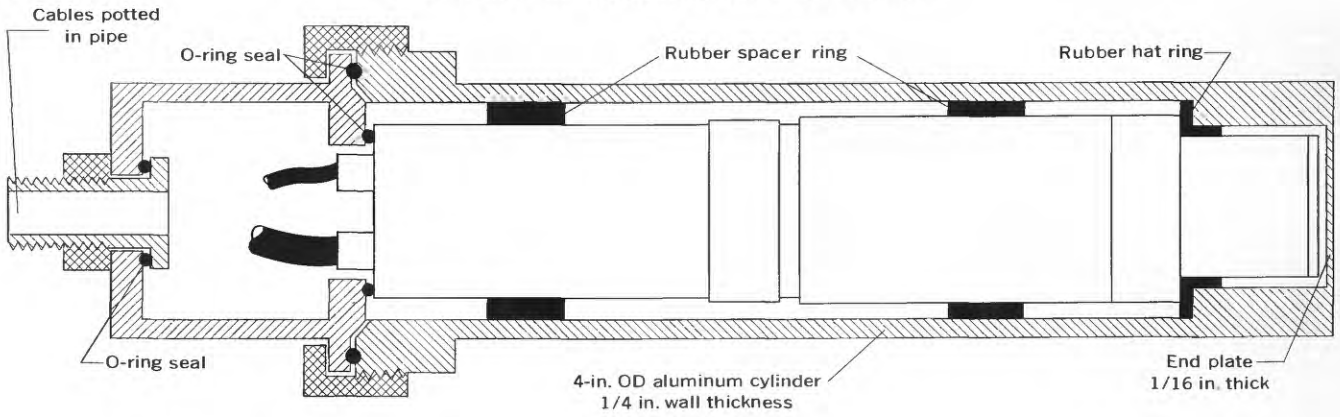

FIGURE 9.—Watertight casing for scintillation detector. Scale 1 inch=3 inches.

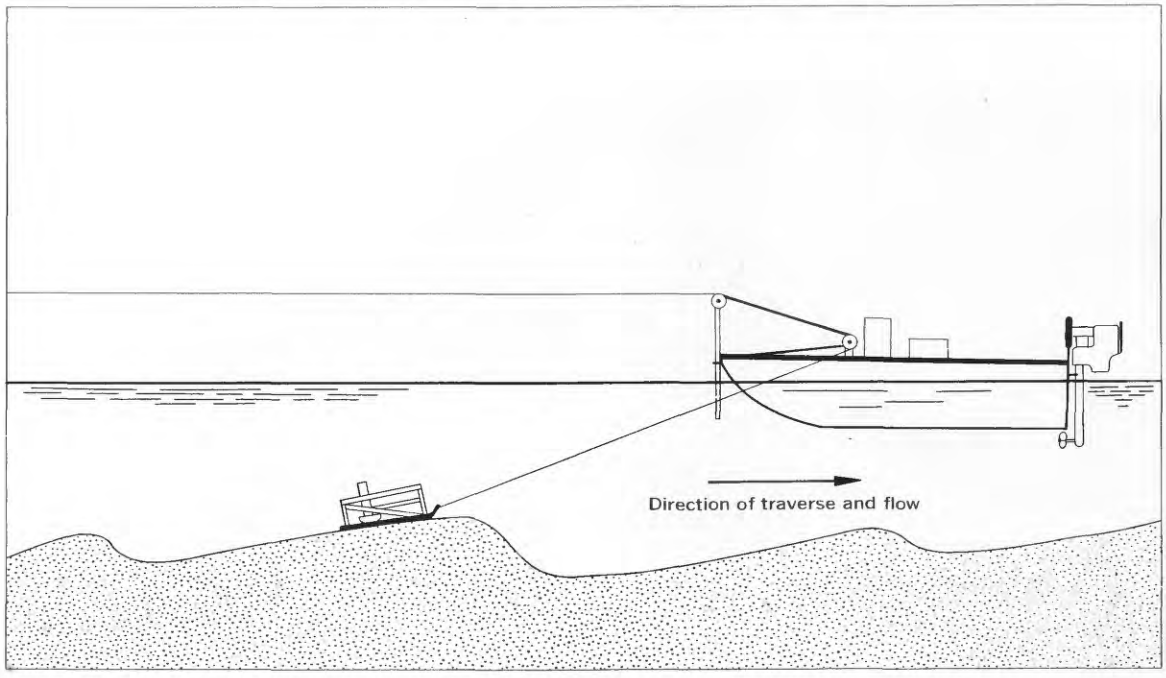

FIGURE 10.—Arrangement of boat and sled for the longitudinal traverses.

on the bed by a wooden dish. The watertight casing for the detector (see fig. 9) was an aluminum cylinder sealed at the bottom with a thin aluminum plate. For the longitudinal traverses, the boat and detector sled were arranged in tandem as shown in figure 10, and the boat, which faced upstream and pulled the detector sled, was maneuvered in a downstream direction by means of an outboard motor having reverse controls. The pulse-height analyzer, count-rate meter, and recorder were mounted in the boat together with a 115-volt a-c power supply, which consisted of a 1-kilovolt-ampere portable gasoline motor-generator unit and an electronic voltage regulator. This power supply proved to be sufficiently stable for satisfactory operation of the radiation-detection equipment. The arrangement of the equipment in the boat is shown in figure 11.

In addition, the experimental equipment included a dual-channel ultrasonic depth sounder (Karaki and others, 1961) capable of providing continuous records of the bed and water-surface profiles, a 400-foot distance-measuring cable and reel, and an automatic distance-marking system (see fig. 12). The distance-measuring cable functioned both as a stay line and as a part of the distance-marking system. In operation, the cable, which was fixed at the upstream end of each 400-foot segment of the test reach, was unwound at a controlled rate allowing the boat and sled to move downstream. When buttons that were located at definite intervals along the cable tripped an event-marking switch, ticks were made on the recorder charts. In this way, the recorder charts were provided with a distance coordinate.

Core samples of the bed material were collected along the test reach to determine the vertical distribution of tracer particles. The cores were sampled with the piston-type sampler shown in figure 13. This instrument was capable of collecting 3-foot cores, which were ejected with a hand-operated jack in 2-inch increments. Each 2-inch increment was collected in a separate container and analyzed for radioactivity. For this purpose, the sled was inverted as in figures 13 and 14, and a scaler was incorporated in the radiation-detection system so that counting rates could be determined more accurately.

FIGURE 11.—Arrangement of instruments in the boat.

FIGURE 12.—Dual ultrasonic depth sounder and distance-marking system.

FIGURE 13.—Equipment for sampling and analyzing the bed material. The 1½-inch-diameter sampler is used to collect 3-foot cores, which are ejected in 2-inch-increments with the hand jack attached to the end of the sampler plunger. Samples are counted with the detector and sled in an inverted position.

FIGURE 14.—Analysis of the vertical distribution of labeled particles in the field. Note the scaler and the inverted detector sled on top of the canopy over the instruments.

CALIBRATION OF RADIATION-DETECTION EQUIPMENT

To establish an absolute relation between the counting rate and the concentration of tracer particles, the detection equipment was calibrated with tracer particles in a laboratory calibration tank (see fig. 42) 4 feet in diameter and about 4 feet high. In the calibration, known amounts of labeled sand were mixed thoroughly

in the tank with sand having a median diameter and size distribution that approximated the natural bed material in the North Loup River. This was done for concentrations of tracer particles that ranged approximately from 0.7 g per cu ft (grams per cubic foot) of sand mixture to 40 g per cu ft. For each concentration, an average counting rate was determined by placing the detector at different locations on the surface of the sand; each counting location was selected so that the geometry of the detector would be similar to that in the natural stream. To reduce the background counting rate, a 9-inch depth of water was maintained over the sand bed throughout the calibration procedure. It was anticipated that the thickness of bed through which the particles would disperse would vary and that the counting rates would be affected accordingly. Therefore, calibrations were made for depths of uniform concentrations ranging from 2 to 18 inches. Two different methods were used to mix the labeled sand with the natural sand in the tank. Initially, a motor-driven post-hole auger was used as a mixer. The auger eventually was replaced by an ordinary concrete mixer. The concrete mixer yielded mixtures of more uniform concentration and was easier to use than the auger.

Throughout the calibration, counting rates were determined on both differential and integral settings of the pulse-height analyzer so that either setting could be used in the field. For integral counting, the lower discriminator setting was 5.0 volts and the high-voltage setting was 900 volts; the 900-volt setting was approximately in the center of a wide voltage range over which the count rates remained virtually constant (center of the plateau). For the differential counting, the gain and high-voltage settings were adjusted so that the 8.5-volt window width corresponded to the 0.40–0.74 Mev energy range. To insure that instrument drift did not alter the range of energies from which counting rates were determined, the detection system was calibrated with a sealed cesium 137 source periodically during each day. The periodic checks indicated that the system was reasonably stable.

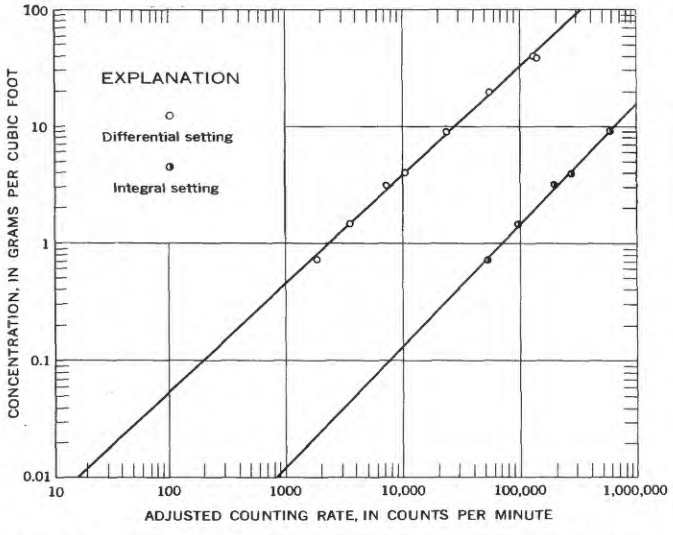

FIGURE 15.—Relations between the concentration of tracer particles in submerged sand and the adjusted counting rate for iridium 192.

The results of the laboratory calibrations are shown in figure 15. This graph is for uniform concentrations mixed to a depth of 8 inches. Figure 16 shows that the counting rate remains virtually constant for all depths of sand greater than about 8 inches; therefore, 8 inches can be considered as an infinite depth. Because the calibrations were made during about a week's time, observed counting rates were adjusted to account for the radioactive decay. All the calibration curves are based on adjusted counting rates that refer to October 26, 1960. The adjusted counting rates were computed using the equation:

$$R_a = (R_o - R_b)e^{0.693\frac{t}{T}}.$$

where

R_a = the adjusted counting rate
R_o = the observed counting rate at time t
R_b = the background counting rate
t = the number of days after October 26, 1960
T = the half-life of iridium 192 (74 days).

Because the data in figure 15 exhibited some scatter, the curves were fitted by the method of least squares. Interestingly, the integral and differential counting curves had slopes that differed slightly from 1.0. Thus, the data indicated that the counting rate is not directly proportional to the concentration, which is contrary to expectation. Spot checks indicated that the calibrations were repeatable. Because the calibration conditions closely approximated the field conditions, the empirical calibration curves shown in figure 15 were used in evaluating the field data.

FIELD PROCEDURES

To insure uninterrupted operation after the tracer particles had been introduced into the stream, auxiliary equipment used during the investigation was installed and all experimental equipment and procedures were tested beforehand in practice runs. The practice runs also provided measurements of background radioactivity along the test reach. For the operation of the boat and detector sled, cables were extended across the stream at the upstream end of the test reach and at 400-foot intervals downstream. The lateral cables downstream were necessary because the distance-measuring cable, which was only 400 feet long, had to be detached, rewound, and attached to the next cable

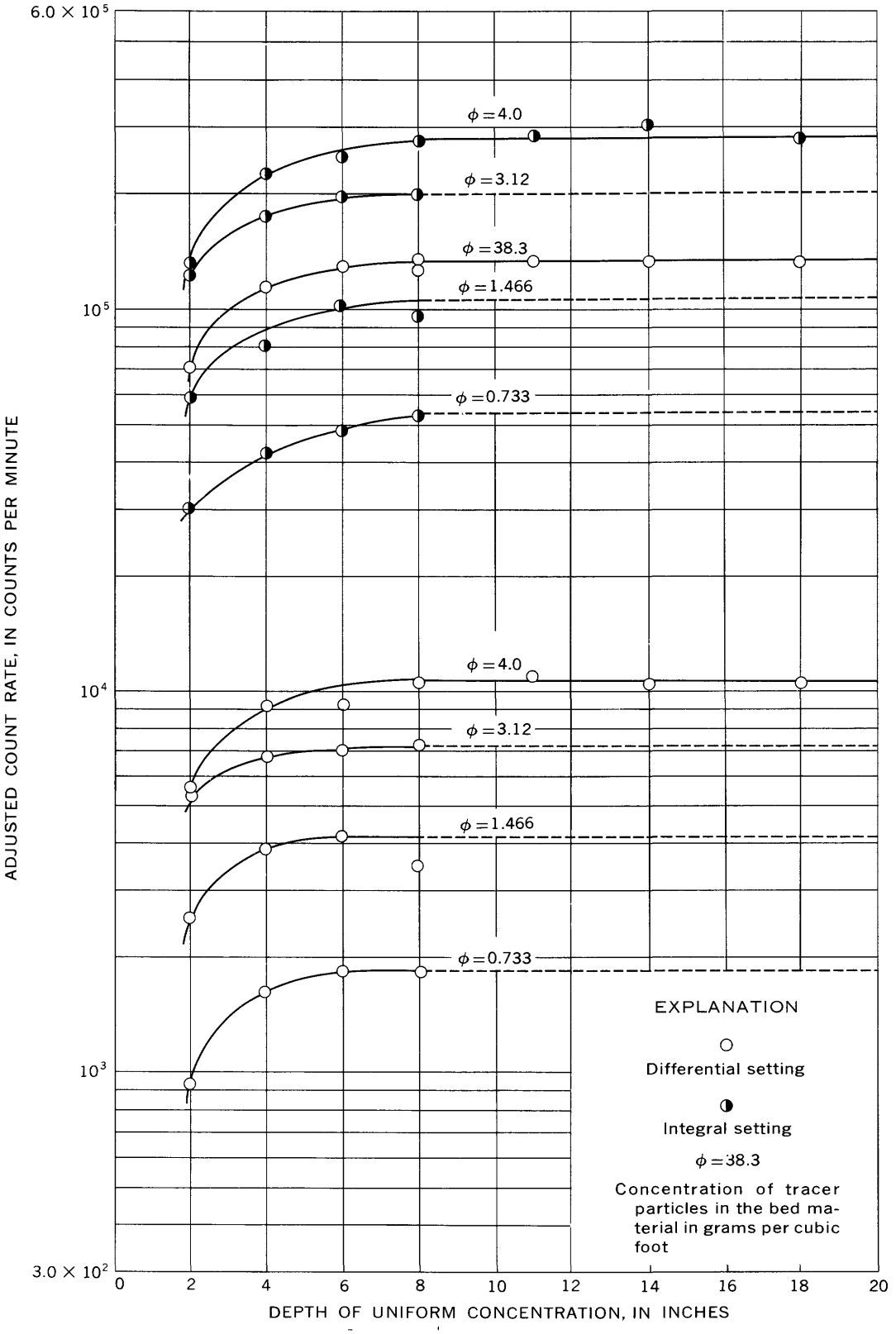

FIGURE 16.—Variation in adjusted count rate with the depth to which different concentrations of tracer particles are uniformly mixed.

downstream in order for the boat to remain moored and for the distance-marking device to be operative throughout the entire reach. For the measurement of water-surface slope, staff gages were placed on both banks at the upstream end of the test reach, on the left bank at two different intermediate positions within the reach, and on both banks at the downstream end of the reach (see fig. 2).

The dosing operation was performed on November 3, 1960, and consisted of depositing 2-pound lots of tracer particles on the streambed at 2-foot intervals across the entire width of the channel. Each 2-pound lot was labeled with 2 mc of iridium 192. About 2 hours after dosing, the first longitudinal traverse was made. Before this traverse, as well as all subsequent ones, the boat was fixed to the first lateral cable and the detector sled was placed by hand upstream from the boat along the tracing path. Prior to the release of the boat from the lateral cable, the background counting rate was recorded for about 2 minutes. When the background counting had been completed, the boat was released and moved downstream under power along a course that was roughly a distance of one-third the channel width away from the bank. During the course of the traverse, the outboard motor was used to position and pull the boat as the reel operator played out the distance-measuring cable, which allowed the boat and detector sled to progress downstream at a controlled rate. The downstream motion was arrested intermittently to allow the scale on the ratemeter to be changed as required by changes in the activity level.

To define the lateral distribution of the tracer particles, lateral traverses were made during the first few days. The lateral traverses were made in the same manner as the longitudinal traverses except that the detector sled was detached from the boat and pulled across the stream by hand.

The bed-material sampling was done initially by collecting cores in both the longitudinal and lateral directions without reference to the position of the dunes on the bed. However, because of the time required for the operation, the procedure was altered and samples were collected only in the troughs on the bed. In the operation, the position of the boat was fixed with the distance-measuring cable and lateral ropes. After positioning, the core sampler was depressed into the bed to its maximum extent and a 3-foot core was extracted. After the sample had been obtained, the boat was pulled to one bank and the 2-inch core increments were ejected into containers for radiation analysis. Each 2-inch increment was counted for a 1-minute period on the detector, which was placed in an inverted position in the boat.

RADIATION SAFETY

As mentioned previously, radiological health factors were considered in the selection of the test reach. In addition to considerations of the location of the test reach, calculations were made to insure that the activity on the tracer particles presented neither an internal nor an external radiation hazard. For the calculations, two different assumptions were considered. The first was that all the activity would be removed from the tracer particles as soon as they were introduced into the water. Under this assumption, computations showed that the activity would be diluted to the maximum permissible concentration[1] in drinking water by the quantity of water flowing past the dosing section in about 2.3 minutes. Inasmuch as the dosing operation would require about 30 minutes, the maximum permissible concentration would never be exceeded. The second assumption was that all the activity would remain on the particles. Under this assumption, the activity on the tracer particles would be dispersed within the bed material to a concentration comparable to the maximum permissible concentration for drinking water when the tracer particles were uniformly distributed throughout a 470-foot length of the test reach. Obviously, the maximum permissible concentration for drinking water is only an approximate index when the medium is the bed material, because, unlike water, large quantities of sand would never be ingested; however, the criterion provides a wide safety margin and therefore is useful. Also, under the second assumption, the tracer particles conceivably could represent an external radiation hazard; however, the depth of water in the stream afforded more than adequate shielding at all times.

To provide quantitative information on levels of radiation in the stream during the experiment, eight pocket dosimeters encased in waterproof tubes were placed on the streambed near one bank at about 100-foot intervals along the upstream end of the test reach. The dosimeter readings showed no trend with distance from the dosing section and indicated an average accumulation of only 8 mr (milliroentgens) for the period November 2–16.

In addition, the experimental procedures were designed to reduce to a minimum the radiation exposure received by project personnel. Precautions were particularly necessary in the operations that required the handling of tracer particles. The tracer particles were packaged by the supplier in No. 3 cans, each of which contained 2 pounds of Ottawa sand labeled with 2 mc of iridium 192. The measured and calculated exposure rates at a distance of 30 inches from

[1] The maximum permissible concentration of iridium 192 in drinking water for unrestricted areas, recommended by the Natl. Comm. on Radiation Protection (U.S. Dept. Commerce, 1959), is 4×10^{-5} μc per ml.

one can of tracer particles were, respectively, 1.2 and 1.1 mr per hr. The intensity of exposure varies approximately inversely with the square of the distance from the can. Thus, even though the level of radiation at 30 inches did not constitute any particular hazard, the cans of particles could not, with safety, be handled directly. To avoid direct handling of the cans, 3-foot tongs and an electric can opener were used. Also, in the calibration procedure when small quantities of tracer particles were separated and weighed, a long-handled scoop was used.

All project personnel were equipped with pocket dosimeters and film badges, and records of radiation exposure were maintained. During the period when the tracer particles were being handled, the maximum dosage received during a single day by any individual was 4 mr, and the average daily dose was 1.5 mr. This is considerably below the average maximum permissible dosage—20 mr per day—for workers in the atomic industries.

PRESENTATION AND DISCUSSION OF DATA

After the dosing and the first runs on November 3, the tracer particles were tracked daily by making longitudinal traverses with the radiation-detection equipment down the left and right sides of the stream. Exceptions to this were on November 9, when only one longitudinal traverse (run 7C), down the center of the stream, was made; on November 11, when additional longitudinal traverses down the center (run 9C) and very near the left bank (run 9La) were made; and on November 14, when no runs were made. In addition, lateral traverses were made on November 4, 5, and 8. Table 1 is a summary of the time, lateral position, and length of all longitudinal traverses, and the time and longitudinal position of all lateral traverses.

Curves that indicate the variation in concentration of tracer particles along the test reach at various times are shown in figures 17–21. These longitudinal concentration-distribution curves were obtained in the following manner from the counting rates that were continuously recorded during the longitudinal traverses. On the recorder chart for each run, the abscissa (distance coordinate) was divided, on the basis of the rate of change of the counting rate, into increments that represented from 5 to 100 feet of reach length. The average counting rate for each distance increment was determined graphically, and the background counting rate was subtracted from the average to obtain the net counting rate. Net counting rates, in turn, were corrected for the radioactive decay that had occurred between the time of the run and the time for which the calibration curves were made (Oct. 26, 1960). By

TABLE 1.—*Time, location, and extent of longitudinal and lateral traverses*

Date (Nov. 1960)	Run	Time of run (p.m., except as indicated)			Time after dosing (hr) [1]	Side of reach monitored	Length (feet) of reach monitored (sta. to sta.) [2]
		Start	End	Mean			
3	1 L	4:00				Left	
3	1 La	4:30	4:40	4:35	2.6	do	0–200
3	1 R	5:10	5:20	5:15	3.2	Right	0–200
3	1 Ra	6:05	6:15	6:10	4.2	do	0–75
4	2 L	11:00 a.m.		11:10 [3]	21.2	Left	0–400
4	2 R	12:00 a.m.		12:10 [3]	22.2	Right	0–400
4	2 Ta [4]			2:30	24.5		[5] 75
4	2 Tb [4]			2:45	24.8		[5] 125
5	3 R	9:55 a.m.	10:35 a.m.	10:15 a.m.	44.2	Right	0–800
5	3 L	11:30 a.m.	12:10	11:50 a.m.	45.8	Left	0–800
5	3 T [4]			1:55			[5] 185
6	4 R	12:15	1:30	12:52	70.9	Right	0–1200
6	4 L	3:15	4:30	3:52	73.9	Left	0–1200
7	5 R	1:30	2:50	2:10	96.2	Right	0–1800
7	5 L	3:45	4:50	4:18	98.3	Left	0–1200
8	6 R	11:30 a.m.	11:50 a.m.	11:40 a.m.	117.7	Right	0–1800
8	6 L	1:45	3:00	2:23	120.4	Left	0–1800
8	6 T [4]			3:30	121.5		[5] 415
9	7 C	11:30 a.m.	12:55	12:12	142.2	Centerline	0–1800
10	8 R	3:30	4:45	4:08	170.1	Right	0–1800
10	8 L	5:20	6:20	5:50	171.8	Left	0–1800
11	9 L	1:45	2:10	1:58	192.0	do	0–400
11	9 La	2:40	3:55	3:18	193.3	do [6]	0–400
11	9 C	5:30	5:40	5:35	195.6	Centerline	0–400
11	9 R	5:55	6:05	6:00	196.0	Right	0–400
12	10 L	11:00 a.m.	12:15	11:38 a.m.	213.6	Left	0–1800
12	10 R	1:50	3:10	2:30	216.5	Right	0–1800
13	11 L	11:50 a.m.	12:40	12:15	238.2	Left	0–1800
13	11 R	3:00	4:25	3:38	241.6	Right	0–1800
15	12 L	10:15 a.m.	11:20 a.m.	10:48 a.m.	284.8	Left	0–1800
15	12 R	12:55	1:55	1:25	287.4	Right	0–1800

[1] Mean time of dosing, 2:00 p.m., Nov. 3, 1960.
[2] Dosing performed at station 0.
[3] Estimated.
[4] Transverse run.
[5] Longitudinal station of transverse run.
[6] Very near bank.

use of the calibration curves in figure 15, the corrected counting rates were converted to concentrations that express the weight of tracer particles per unit volume of natural sand.

The background counting rate that was used to compute the net counting rate for each traverse was a time-weighted average, which had been measured just upstream from the dosing section prior to the traverse. The individual time-weighted rates were used to compensate for any instrument drift that may have occurred as a result of differences in operating conditions from time to time and because reconnaissance measurements along the reach indicated that the background counting rate varied only with time and not location. When the pulse-height analyzer was on the differential setting, the background counting rate usually averaged about 300 cpm; when it was on the integral setting, background averaged about 3,000 cpm.

The longitudinal-distribution curves indicate that the distributions along the left and right sides of the test reach were different. A significant quantity of the tracer particles on the left side seemingly was trapped in a deep trough near the dosing station and remained buried beyond the range of the radiation-detection equipment for several days. Evidently, one or more dunes with very deep troughs existed, at the time of the dosing, along the left bank of the stream at the up-

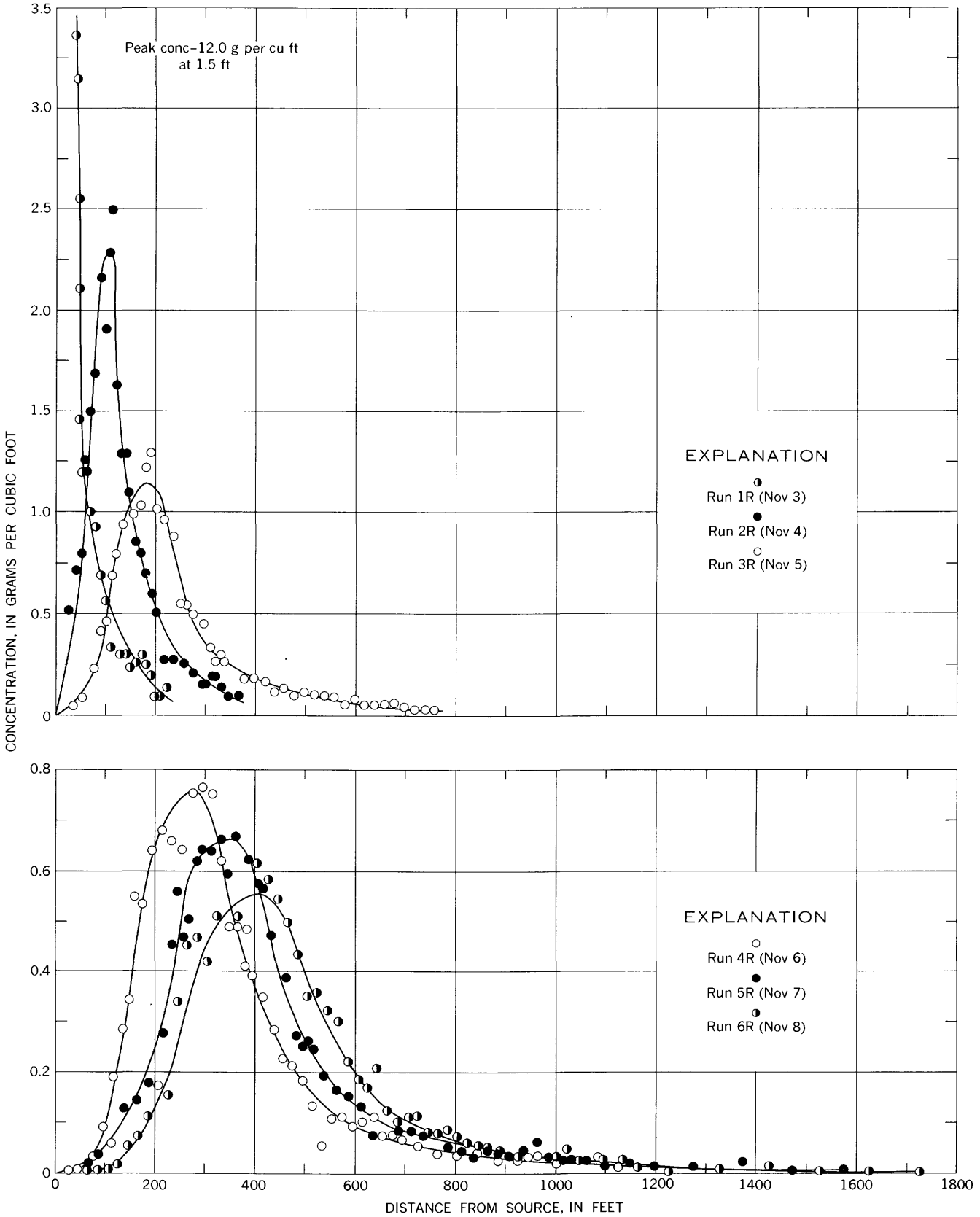

FIGURE 17.—Longitudinal distribution of labeled particles along the right side of the channel, November 3–8, 1960.

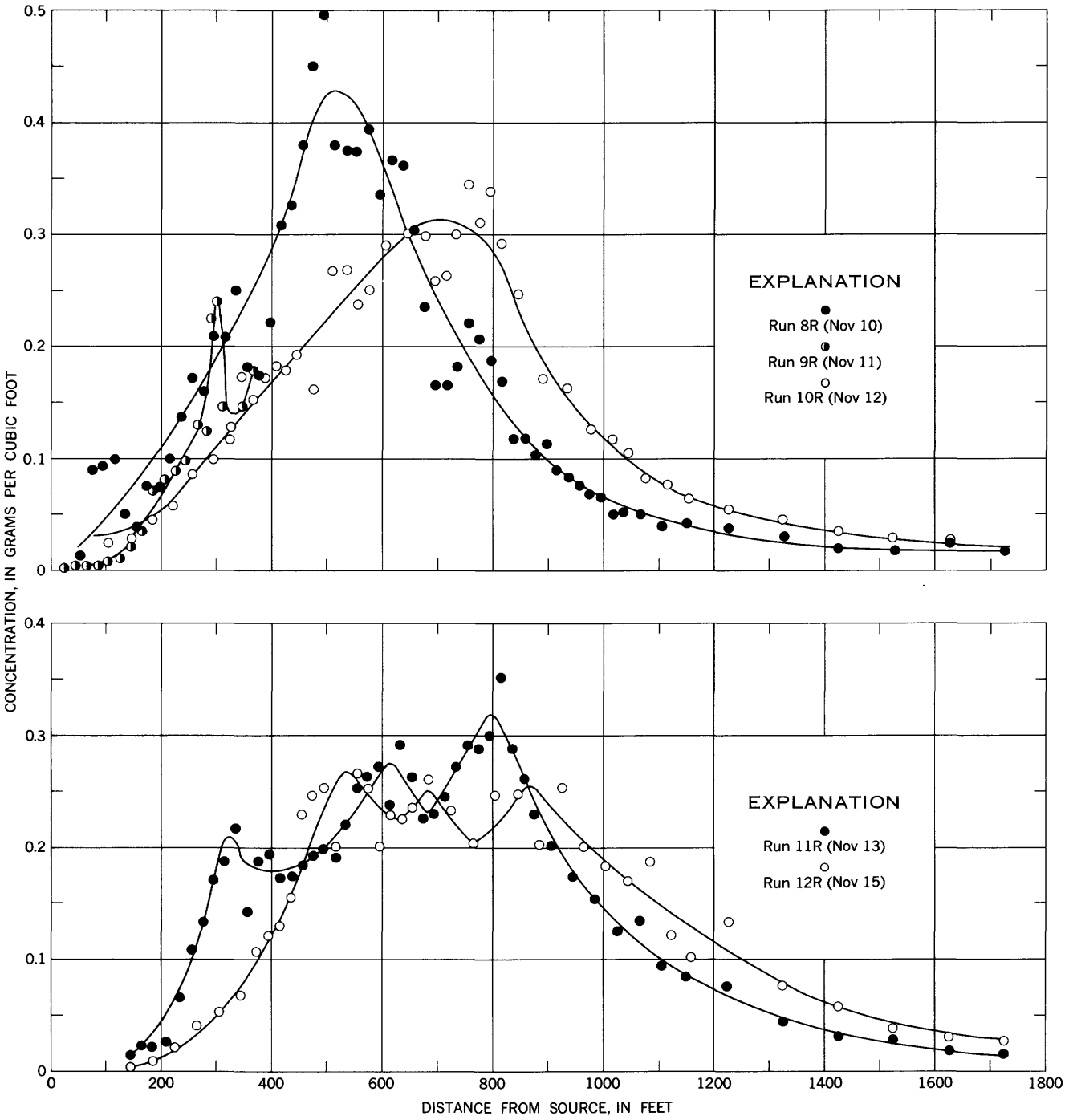

FIGURE 18.—Longitudinal distribution of labeled particles along the right side of the channel, November 10–13, 15, 1960.

stream end of the test reach. Subsequently, a train of small dunes passed over these deep troughs and trapped some of the tracer particles. It was not until about November 10 (run 8) that another train of dunes with deep troughs passed through the upstream end of the test reach and released the trapped particles, which were then free to disperse downstream in a more normal manner.

The dispersion of tracer particles along the right side of the test reach seems to have proceeded normally until about November 11 (run 9), when particles that had been trapped on the left side began to disperse laterally toward the right side of the stream. The distribution defined by run 7C on November 9, indicates that a relatively small quantity of tracer particles had been trapped near the center of the stream and began to

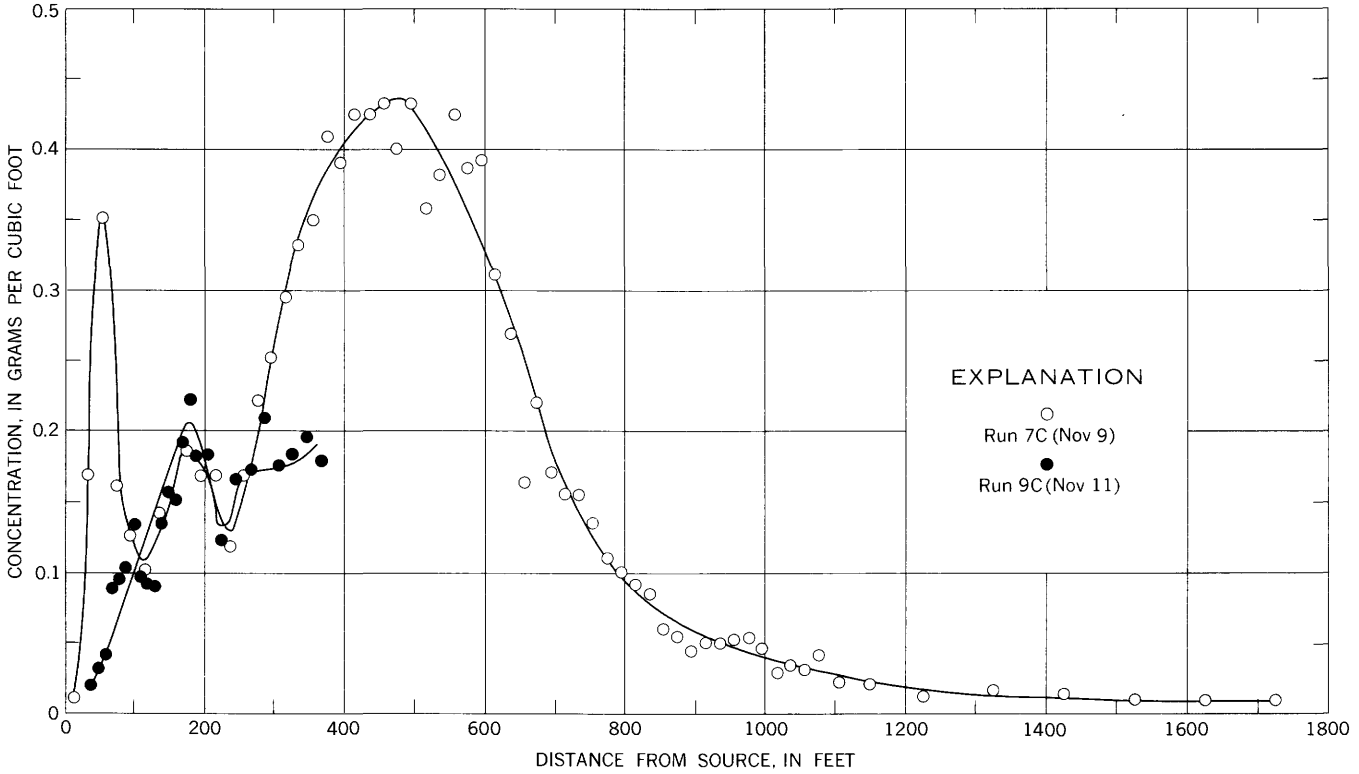

FIGURE 19.—Longitudinal distribution of labeled particles along the center of the channel, November 9 and 11, 1960.

disperse downstream somewhat sooner than the particles that had been trapped on the left side.

As a result of the temporary storage, the distribution curves for the left side of the test reach are less indicative of the general distribution that applies for the average flow conditions than those for the right side. However, the fact that particles were buried demonstrates that under similar conditions highly concentrated deposits of contaminated particles could remain buried for considerable periods of time and then suddenly be released.

The normal dispersion rate was reduced somewhat on the mornings of November 9 and 10, when the water temperature was 0°C and there was heavy frazil ice (fig. 22) in the stream; the ice melted by noon on both days. Apparently, the ice damped the turbulence in the flow sufficiently to reduce significantly the transport and dispersion of the bed-material load. After the ice melted, the transport and dispersion increased to its earlier rate.

The lateral distribution of the tracer particles is illustrated in figures 23 and 24. In the graphs for November 4 and 5, the differences between the amounts of tracer particles available for transport and dispersion on the right side and on the left side are evident. However, the graph for November 8 shows that as time went on, the particles became distributed reasonably uniformly across sections that were fairly distant from the source.

The vertical distribution of tracer particles in the streambed, as determined from the core-sampling data, is shown in figures 25–29. The graphs show that although the variation in counting rate with depth into the bed was considerable at most of the sampling locations, there was no regular vertical distribution pattern. Hence, a vertical concentration gradient cannot be evaluated with any degree of certainty. The variations probably resulted largely from the passage of dunes having different heights, mean elevations, and concentrations of tracer particles. As a result of the irregularities of the dunes, neither the distance below the water surface, distance below the bed surface, nor depth of activity can be used to normalize the vertical distribution of count rate. Hence, the distributions from the separate verticals cannot be combined to provide an average gradient. However, the distributions from the separate verticals can be combined to indicate the average depth of the zone through which the sediment particles moved; the average depth to which tracer particles extended below the bed surface (average depth of the zone of movement) was 1.45 feet.

General hydraulic and sediment data were collected several times during the course of the experiment.

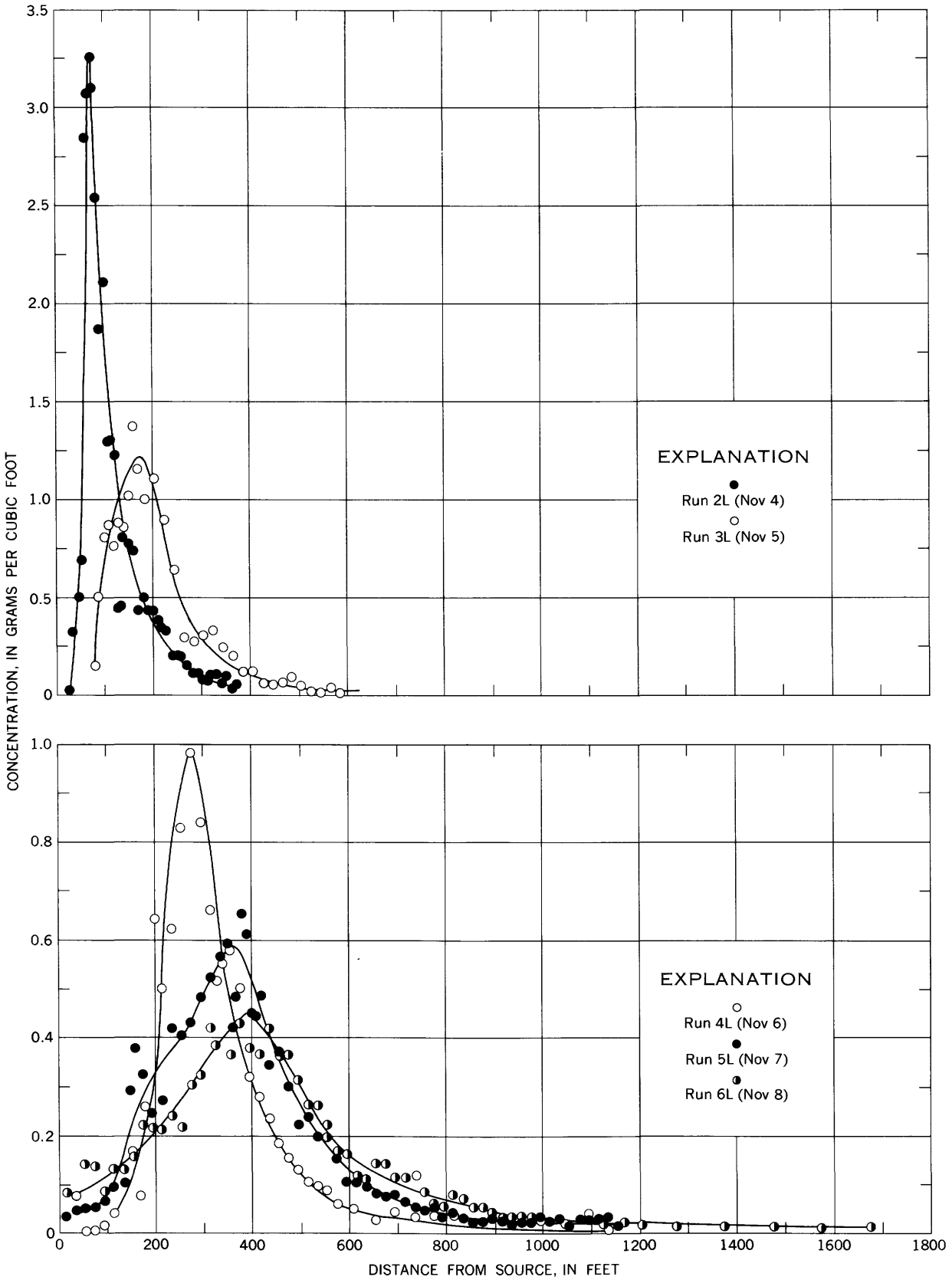

FIGURE 20.—Longitudinal distribution of labeled particles along the left side of the channel, November 4-8, 1960.

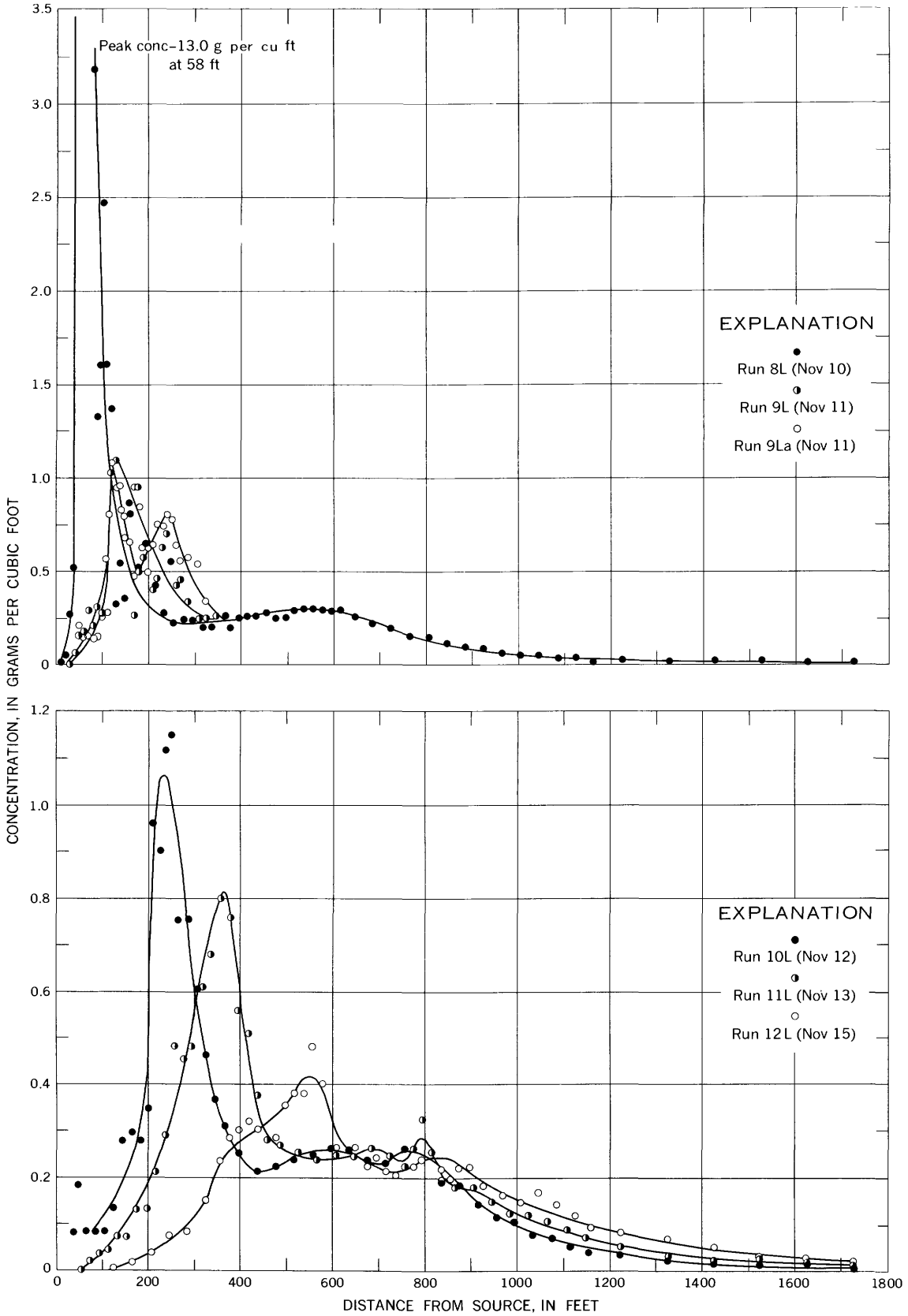

FIGURE 21.—Longitudinal distribution of labeled particles along the left side of the channel, November 10–13, 15, 1960.

FIGURE 22.—Frazil ice in the stream, November 9.

Summaries of these data are presented in tables 2 and 3. The hydraulic data include information on water-discharge measurements, water-surface slopes, roughness coefficients, water temperatures, and the

TABLE 2.—*Summary of hydraulic data*

Date (Nov. 1960)	Time	Water-discharge measurement: Discharge (cfs)	Width (ft)	Mean depth (ft)	Area (sq ft)	Mean velocity (fps)	Water-surface slope×10³	Roughness coefficient $\left(\frac{C}{\sqrt{g}}\right)$	Water temperature (°C)	Mean depth in reach (ft)
4	9:00 a.m.						0.839			
4	11:30 a.m.	263	47.4	2.47	117	2.25	[1].839	8.7	6	2.3
5	9:00 a.m.						.833		2.5	
5	11:00 a.m.								4	2.7
6	10:00 a.m.								3	
6	12:00 a.m.								5	2.5
6	5:00 p.m.	249	54	2.13	115	2.17	.844	9.0	6	
7	10:00 a.m.						.805		3	
7	2:00 p.m.								6	2.4
7	5:00 p.m.								7	
8	11:00 a.m.						.821		4	
8	1:00 p.m.								4	2.7
8	2:00 p.m.								4	
9	9:00 a.m.						.816		0	1.8
9	5:00 p.m.						.810		1	
9	5:00 p.m.	251	56	1.91	167	2.35	[1].810	10.5	1	
10	9:30 a.m.						.810		0	
10	2:00 p.m.								2	
10	5:00 p.m.								3.5	2.4
11	11:00 a.m.						.883		2.5	
11	3:00 p.m.						.860		5	
11	5:00 p.m.								6	
12	10:00 a.m.						.815		4	
12	3:00 p.m.						.826		8	2.5
12	4:15 p.m.	255	57	2.02	115	2.22	[1].826	9.6	8	
13	10:00 a.m.						.838		4	
13	5:30 p.m.						.816		8	2.5
15	9:30 a.m.						.878		5.5	
15	1:00 p.m.						.860		8	2.6
16	3:30 p.m.	260	53.4	2.06	110	2.37	[1].860	9.9		

[1] Estimated.

TABLE 3.—*Summary of sediment data*

[Particle size distribution of all sediment determined by means of visual-accumulation tube. Bed material, collected Nov. 16, 1960, was also analyzed with sieve]

MEASURED SUSPENDED SEDIMENT

Date of collection (Nov. 1960)	Time (p.m.)	Water discharge (cfs)	Water temperature (°C)	Concentration (ppm)	Percent finer than indicated size, in millimeters: 0.0625	0.088	0.125	0.175	0.250	0.350	0.500	Measured suspended-sediment discharge (tons per day)
4	12:30	263	6	634	10	14	28	58	89	100	------	450
9	6:10	251	1	648	7	12	28	60	88	98	100	439
12	5:15	255	8	390	15	22	38	64	88	100	------	269
16	4:30	260	--------	498	10	13	27	61	87	100	------	350

BED MATERIAL

Depth below trough surface (in.)	Percent finer than indicated size, in millimeters: 0.088	0.125	0.175	0.250	0.350	0.500	0.700	1.000	1.651	3.327	9.424
([1])	0	2	6	29	68	91	96	97	98	99	100
0–12	0	1	6	27	65	87	92	94	97	99	100
12–24	0	1	8	32	66	91	97	--------	98	100	--------
24–36	--------	0	3	18	55	86	98	99	100	--------	--------
0–12	--------	0	4	25	69	93	99	--------	100	--------	--------
12–24	0	1	5	21	45	87	97	--------	99	100	--------
24–36	0	1	4	15	41	70	84	90	93	99	100

LABELED OTTAWA SAND

Percent finer than indicated size, in millimeters: 0.175	0.250	0.350	0.500
0	9	81	100

[1] Composite of 3-ft cores collected throughout test reach.

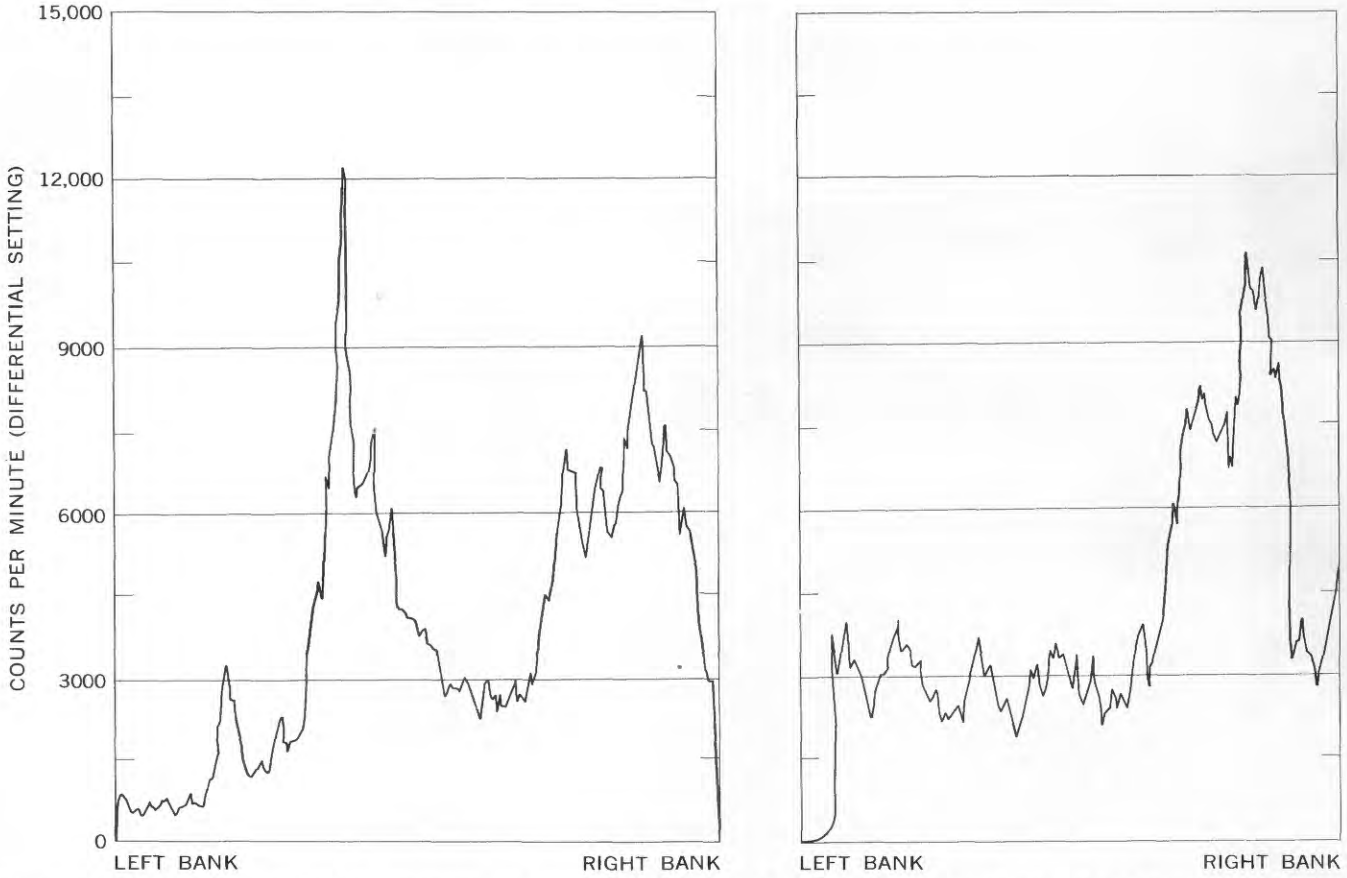

FIGURE 23.—Lateral distribution of labeled particles downstream from the source on November 4, 1960. Left graph shows distribution 75 feet downstream (2:30 p.m.). Right graph shows distribution 125 feet downstream (2:45 p.m.).

mean depths in the reach. The sediment data include information on the measured suspended sediment, bed material, and tracer particles. During the period November 4–16, the water discharge was measured five times and the suspended sediment was sampled four times. The measured water discharges ranged from 249 to 263 cfs and averaged 256 cfs. Suspended-sediment concentrations ranged from 390 to 648 ppm (parts per million) and averaged 542 ppm, and measured suspended-sediment discharges ranged from 269 to 450 tons per day and averaged 377 tons per day. The mean depths for the entire reach, which were determined from the records obtained with the ultrasonic depth sounder, ranged from 1.8 to 2.7 feet. During the course of the experiment, the water temperature ranged from 0° to 8°C and averaged about 5°C. Usually, the water gradually warmed during the day. As previously mentioned, on the mornings of November 9 and 10 the water temperature was 0°C and the stream contained heavy frazil ice.

The streambed was formed of dunes that moved slowly downstream. The size of the individual dunes varied greatly; however, an average dune was about 1.0–1.5 feet high at the crest and about 10–15 feet long. Typical records of the bed-surface profile, as defined by the ultrasonic depth sounder, are shown in figure 30. The roughness coefficients associated with the bed form were within the range of values usually associated with dunes; that is, values of $\frac{C}{\sqrt{g}}$, where C is the Chezy coefficient and g is the acceleration of gravity, ranged from 8.7 to 10.5. These values correspond, respectively, to values of the Manning n of 0.035 and 0.028.

DERIVATION OF CONCENTRATION-DISTRIBUTION AND RELATED FUNCTIONS

The part of the total sediment discharge that is composed of particles having sizes the same as those of particles commonly found in the bed material is called the bed-material discharge. The individual particles of the bed-material discharge move in a discontinuous manner involving alternate transportation and storage. During the storage phase, the particles are a part of the bed material. During the transport phase, their downstream progress may be by rolling or sliding in almost continuous contact with the streambed or by temporary entrainment within the body of the flow.

Ordinarily, the sediment that moves in contact with the bed is called the bedload, and the sediment that is entrained in the flow is called the suspended load. Regardless of the mode of transport, all particles associated with the bed-material discharge move in a series of discrete steps. Einstein (1950) indicated that the average distance traveled between consecutive points of deposition may be assumed to be 100 grain diameters for particles of average sphericity. Whether or not 100 diameters is a valid estimate for all sediments is of no particular significance in this discussion. The chief point is that the particles move in discrete steps. Presumably, the distance traveled during each step by the entrained particles will be greater than the distances traveled by bedload particles, and the lengths of the individual steps vary to a considerable degree. Thus, if a group of particles is released instantaneously from a point or line source, the particles will not move downstream in a body but will be dispersed along the length of the channel. In addition to being distributed longitudinally, the particles will be dispersed vertically in a layer parallel to and immediately below the bed surface. The lower boundary of the layer will be determined by the characteristics of the bed forms.

Randomness is associated with many of the various physical factors that combine to determine the length of a step and the time between the steps of a particular particle under a given set of conditions. Among these factors are turbulence, the transport characteristics of the particle, the location and orientation of the particle, and the dimensions of the bed forms. Because of the randomness of these physical factors, the dispersion of bed-material particles seems to possess the basic attributes of a random process. By random process is meant a repetitive process in which any single trial can have any one of a number of possible outcomes but the actual outcome of a trial is governed by chance and cannot be predicted. Thus, the use of probability theory is appropriate in deriving a distribution function for describing the dispersion of tracer particles released simultaneously from a source in the streambed.

Einstein (1937) considered bedload transport from the viewpoint of probability theory. Beginning with virtually the same assumptions, Einstein arrived at distribution functions that are identical with those obtained in the following derivation. However, Einstein's method of derivation was considerably different.

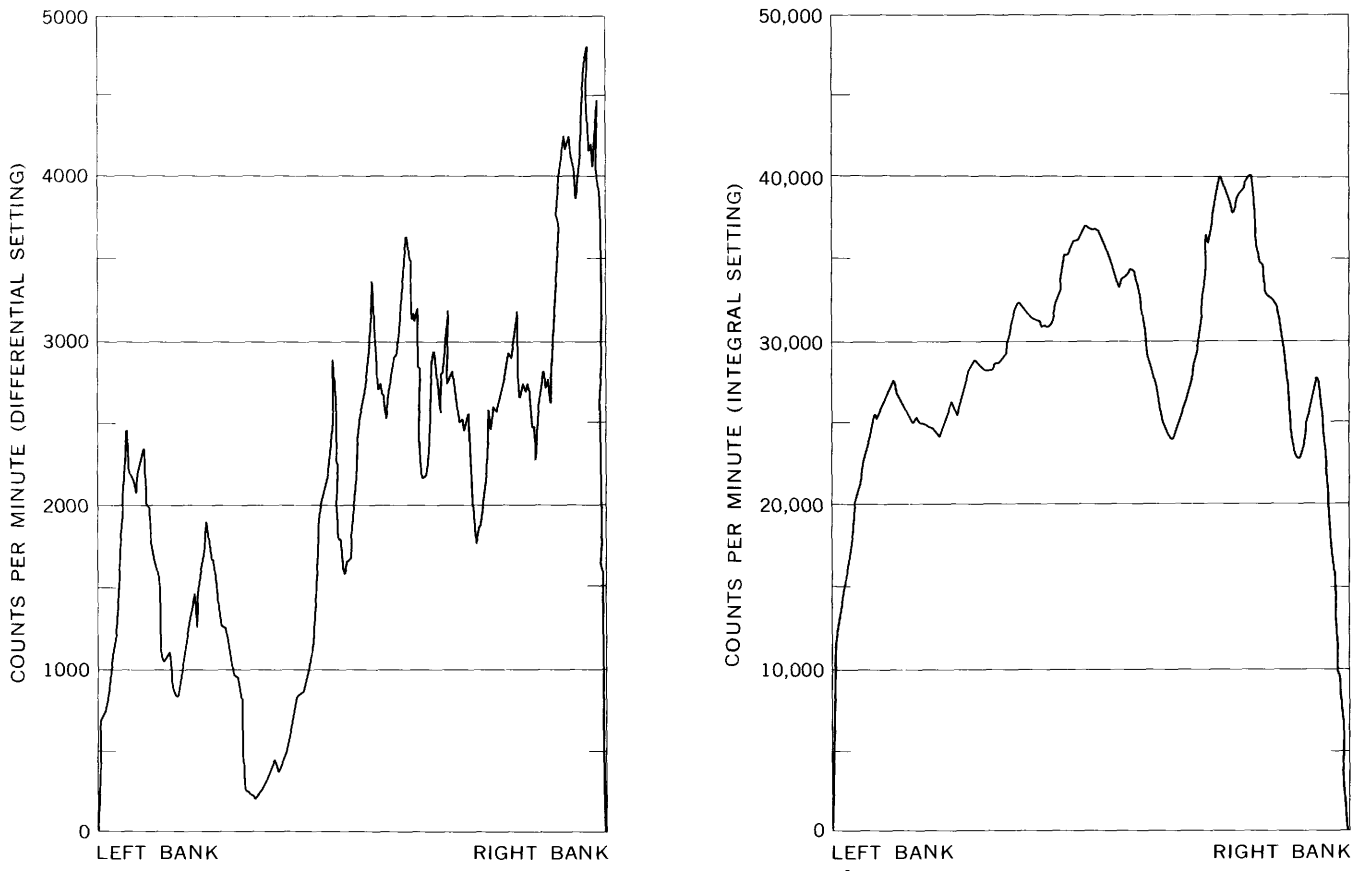

FIGURE 24.—Lateral distribution of labeled particles downstream from the source on November 5 and 8, 1960. Left graph shows distribution 185 feet downstream (Nov. 5, 1:55 p.m.). Right graph shows distribution 415 feet downstream (Nov. 8, 3:30 p.m.).

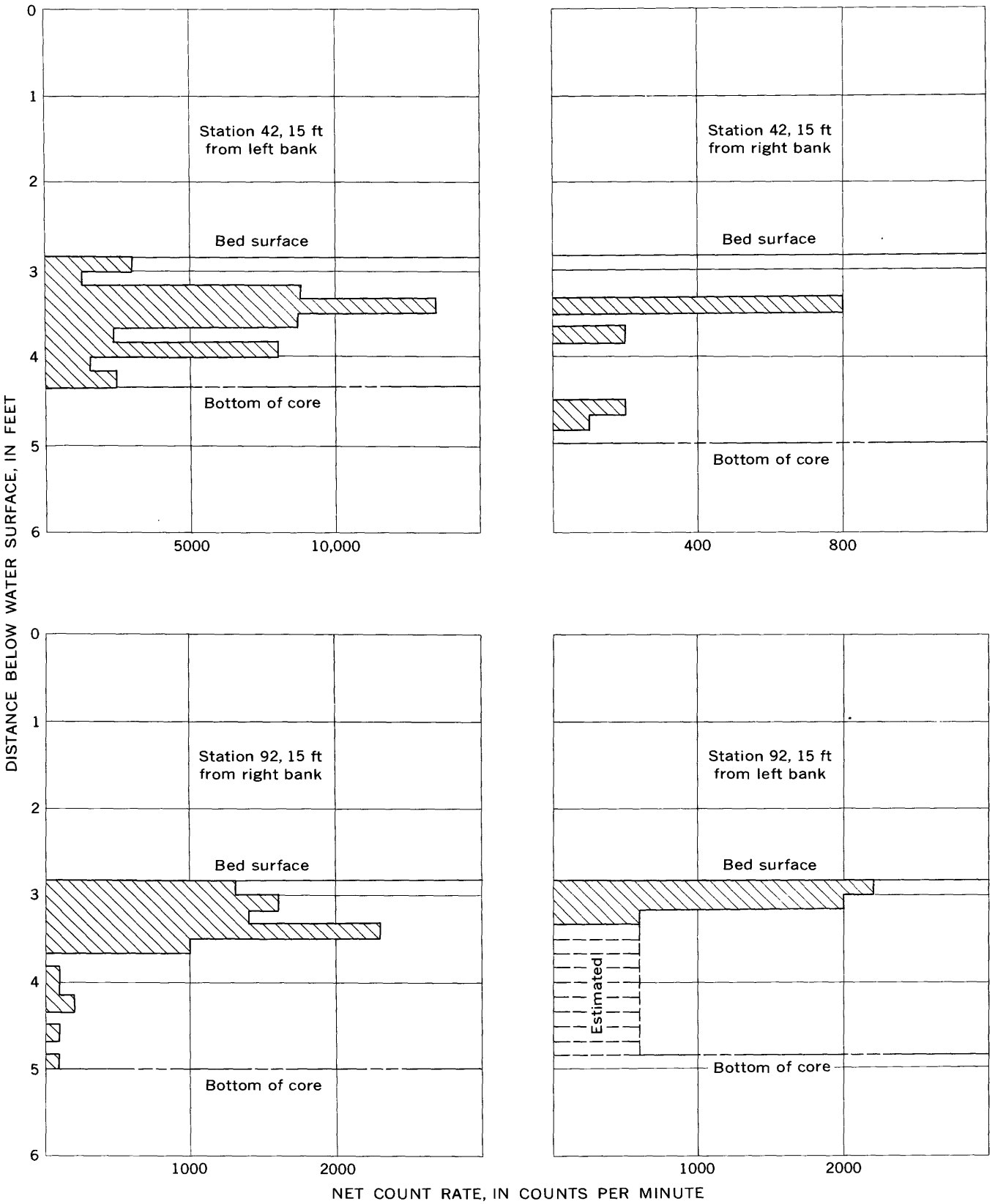

FIGURE 25.—Vertical distribution of labeled particles at selected verticals on November 4, 1960.

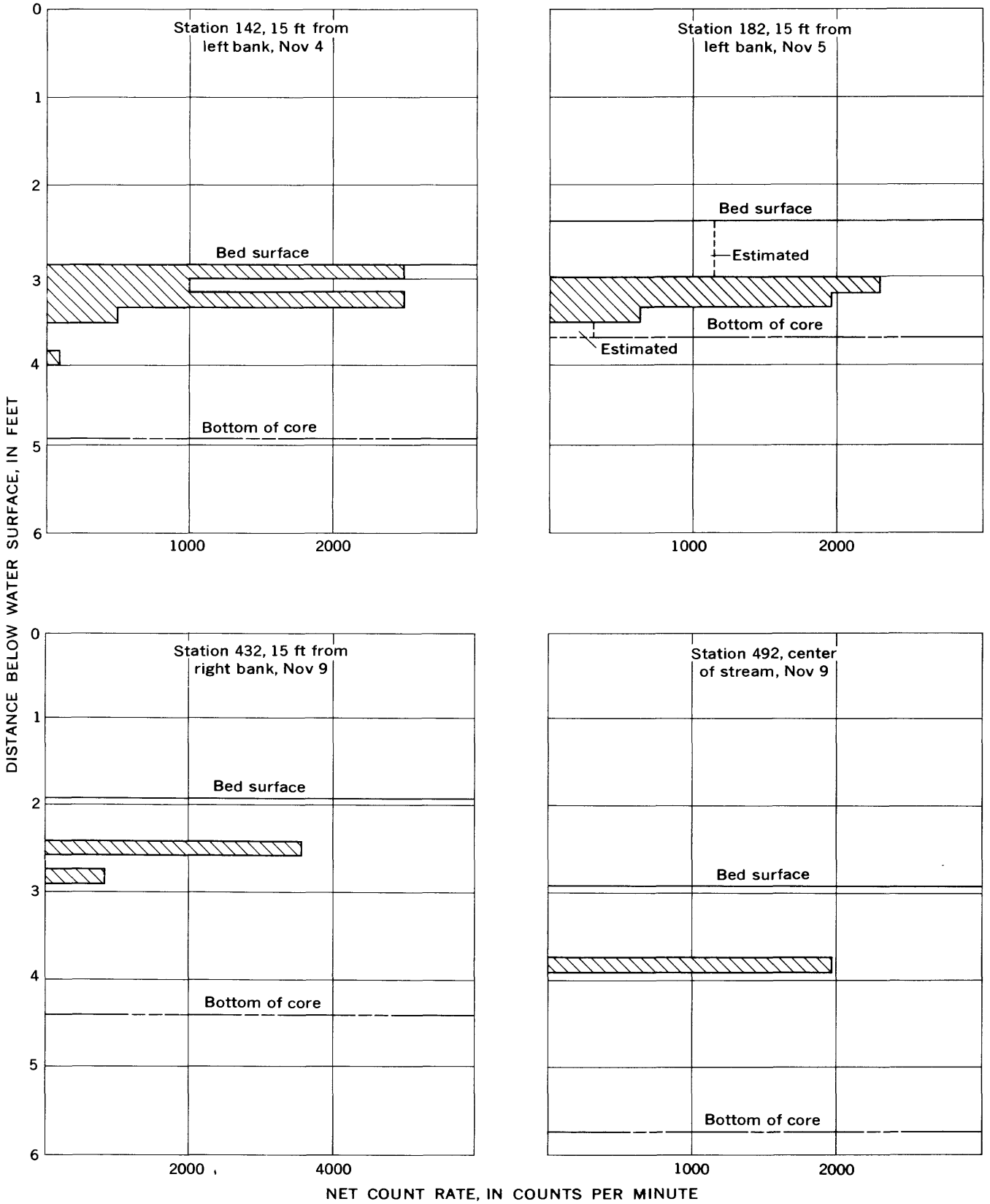

FIGURE 26.—Vertical distribution of labeled particles at selected verticals on November 4, 5, and 9, 1960.

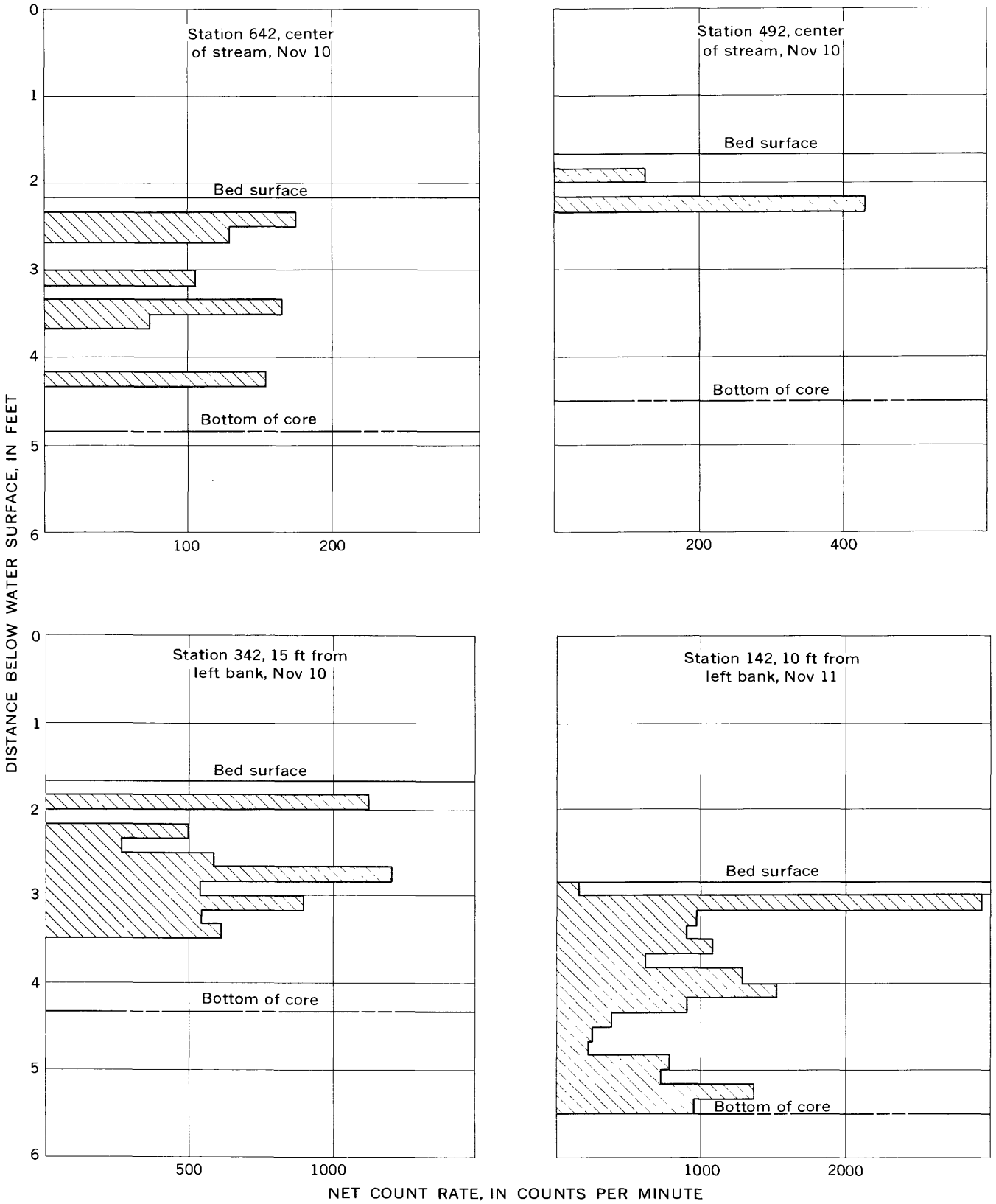

FIGURE 27.—Vertical distribution of labeled particles at selected verticals on November 10 and 11, 1960.

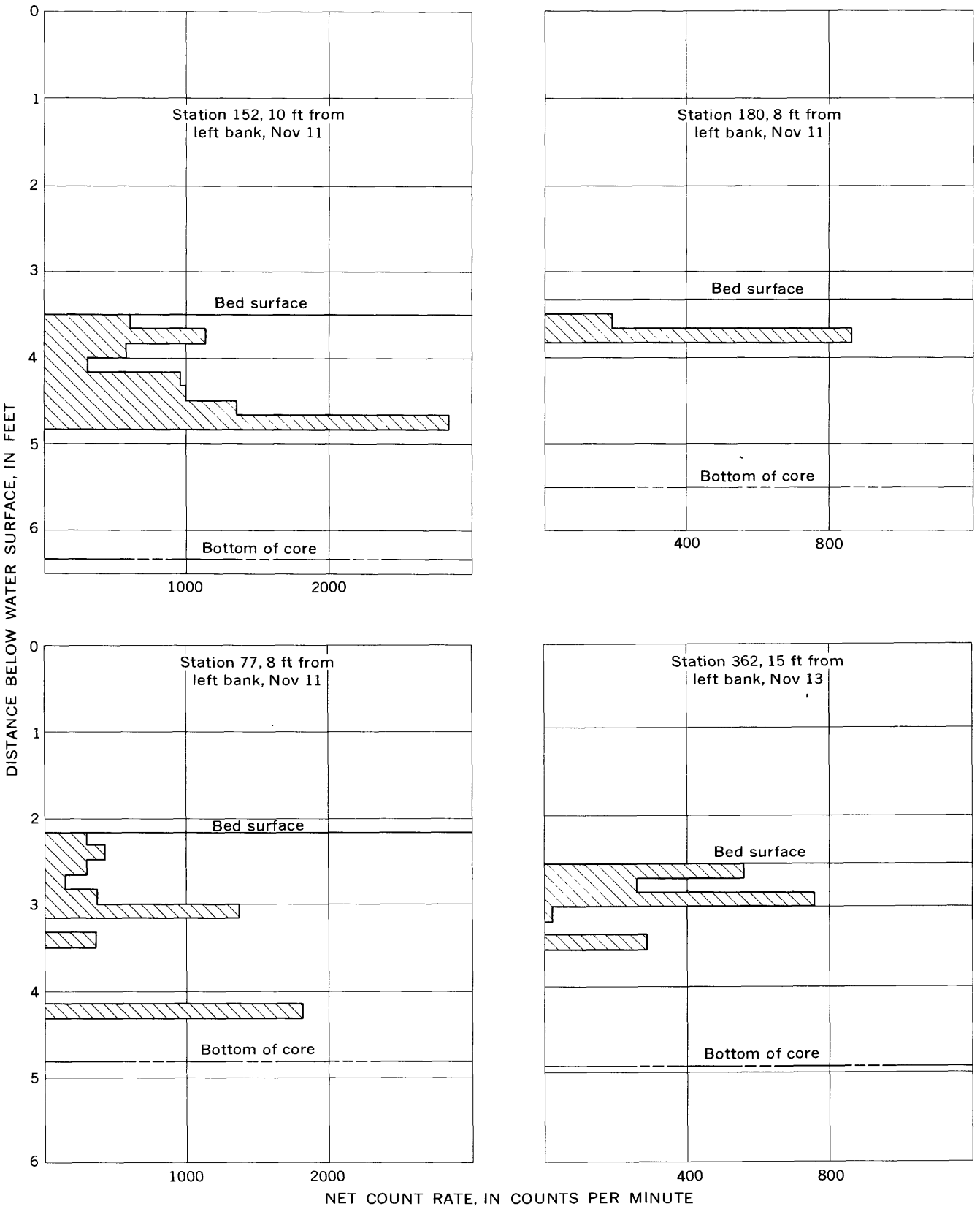

FIGURE 28.—Vertical distribution of labeled particles at selected verticals on November 11 and 13, 1960.

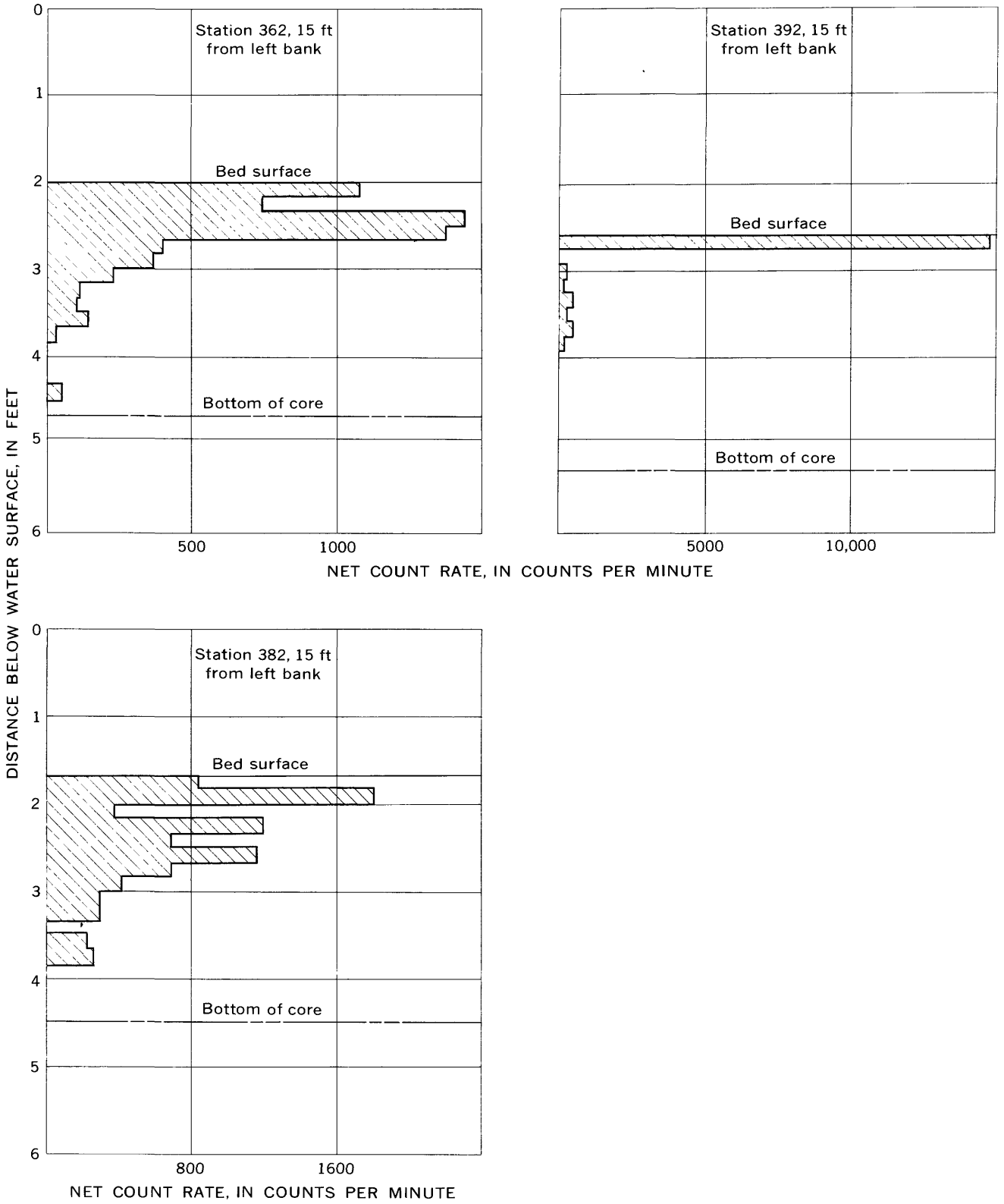

FIGURE 29.—Vertical distribution of labeled particles at selected verticals on November 13, 1960.

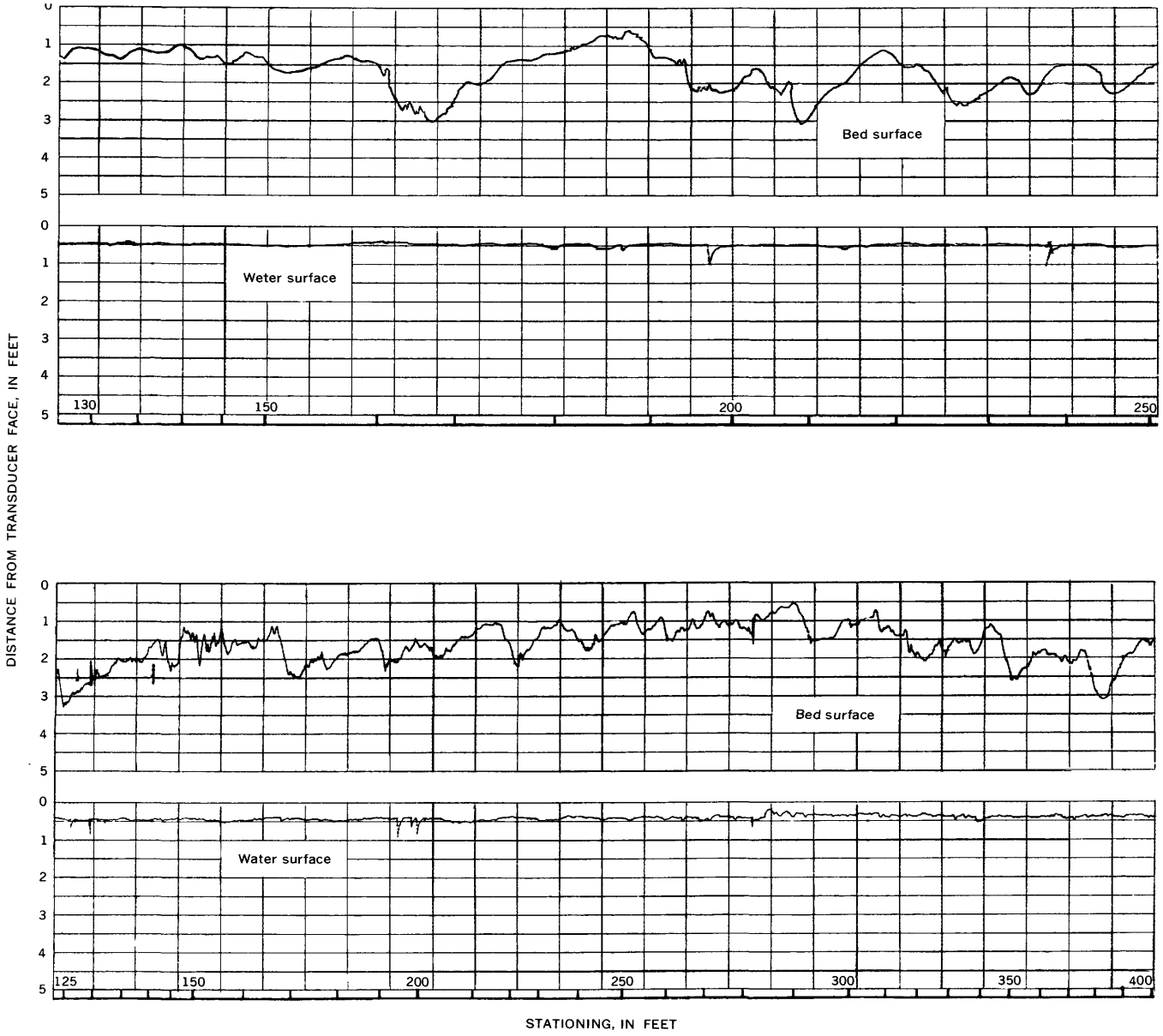

FIGURE 30.—Water- and bed-surface profiles defined by the dual channel stream monitor. (From Hubbell and Haushild, 1962.) In top graph, traverse speed is approximately 15 feet per minute; in bottom graph, 33 feet per minute.

THE CONCENTRATION-DISTRIBUTION FUNCTION

Assume a straight, uniform alluvial channel in which the water and bed-material discharges per unit width are uniform and constant. Now, consider a group of tracer particles having identical transport characteristics. Let these particles be released simultaneously, at time $t=0$ and station $x=0$, from a uniformly distributed plane source that extends laterally across the channel and vertically from the surface of the bed to the lower limit of the zone of particle movement. Also, let the tracer particles move and disperse downstream in such a way that there is no tendency for a vertical concentration gradient of tracer particles to develop in the bed.

If the number of tracer particles is small enough so that the bed-material discharge is virtually unchanged by the release of the particles, yet is large enough to approximate an infinite population, the stepwise movements of the tracer particles can be considered as sequences of occurrences of an event in a continuum of space, and the longitudinal distribution of the tracer particles will correspond to a probability-density function.

Let E represent the event that a tracer particle begins and terminates a step in the downstream direction. Also, let the probability of E occurring while the particle remains within a random length increment $(x, x+\Delta x)$ be $k_1\Delta x$, where k_1 is a constant for

all tracer particles and $k_1\Delta x$ is independent of x and the number of times that E has occurred previously. Furthermore, let Δx be sufficiently small so that the probability of two or more successive occurrences of E while the particle is in $(x, x+\Delta x)$ is negligibly small.

According to these hypotheses, a tracer particle that is in the increment $(x, x+\Delta x)$ may, when it moves, either remain in the increment or be transported out of the increment; but, it may not be in the same increment at the termination of a second step. The corresponding probabilities are $(k_1\Delta x)$ that E will occur once and $(1-k_1\Delta x)$ that E will not occur. With these probabilities, a formula can be derived for the probability, $p(i; x+\Delta x)$, that E will occur exactly i times while the particle is being transported over the distance $(0, x+\Delta x)$. If this distance is divided into the two increments $(0, x)$ and $(x, x+\Delta x)$, E may occur i times in either of two mutually exclusive ways. These are:

1. E may occur i times in $(0, x)$ and zero times in $(x, x+\Delta x)$.
2. E may occur $i-1$ times in $(0, x)$ and one time in $(x, x+\Delta x)$.

By applying the multiplication theorem for the probabilities of independent events, the respective probabilities for these two ways are $[p(i; x)][(1-k_1\Delta x)]$, and $[p(i-1; x)](k_1\Delta x)$. By the addition theorem for the probabilities of mutually exclusive events,

$$p(i; x+\Delta x)=[p(i; x)][(1-k_1\Delta x)]+[p(i-1; x)](k_1\Delta x)$$ [2]

or

$$\frac{p(i; x+\Delta x)-p(i; x)}{\Delta x}=k_1[p(i-1; x)-p(i; x)]$$

which approaches the differential equation

$$\frac{d[p(i; x)]}{dx}=k_1[p(i-1; x)-p(i; x)] \quad (1)$$

as a limit as Δx approaches zero. By a similar process of reasoning, when no events occur $(i=0)$,

$$\frac{d[p(0; x)]}{dx}=-k_1[p(0; x)]. \quad (2)$$

With conditions $p(0; 0)=1$ and $p(i; 0)=0$ for $i\geq 1$, the solution to equations 1 and 2 is

$$p(i; x)=\frac{e^{-k_1x}(k_1x)^i}{i!}, \quad i=1, 2 \ldots, \quad (3)$$

which is the Poisson probability mass function with parameter k_1x. Equation 3 expresses the probability that E will occur exactly i times as the given tracer particle is transported the distance $(0, x)$.

[2] The notation and terminology in this section are for the most part consistent with those of Parzen (1960).

The distribution function corresponding to equation 3 may be stated

$$F(n-1; x)=\sum_{i=0}^{n-1}\frac{1}{i!}(k_1x)^ie^{-k_1x} \quad (4)$$

where $F(n-1; x)$ is the probability that the number of occurrences of E as the particle is transported over the distance $(0, x)$ is less than n. Then $1-F(n-1; x)$ is the probability that the number of occurrences of E in $(0, x)$ is equal to or greater than n, which is also the probability that at the completion of the nth occurrence of E the particle will have been transported a distance equal to or less than $(0, x)$. Hence, $1-F(n-1; x)$ is equivalent to the distribution function $F(x; n)$ for the location of the particle at the completion of the nth event. Differentiation of $F(x; n)$ with respect to x yields the probability density function

$$f(x; n)=k_1e^{-k_1x}\frac{(k_1x)^{n-1}}{\Gamma(n)} \quad (5)$$

where $\Gamma(n)$ is the gamma function (generalized factorial function) of n. Equation 5 is the probability density function for the gamma distribution with parameters n and k_1. When multiplied by dx, it expresses the probability that at the completion of the nth step the given tracer particle will be located in the length increment $(x, x+dx)$, which is to say that the particle will have been transported the exact distance $(0, x)$.

The mean distance over which a particle would be transported during n repeated occurrences of E is

$$x_n=\int_0^\infty xf(x; n)dx=\frac{n}{k_1}.$$

Thus $k_1=n/x_n$ may be interpreted as the mean rate of occurrences of E with respect to x. Also, the mean step length for any single occurrence of E is $1/k_1$.

Considering now the movements of a tracer particle with respect to time, E may also be defined as the event that a tracer particle begins and terminates a rest period between successive steps in the downstream direction. The same considerations that apply to the number of occurrences of E in $(0, x)$ apply also to the number of occurrences of E in $(0, t)$. Thus, assuming that the total traveltime is negligible in comparison to the total rest time, the probability that a tracer particle will have completed exactly i rest periods in the elapsed time $(0,t)$ is expressed by the probability mass function

$$p(i; t)=\frac{e^{-k_2t}(k_2t)^i}{i!}, \quad i=1,2 \ldots, \quad (6)$$

and the probability density function for the total elapsed time at the completion of the nth rest period is

$$f(t; n)=k_2 e^{-k_2 t}\frac{(k_2 t)^{n-1}}{\Gamma(n)} \tag{7}$$

where k_2 is analogous to k_1 and may be interpreted as the mean rate of occurrence of rest periods with respect to t. Also, the mean duration of any single rest period is $1/k_2$.

Up to this point, the notation $(x; n)$, $(i; x)$, $(t; n)$, and so on, prefixed by p, f, or F, has been used to denote various probability functions. The first term in the parentheses denotes the variable with respect to which probability is distributed. The second term, following the semicolon, specifies a qualifying condition. For example, $p(n; t)$ denotes the probability that E will occur exactly n times during the specified time interval $(0, t)$ following release from the source. Likewise, $f(x; n)$ denotes the probability density for the total distance, x, moved by the particle at the completion of the nth step. In the development that follows, it is convenient to use different notations to express the same probability functions. Usage of the concept of conditional probability requires that the symbol $f(x; n)$ be replaced by $f(x|n)$, which denotes the conditional probability density for the total distance moved given that the particle has taken n steps. Also, the symbol $p(n; t)$ is replaced by $p_t(n)$. In the subscript system of notation, the qualifying condition is denoted by the subscript instead of by the term following the semicolon.

As a tracer particle moves downstream in discrete steps, each rest period is followed by a step which in turn is followed by another rest period, and so on. Therefore, on the assumption that the particle is initially at rest and begins its first rest period at $t=0$, during any given rest period the particle must have undergone the same number of complete rest periods as steps; hence, a particle that has taken n steps will have also undergone n rest periods.

Use of the concept of conditional probability enables derivation of the density function $f_t(x)$, from which the probability of the location of the tracer particle in any length increment $(x+dx)$ at time t, can be obtained. To this end it is convenient to express equation 5 in the form of a conditional probability-distribution function as follows:

$$F(x|n)=\int_0^x f(x'|n)dx'=P[x'\leq x|i=n] \tag{5a}$$

where

P denotes probability
x' = a dummy variable of integration.

If one considers the two events A' and B', the conditional probability that A' will occur given that B' has occurred is defined as

$$P[A'|B']=\frac{P[A', B']}{P[B']}$$

where $[A', B']$ represents the joint occurrence of A' and B'. Applying this definition,

$$F_t(x|n)=P_t[x'\leq x|i=n]=\frac{P_t[x'\leq x, i=n]}{P_t[i=n]}$$

$$=\frac{P_t[x'\leq x, i=n]}{p_t(n)}, \qquad 0<t<\infty.$$

When n is given, knowledge of t adds no information; hence,

$$F_t(x|n)=F(x|n)$$

and

$$P_t[x'\leq x, i=n]=F(x|n)\,p_t(n). \tag{8}$$

The marginal distribution function in x corresponding to the joint probability function in equation 8 is

$$F_t(x)=\sum_{n=0}^{\infty} P_t[x'\leq x, i=n]=\sum_{n=0}^{\infty} F(x|n)\,p_t(n)$$

$$=\sum_{n=1}^{\infty} F(x|n)\,p_t(n)+F(x|0)\,p_t(0). \tag{9}$$

Differentiation of equation 9 with respect to x yields the density function for x at time t

$$f_t(x)=\frac{\partial}{\partial x}[F_t(x)]=\sum_{n=1}^{\infty} f(x|n)\,p_t(n)+p_t(0)\frac{\partial}{\partial x}[F(x|0)].$$

Introducing into this equation

$$f(x|n)=f(x; n)=k_1 e^{-k_1 x}\frac{(k_1 x)^{n-1}}{\Gamma(n)} \tag{5}$$

$$\left.\begin{aligned} p_t(n)&=p(n; t)=\frac{e^{-k_2 t}(k_2 t)^n}{n!}\\ p_t(0)&=p(0; t)=e^{-k_2 t}\\ F(x|0)&=1, \end{aligned}\right\} \tag{6}$$

the density function for x at time t can be written

$$f_t(x)=k_1 e^{-(k_1 x+k_2 t)}\sum_{n=1}^{\infty}\frac{(k_1 x)^{n-1}}{\Gamma(n)}\frac{(k_2 t)^n}{n!}, \qquad x>0, \tag{10}$$

which transforms readily into

$$f_t(x)=k_1 e^{-(k_1 x+k_2 t)}\sqrt{\frac{k_2 t}{k_1 x}}\,I_1(2\sqrt{k_1 x k_2 t}), \qquad x>0, \tag{10a}$$

where $I_1(2\sqrt{k_1 x k_2 t})$ is a modified Bessel function of the first kind of order one. Values of this Bessel function are given in tabular form in many mathematics reference books, such as that of Korn and Korn (1961).

Equations 10 and 10a were first derived by Einstein (1937).

It should be noted that the integral of the density function in equations 10 and 10a over the entire range of x is

$$\int_0^\infty f_t(x)dx = 1 - e^{-k_2 t} = 1 - p_t(0)$$

where $p_t(0)$ is the probability that the particle has not yet moved from the origin at time t. Thus the density function $f_t(x)$ applies only to particles that have taken at least one initial step.

If, as assumed initially, a very large number of tracer particles that are initially distributed uniformly in a plane extending throughout the zone of movement at $x=0$ all begin their first rest period at $t=0$, the density function, $f_t(x)$, as defined by equations 10 and 10a can be used to estimate the concentration $\phi(x, t)$ of tracer particles in the bed at any distance, x, downstream from the source at time t. In fact, $\phi(x, t)$ will be directly proportional to $f_t(x)$ if the following conditions are satisfied: (1) The average depth to which the tracer particles are distributed remains constant downstream from the source; (2) the concentration of tracer particles does not, on the average, vary with depth below the bed surface; (3) at any given instant, no significant fraction of the tracer particles are in suspension. Given these conditions, if the concentration of tracer particles is defined as the weight of tracer particles per unit volume of bed material, the concentration is

$$\phi(x, t) = \frac{W}{Bd} f_t(x)$$

where

W = the total weight of tracer particles placed in the channel
B = the width of the channel
d = the average depth beneath the bed surface to which the tracer particles are distributed.

Thus, the concentration-distribution function at time t for tracer particles that have moved from the origin where they began their first rest period at $t=0$ is

$$\phi(x, t) = \frac{Wk_1}{Bd} e^{-(k_1 x + k_2 t)} \sum_{n=1}^{\infty} \frac{(k_1 x)^{n-1}}{\Gamma(n)} \frac{(k_2 t)^n}{n!} \tag{11}$$

or

$$\phi(x, t) = \frac{Wk_1}{Bd} e^{-(k_1 x + k_2 t)} \sqrt{\frac{k_2 t}{k_1 x}} I_1(2\sqrt{k_1 x k_2 t}). \tag{11a}$$

Either of these forms of the concentration-distribution function can be used to compute the concentration of tracer particles in the bed at any distance downstream from the source at any given time after release; however, computation is considerably easier with the second form. Computation of concentrations is facilitated still further by writing equation 11a in the form

$$\phi(x, t) = \frac{Wk_1}{Bd} e^{-(\sqrt{k_1 x} - \sqrt{k_2 t})^2} \sqrt{\frac{k_2 t}{k_1 x}} [e^{-z} I_1(z)] \tag{11b}$$

where $z = 2\sqrt{k_1 x k_2 t}$.

Significant properties of the concentration-distribution function with respect to x for a given t are as follows:

Area under the distribution curve:

$$A = \int_0^\infty \phi(x, t)dx = \frac{W}{Bd}(1 - e^{-k_2 t})$$

Mean:

$$\bar{x} = \frac{k_2 t}{k_1}$$

Mean rate of movement of tracer particles:

$$\frac{d\bar{x}}{dt} = \frac{k_2}{k_1}$$

Variance:

$$\sigma_x^2 = \frac{2k_2 t}{k_1^2} = \frac{2\bar{x}}{k_1}$$

Mode:

$x_m = x$ evaluated when $\frac{\partial f_t(x)}{\partial x} = 0$, in which case

$$\frac{k_1 x}{k_2 t} = \left\{\frac{I_2(2\sqrt{k_1 x k_2 t})}{I_1(2\sqrt{k_1 x k_2 t})}\right\}^2$$

where $I_2(2\sqrt{k_1 x k_2 t})$ is a modified Bessel function of the first kind of order two.

RELATED DISTRIBUTION FUNCTIONS

If a tracer particle is introduced into the channel at $x=0$ in such a way that it takes its first step at time $t=0$, then during any given rest period the number of rest periods it will have completed will be one less than the number of steps. Equation 9 then becomes

$$F_t^*(x) = \sum_{n=1}^{\infty} F(x|n) p_t(n-1) \tag{12}$$

where the asterisk denotes the initial condition of beginning with motion. Likewise equations 10 and 10a become

$$f_t^*(x) = k_1 e^{-(k_1 x + k_2 t)} \sum_{n=1}^{\infty} \frac{(k_1 x)^{n-1}}{\Gamma(n)} \frac{(k_2 t)^{n-1}}{(n-1)!} \tag{13}$$

and

$$f_t^*(x) = k_1 e^{-(k_1 x + k_2 t)} I_0(2\sqrt{k_1 x k_2 t}) \tag{13a}$$

where $I_0(2\sqrt{k_1 x k_2 t})$ is a modified Bessel function of the first kind of order zero. As were equations 10 and 10a, equations 13 and 13a were first derived by Einstein (1937).

In a manner analogous to that which was used to obtain the concentration-distribution function, $\phi(x,t)$, which specifies the concentration of tracer particles in the bed at any distance x and any time t, a discharge-distribution function, $\psi(t,x)$, which specifies the discharge of tracer particles past a cross section at any distance x downstream from the source at any time t, can be obtained from the density function $f_x(t)$. A tracer particle that begins its first rest period at the origin at $t=0$ will, as it passes a point a distance x downstream from the origin, have completed one less step than rest periods. Thus, the probability density $f_x(t)$, which relates to the probability that the particle will pass the point x during the time interval $(t, t+dt)$, corresponds to $f_t^*(x)$, except that the variables x and t and the constants k_1 and k_2 are interchanged so that

$$f_x(t)=k_2e^{-(k_1x+k_2t)}\sum_{n=1}^{\infty}\frac{(k_2t)^{n-1}}{\Gamma(n)}\frac{(k_1x)^{n-1}}{(n-1)!} \tag{14}$$

or

$$f_x(t)=k_2e^{-(k_1x+k_2t)}I_0(2\sqrt{k_1xk_2t}). \tag{14a}$$

If a large number of tracer particles are placed in the channel, again as a uniformly distributed plane source at $x=0$, and all the particles begin their first rest period at $t=0$, the estimated discharge $\psi(t,x)$ of tracer particles in weight per unit time per unit of cross-sectional area is proportional to $f_x(t)$, where W/Bd is again the constant of proportionality. The discharge-distribution function is

$$\psi(t,x)=\frac{Wk_2}{Bd}e^{-(k_1x+k_2t)}\sum_{n=1}^{\infty}\frac{(k_2t)^{n-1}}{\Gamma(n)}\frac{(k_1x)^{n-1}}{(n-1)!} \tag{15}$$

or

$$\psi(t,x)=\frac{Wk_2}{Bd}e^{-(k_1x+k_2t)}I_0(2\sqrt{k_1xk_2t}). \tag{15a}$$

APPLICATION OF CONCENTRATION-DISTRIBUTION FUNCTION TO EXPERIMENTAL DATA

To use the theoretically derived concentration-distribution function, the constants k_1 and k_2 must be evaluated. Presumably, values for these constants are related to various hydraulic and sediment factors; however, until the nature of the relations is known, the constants must be determined from observed distributions. To make the determinations, certain characteristics of the observed and theoretical distributions are equated. These characteristics are the time rate of movement of the mode (peak) along the channel and the time rate of attenuation of the peak relative concentration, per foot of width; relative concentration is defined as the ratio of concentration at a point to the area under the concentration-distribution curve. Experimental data related to these rates are listed in table 4.

TABLE 4.—*Some characteristics of the observed distributions*

Run	Time after dosing (hr) [1]	Distance from source (ft)		Peak concentration (g per cu ft)	Area under concentration-distribution curve (g per sq ft)	Peak relative concentration per foot of width
		Mean	Mode			
2 R	22.3	131	107	2.28	249	0.0092
2 L	21.2	115	73	3.26	238	.0137
3 R	44.2	244	182	1.14	236	.0048
3 L	45.8	213	172	1.22	204	.0060
4 R	70.9	354	270	.76	228	.0033
4 L	73.9	336	275	.98	194	.0051
5 R	96.2	458	347	.66	213	.0031
5 L	98.3	406	363	.59	[2] 179	.0033
6 R	117.7	491	410	.56	217	.0026
6 L	120.4	499	388	.45	[2] 170	.0026
7 C	142.2	547	475	.44	[2] 197	.0022
8 R	170.1	635	510	.43	[2] 199	.0022
8 L	171.8	670	550	.30	[2] 168	.0018
11 R	241.6	835	801	.32	[2] 166	.0019
12 R	287.4	930	869	.25	[2] 162	.0015

[1] Dispersion time.
[2] Based on a distribution adjusted to eliminate the influence of the delayed release of buried tracer particles (see figs. 34–40).

According to the theory, the rate of movement of the mode is

$$\frac{dx_m}{dt}\approx\frac{k_2}{k_1} \tag{16}$$

for $k_2t\geq$ about 4. In figure 31, the position of the modes of the observed distributions are plotted as a function of the dispersion time. The slope of the straight part of the line that defines the rate of movement of the mode is

$$\frac{dx_m}{dt}=3.00\text{ ft per hr}\approx\frac{k_2}{k_1}.$$

According to the theoretical concentration-distribution function the peak relative concentration is given by

$$\frac{\phi(x,t)_{\max.}}{A}=\frac{\phi(x,t)_{\max.}}{\frac{W}{Bd}(1-e^{-k_2t})}=\frac{f_t(x)_{\max.}}{(1-e^{-k_2t})} \tag{17}$$

where $f_t(x)_{\max.}$ is equal to $f_t(x)$ evaluated for the condition

$$\frac{k_1x}{k_2t}=\left\{\frac{I_2(2\sqrt{k_1xk_2t})}{I_1(2\sqrt{k_1xk_2t})}\right\}^2.$$

As the dispersion time increases the probability that a particle is still at the origin, $p_t(0)=e^{-k_2t}$, approaches zero so that for $k_2t\geq$ about 3

$$\frac{\phi(x,t)_{\max.}}{A}\approx f_t(x)_{\max.} \tag{17a}$$

In figure 32, the values of the observed peak relative concentration, $\phi_{\max.}/A$, are plotted on logarithmic coordinates as a function of the dispersion time. In figure 33 the ratio of the theoretical peak relative concentration (as given in eq 17a) to k_1 is plotted, also on logarithmic coordinates, as a function of k_2t. Because the respective abscissas and ordinates of figures 32 and 33 differ only by the constants of proportionality k_1

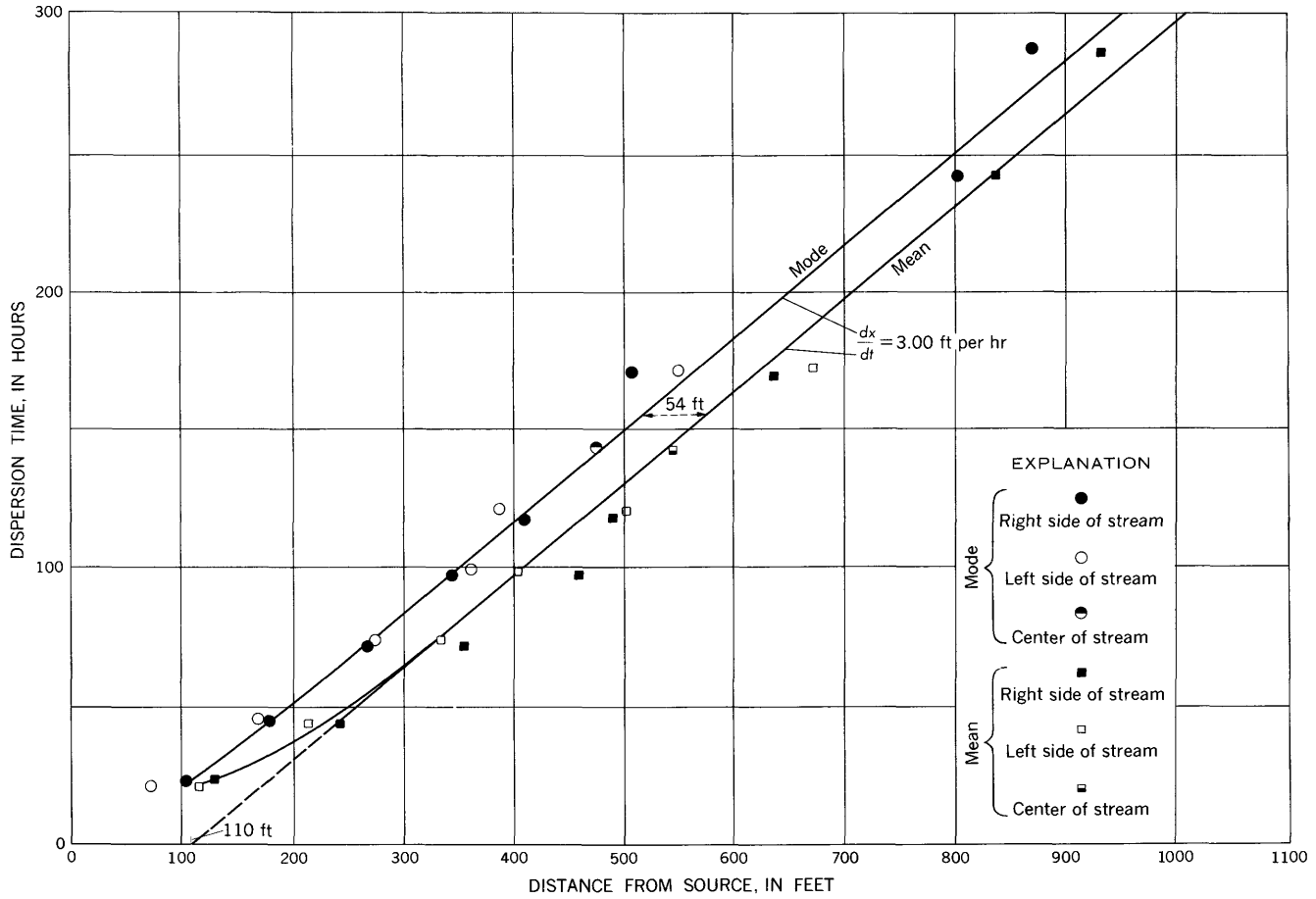

FIGURE 31.—Location of mode and mean as a function of dispersion time.

and k_2, these constants may be evaluated by superimposing figure 32 over figure 33 in the position where (1) the experimental data best fits the theoretical curve, and (2) k_2/k_1 equals 3.00 feet per hour. When the data are superimposed over the theoretical curve in this position,

$$k_1=\frac{\phi_{max.}/A}{\frac{1}{k_1}f_i(x)_{max.}}=\frac{1}{36}\,\text{ft}^{-1}$$

and

$$k_2=\frac{k_2 t}{t}=\frac{1}{12}\,\text{hr}^{-1}.$$

The theoretical attenuation curve for these values of k_1 and k_2 is shown in figure 32. Because the data for runs 3R, 4R, 5R, 6R, and 7C are considered to be the most reliable, the points representing these runs were weighted accordingly in fitting the data. In both figures 31 and 32, values for the points representing the mode in runs 5L, 6L, 7C, 8R, 8L, 11R, and 12R were obtained from modifications of the distribution curves. The curves were modified by substituting estimated curves for the parts that reflected the dispersion of the particles that were buried initially on the left side of the stream.

Theoretically derived distribution curves for times equal to those for the observed distributions were determined from equation 11 and the computed values for k_1 and k_2. It is significant to note that in figure 31 the extension of the straight line part of the curve that defines the rate of movement of the mean does not pass through the origin but intersects the x axis at $x=110$ feet. The displacement of the curve from the origin at zero dispersion time is a major discrepancy, for the mean of the derived distribution function varies directly with the time and should be zero when the dispersion time is zero. To compute theoretical distribution curves that coincided well at the modes with the observed distributions, the origin of the theoretical distribution curves had to be displaced to $x=110$ feet. This procedure seemed to be justified because for dispersion times greater than about 70 hours the mean preceded the mode (see fig. 31) approximately by the distance $\frac{1.5}{k_1}$ (54 ft), which is in accordance with the characteristics of the derived distribution function. The theoretical curves, along with the corresponding observed distribution curves, are shown in figures 34–40. The crosshatched areas under the measured

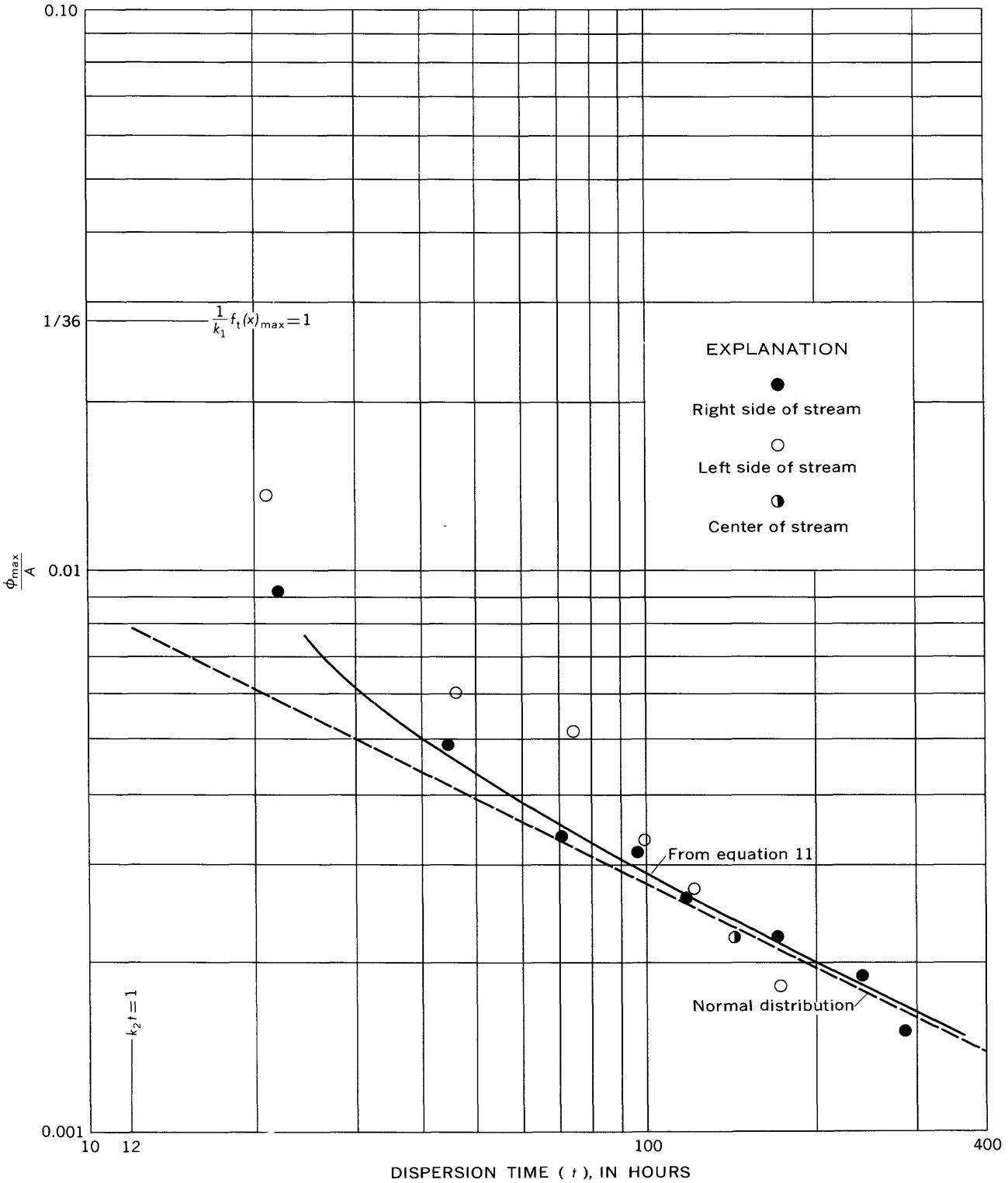

FIGURE 32.—Attenuation of observed peak relative concentration with dispersion time.

curves in figures 36–40 represent estimates of the increase in area under the distribution curve that resulted from the delayed release of tracer particles that had been buried on the left side of the stream near the upstream end of the test reach. Distribution curves are not shown for run 9, because the observed distribution curves span only the first 400 feet of the test reach, and for runs 10L, 10R, 11L, and 12L, because the areas under the observed distribution curves that resulted from the delayed release of buried tracer

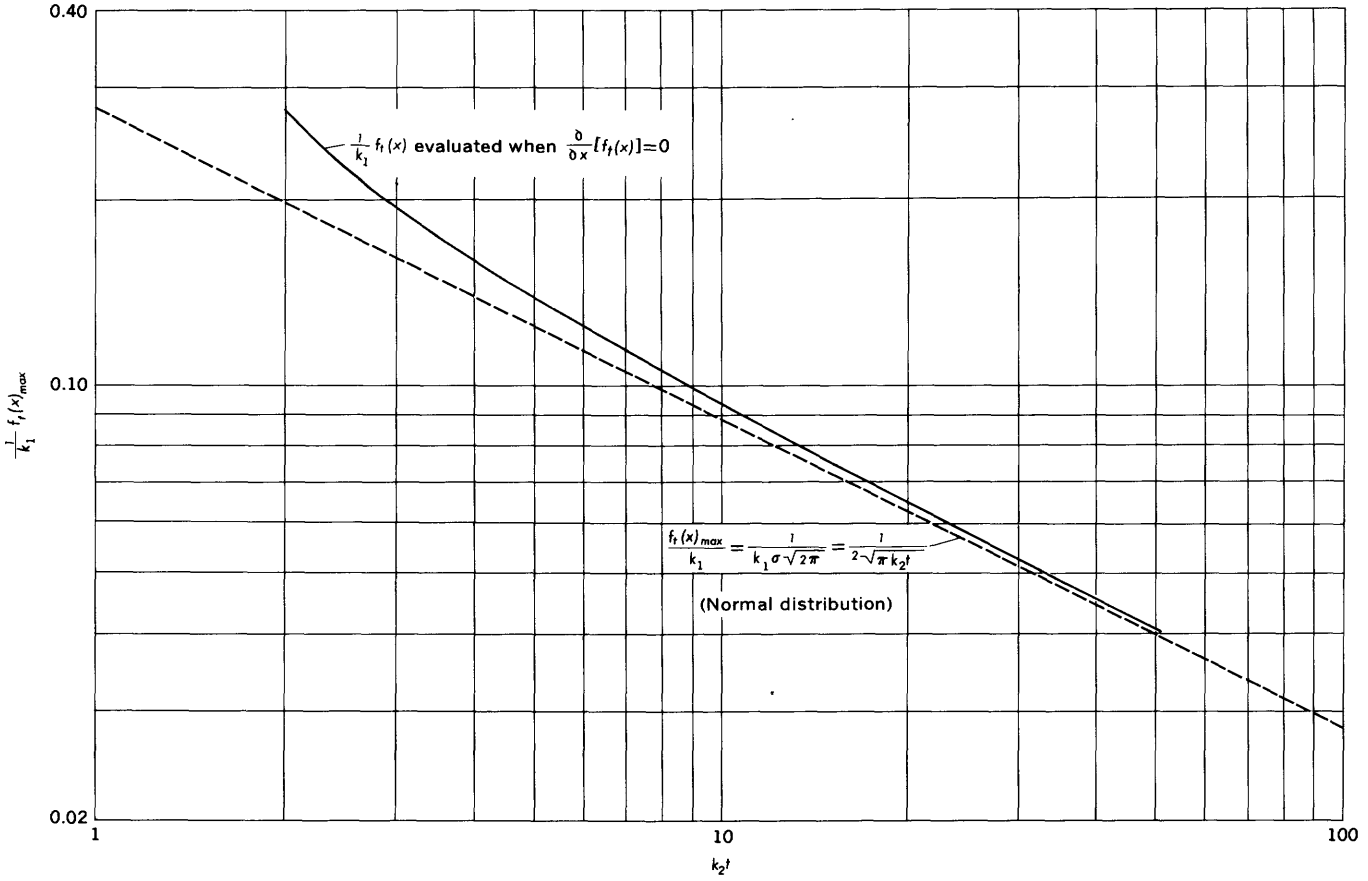

FIGURE 33.—Attenuation of peak according to theoretical function.

particles could not be isolated with confidence from the residual areas. Also, no distribution curves are shown for runs 2R and 2L. This is because the theoretical concentration-distribution function is not applicable to the conditions of the experiment for values of k_2t less than 2. In the range $0<k_2t<2$, the peak of the theoretical distribution curve coincides with the origin where concentration is not defined.

In general, the theoretical and observed distribution curves agree fairly well and exhibit the same characteristics throughout almost the full range of dispersion times. At small dispersion times both sets of distribution curves are markedly skewed in the upstream direction. As the dispersion time increases, they tend to become symmetrical at approximately the same rate. In addition, the rates of attenuation of the peak concentrations with respect to time in both sets of curves are similar and approach the attenuation rate of the normal distribution (see figs. 32 and 33).[3] In some respects, however, the theoretical and observed distribution curves do not agree. One difference is the way in which the concentrations decrease downstream from the peak; the observed concentrations decrease more rapidly immediately downstream from the peak and less rapidly at the tail than do the theoretical concentrations. Another difference is the displacement of the origin of the theoretical distribution curves downstream from the actual source ($x=0$); this is particularly evident in the early runs. Both of these differences can be traced to discrepancies between certain physical features of the experiment and the corresponding assumptions and (or) hypotheses on which the theoretical distribution is based.

Probably the most significant discrepancy is that the theory applies only to a group of tracer particles that have identical transport characteristics, whereas the size (therefore the transport characteristics) of the tracer particles actually used in the experiment varied over a range. Thus, because each set of transport characteristics has a corresponding distribution function, the observed distribution curves are actually the resultant summations of many separate distribution functions, each of which is associated with a different particle size. The size distribution of the tracer particles indicates that at least 80 percent of the particles could have been transported in suspension at one time or another. This factor undoubtedly contributed to the long tails of the observed distribution curves.

[3] Although for large t the distribution function $f_t(x)$ exhibits similar geometric characteristics, it does not in a rigorous sense converge to a normal distribution.

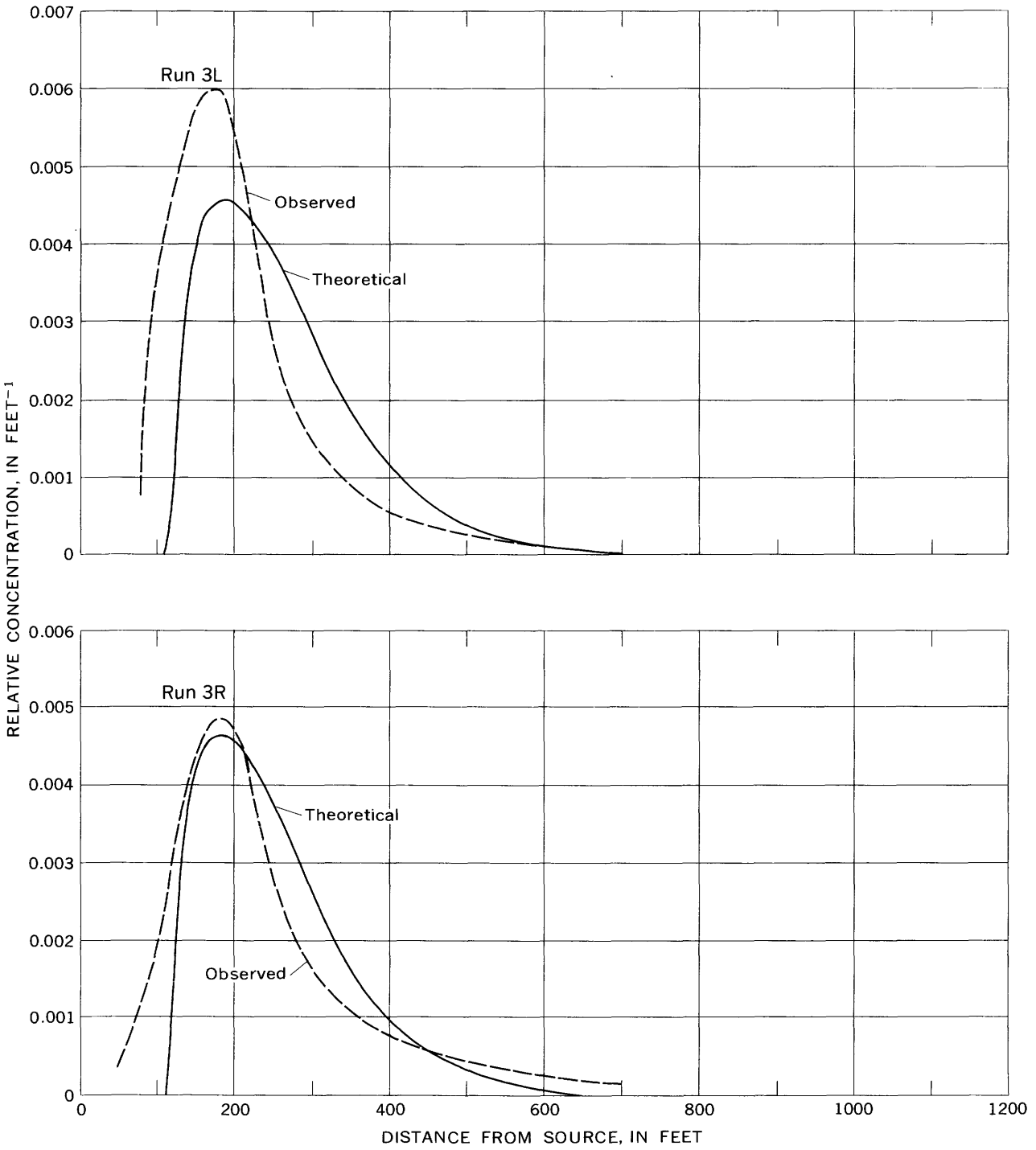

FIGURE 34.—Theoretical and observed longitudinal distribution of tracer particles, runs 3R and 3L.

This conclusion is supported by the results of a similar experiment reported by Lean and Crickmore (1960). In their experiment, the tracer particles were composed of a representative sample of the bed material, which included a fairly wide range of particle sizes. For comparable dispersion times, the distribution curves resulting from their experiment had tails in the downstream direction that are much more pronounced.

The other major discrepancy between the actual experimental conditions and the requirements of the theory concerns the source. The theory requires that the tracer particles be released from a uniformly concentrated plane source extending from the surface of the bed to the lower limit of the zone of particle movement and covering the width of the channel. However, in the experiment the source consisted of a series of

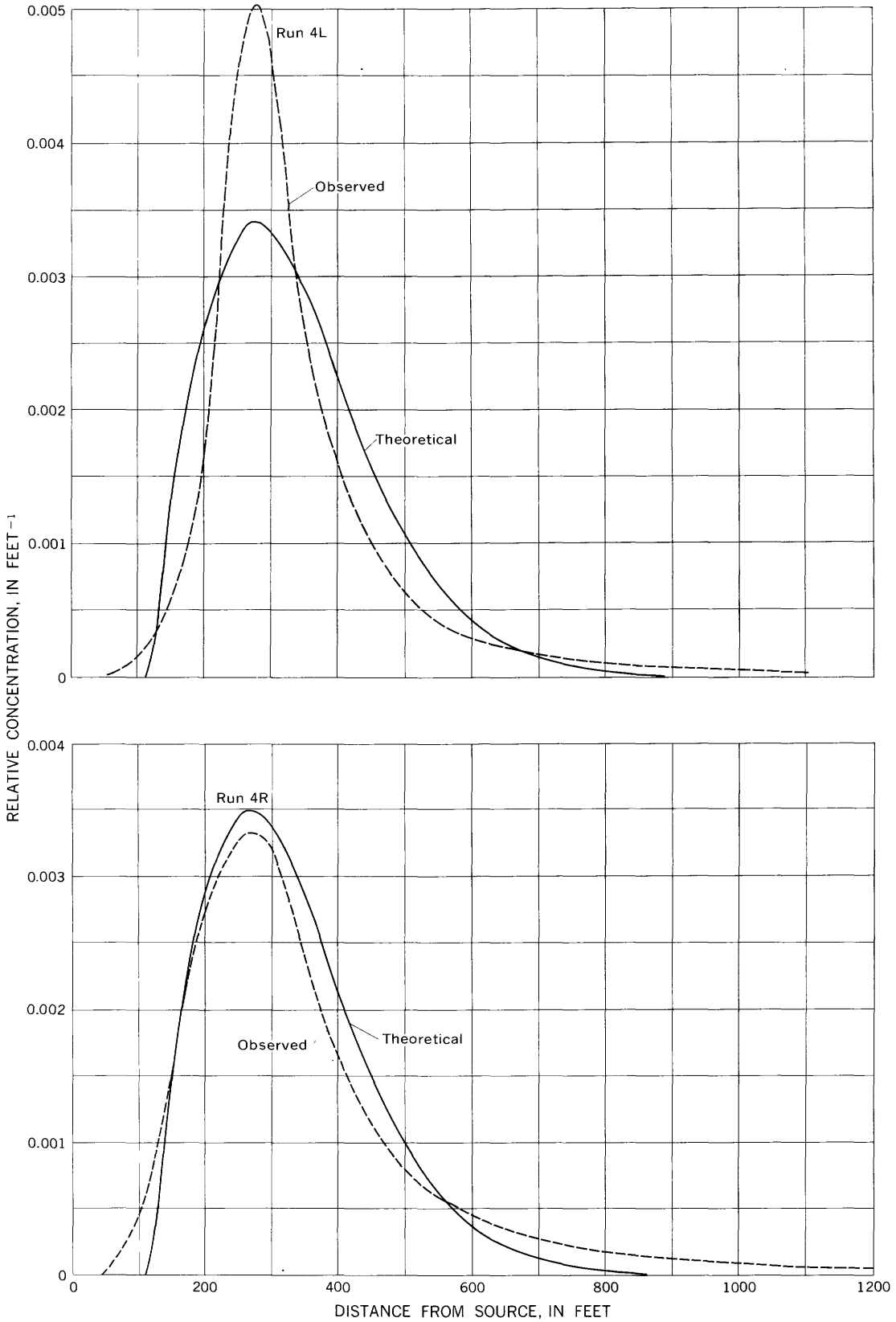

FIGURE 35.—Theoretical and observed longitudinal distribution of tracer particles, runs 4R and 4L.

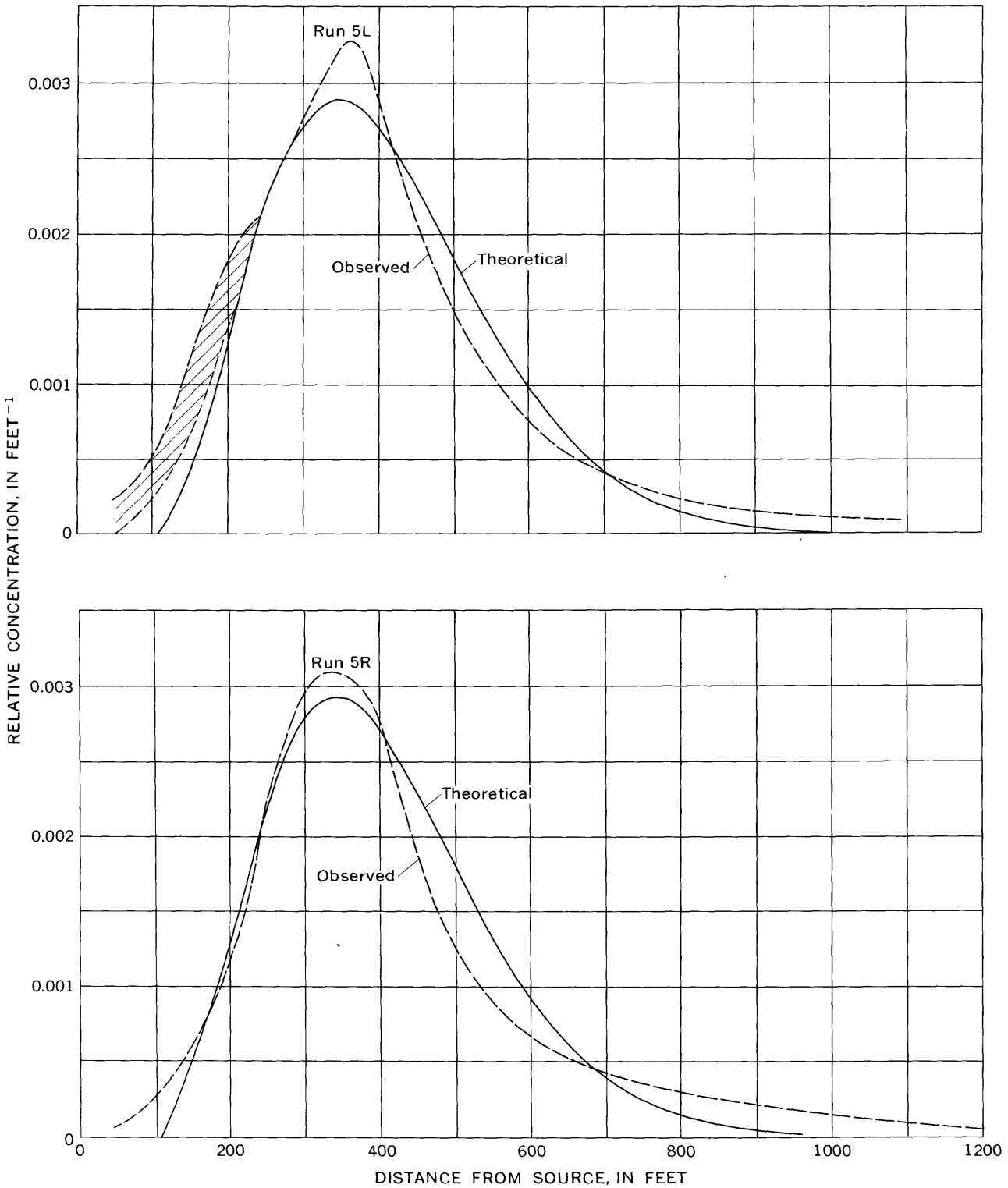

FIGURE 36.—Theoretical and observed longitudinal distribution of tracer particles, runs 5R and 5L. Crosshatching denotes estimated increase in area under distribution curve due to delayed release of buried tracer particles.

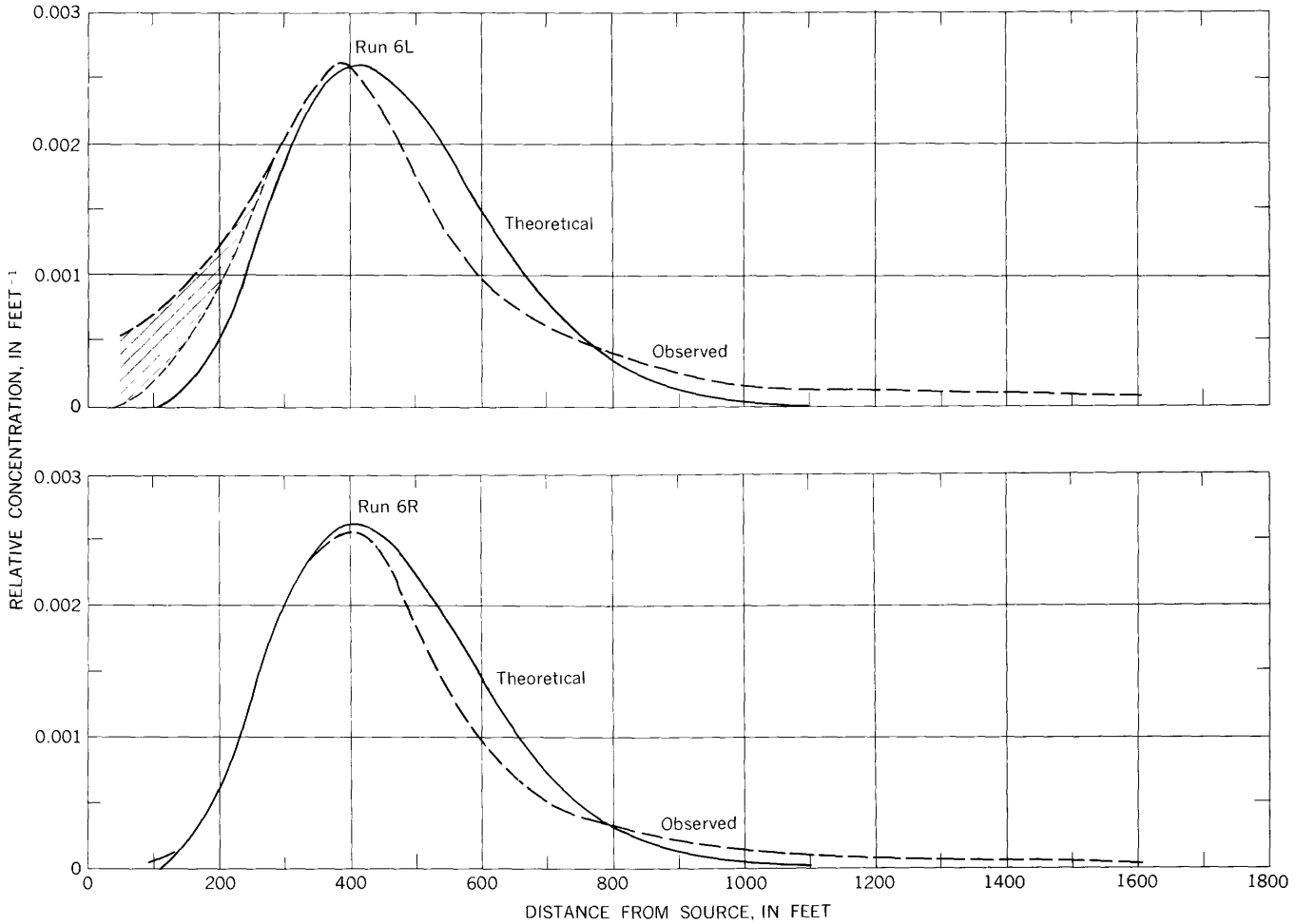

FIGURE 37.—Theoretical and observed longitudinal distribution of tracer particles, runs 6R and 6L. Crosshatching denotes estimated increase in area under distribution curve due to delayed release of buried tracer particles.

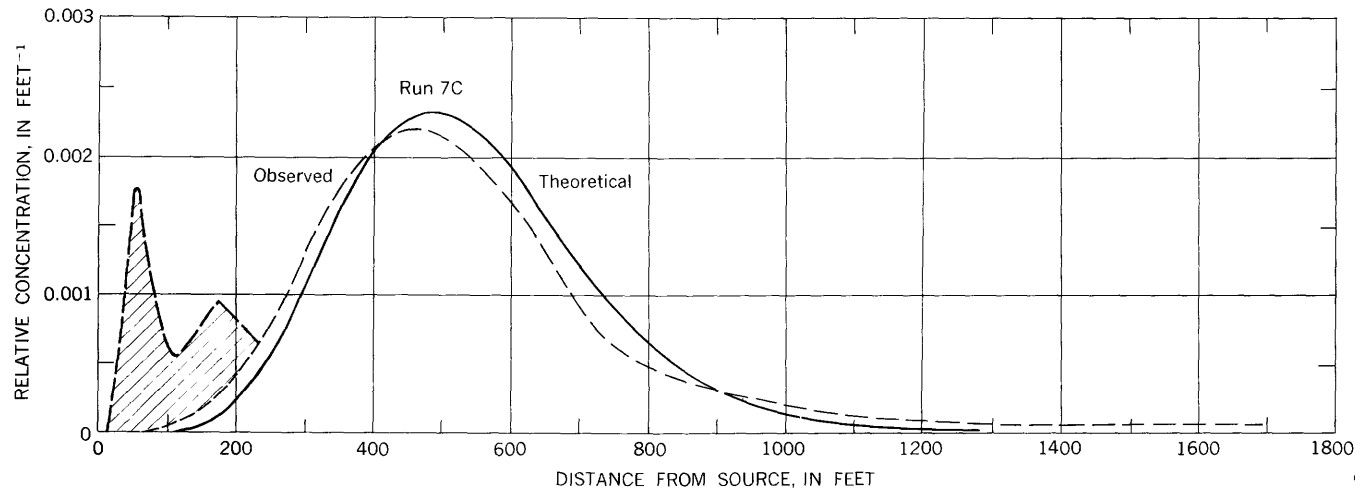

FIGURE 38.—Theoretical and observed longitudinal distribution of tracer particles, run 7C. Crosshatching denotes estimated increase in area under distribution curve due to delayed release of buried tracer particles.

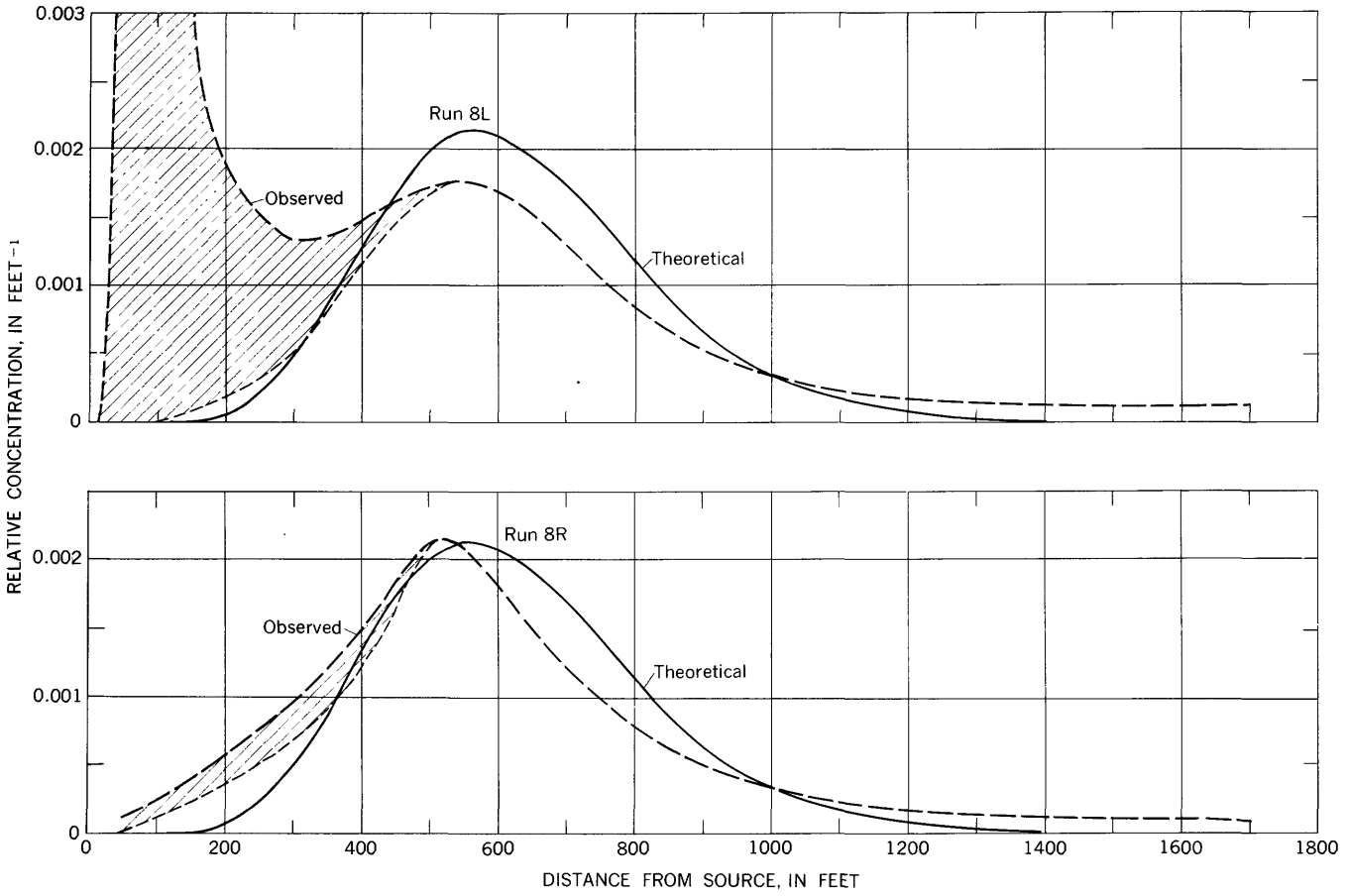

FIGURE 39.—Thecretical and observed longitudinal distribution of tracer particles, runs 8R and 8L. Crosshatching denotes estimated increase in area under distribution curve due to delayed release of buried tracer particles.

point sources, on the surface of the bed, extending across the channel. Undoubtedly, an initial mixing period was required for the tracer particles to become dispersed uniformly throughout the zone of particle movement. During this mixing period the quantity of tracer particles available for transport and dispersion at any given time was probably greater than it would have been had the tracer particles initially been distributed uniformly with respect to depth. This is probably one reason why the origins of the theoretical and observed curves do not coincide (see fig. 31). The fact that the rate of movement of the mean tended to decrease and become constant after about 70 hours may also have been partly caused by a fairly rapid passage of the finer tracer particles through and out of the test reach.

A third way in which the observed distribution data differed from the theory was that the area under the observed distribution curves tended to decrease as the dispersion time increased. The total reduction in the area under the curves during the 13-day period of the experiment was about 35 percent of the area that was observed 1 day after the release of the tracer particles. The rate of decrease is roughly linear. In the analysis, the decrease in area was compensated for by expressing the concentration of tracer particles in terms of relative concentration, ϕ/A. Probably, the major factor contributing to the reduction in area was the removal of some of the radioactive label from the tracer particles by abrasion. Another contributing factor may have been that a significant quantity of the finer tracer particles passed through and out of the test reach during the course of the experiment.

In summary, the observed distribution curves are approximated reasonably well by curves that are based on the theoretical distribution function. Probably, the major differences between the observed and theoretical distributions can be attributed to discrepancies between certain physical features of the experiment and the corresponding assumptions on which the theory is based. In addition, because the constants, k_1 and k_2, were determined by a forced match between observed data and a theoretical curve, their values are empirical and are not necessarily theoretically significant.

BED-MATERIAL TRANSPORT

Most existing measurement techniques and theories for determining bed-material discharge are directed

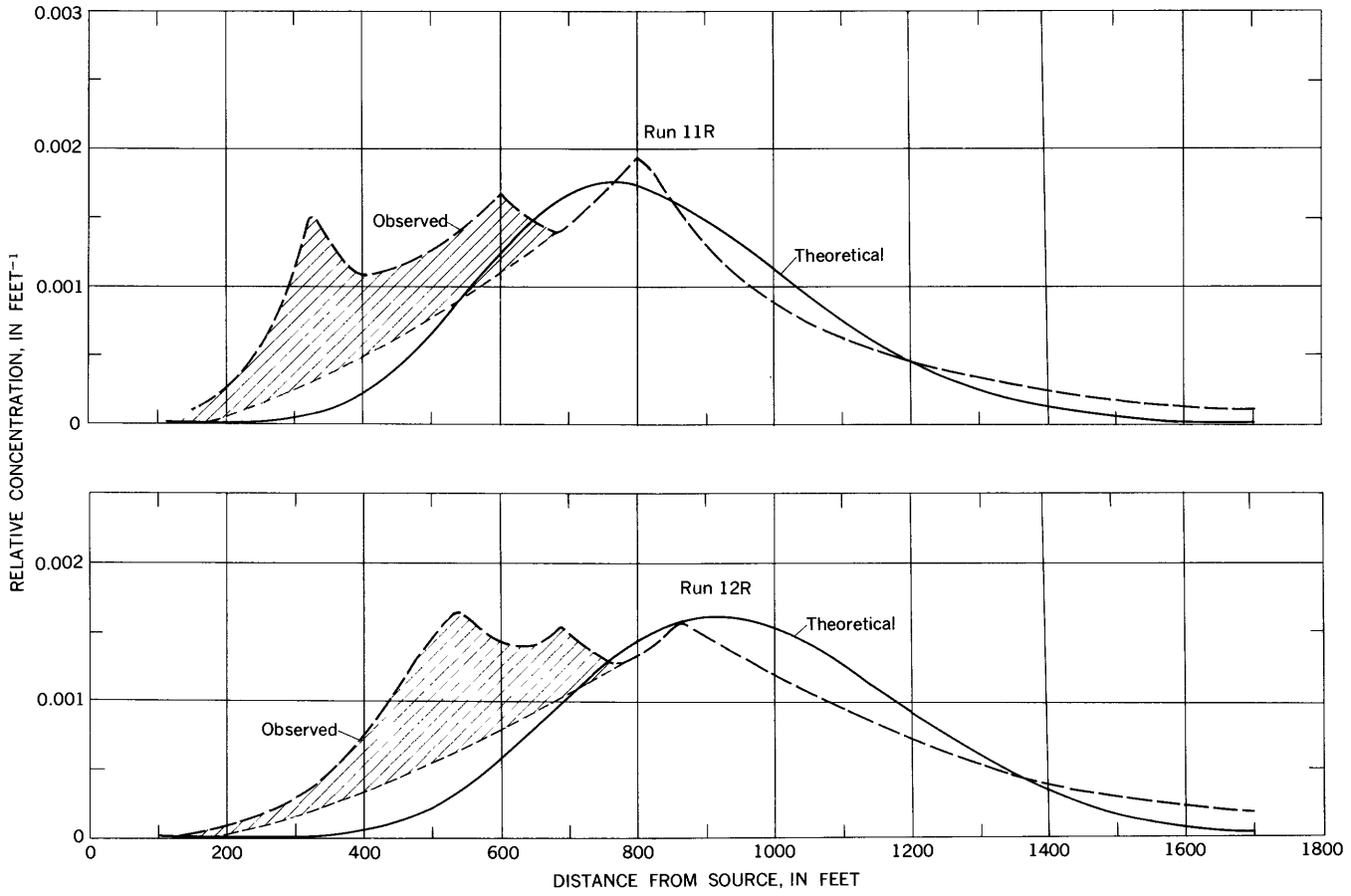

FIGURE 40.—Theoretical and observed longitudinal distribution of tracer particles, runs 11R and 12R. Crosshatching denotes estimated increase in area under distribution curve due to delayed release of buried tracer particles.

toward evaluating the flux of sediment particles past a stationary cross section. With the recent advent of radioactive-tracer and other methods for utilizing labeled sediment particles, a new approach has become feasible. The new approach is based on the determination of how the position of a particular group of tagged bed-material particles varies with time. Consider, within the framework of the same restrictions that were assumed in the derivation of the theoretical concentration-distribution function, a group of tracer particles released from a plane source in the bed of a channel. Assume now, however, that the transport characteristics of the tracer particles simulate those of the bed material. As the tracer particles move downstream they disperse so that at any time, t, after release they are distributed about some mean distance from the source, $\bar{x}$. Hence, the ratio, $\bar{x}/t$, defines the mean velocity of the bed-material particles in the downstream direction. Correspondingly, the bed-material discharge, Q_s, in weight per unit time is

$$Q_s=\gamma_s(1-\lambda)Bd\frac{\bar{x}}{t}=\gamma_s(1-\lambda)\frac{W}{A}\frac{\bar{x}}{t} \tag{18}$$

where

λ=the fraction of volume of bed material, in place, not occupied by particles (porosity)

γ_s=the specific weight of the bed material.

If all the bed-material particles have virtually the same transport characteristics, the tracer particles will be distributed according to equation 11 and k_2/k_1 may be substituted for $\bar{x}/t$ in equation 18. If the tracer particles are selected to simulate only bed-material particles possessing a certain characteristic such as the same size, shape, or specific gravity, the discharge of such particles $(Q_s)_c$ is

$$(Q_s)_c=i_c(\gamma_s)_c(1-\lambda)Bd\left(\frac{\bar{x}}{t}\right)_c$$
$$=i_c(\gamma_s)_c(1-\lambda)\left(\frac{W}{A}\right)_c\left(\frac{\bar{x}}{t}\right)_c \tag{19}$$

where

i_c=the ratio of the volume of particles possessing the characteristic to the volume of bed-material particles in the zone of particle movement

c= a subscript that denotes terms associated with the particles possessing the characteristic.

Although both equations 18 and 19 have the form of a continuity equation, the concept of continuity applies only in a statistical sense. Actually, particles move only when they are exposed on the surface of the bed or when they are in suspension. The particles move in a series of discrete steps and are buried in the bed, for varying periods of time, between the steps. Thus, the mean particle velocity, $\bar{x}/t$, represents the average rate of movement during a total elapsed time. The use of the cross-sectional area, Bd, as the zone of movement is based on the assumption that each observed distribution is representative of the true distribution of the tracer particles at some given instant regardless of whether or not all the particles actually moved through Bd and whether or not some of the particles were in movement (either as bedload or as suspended load) during the time of the distribution observation. This assumption seems quite reasonable because the rate of change of the distribution curves is low and the time required to observe each distribution is short.

Equations 18 and 19 are similar to the bed-material transport equations derived by Lean and Crickmore (1960). However, in their analysis, Lean and Crickmore devoted considerable attention to establishing the local flux of tracer particles as a function of vertical position within the bed.

In the experiment, the following conditions were either known or determined experimentally:

$i_c = 0.65$ (fraction of the bed material within the approximate size range of the tracer particles, which is 0.225–0.420 mm)

$\gamma_s(1-\lambda) = 100$ lb per cu ft $= 0.05$ ton per cu ft

$W = 40$ lb $= 18{,}200$ g

$A = 249$ g per sq ft

$\bar{x}/t = \frac{d\bar{x}}{dt} = 3$ ft per hr $= 72$ ft per day.

The value of $(Q_s)_c$ for these conditions, as computed with equation 19, is 171 tons per day. Unfortunately, this value cannot be compared with a measured discharge to ascertain its accuracy because, at the present time, available equipment is not capable of measuring the sediment discharge on or very near the streambed. However, it can be compared with a discharge computed according to some reliable method. Of available methods for determining bed-material discharge in the North Loup River, the modified Einstein procedure (Colby and Hembree, 1955) is probably the most reliable. The procedure was developed with data from Nebraska sandhill streams, and its accuracy and applicability have been verified (Colby and Hembree, 1955; Hubbell and Matejka, 1959).

The value of $(Q_s)_c$ as computed with the modified Einstein procedure for the 65 percent of the bed material that is in the 0.225–0.420 mm size range is 192 tons per day. (Data from tables 2 and 3 for Nov. 9, 12, and 16 were used in the computation.) The agreement between the values of $(Q_s)_c$ as computed by the two methods (171 tons per day vs. 192 tons per day) is remarkably good. Actually, the two methods should not give exactly the same values because the distribution of the tracer particles within the 0.225–0.420 mm size range differs from the distribution of the bed material in the same range (see fig. 5).

APPLICABILITY OF RESULTS

The theory and experiment discussed in the preceding sections are based on the idealized concept of an instantaneous source of contaminated particles that are distributed uniformly over a plane which extends laterally across the width of the stream and vertically from the surface of the bed to the lower limit of the zone of particle movement. Although such idealized source conditions exist rarely, if ever, in nature, the concentration-distribution function corresponding to an instantaneous plane source (eq 11) is of fundamental practical importance. This is because a concentration-distribution function corresponding to any defined source distribution in space and time can be obtained from the instantaneous plane source function by the technique of mathematical superposition (that is, the convolution integral). The above statement applies to the discharge-distribution function (eq 15) also.

Some examples of concentration-distribution functions corresponding to source distributions where the source strength varies with longitudinal distance and (or) time are listed below. In these examples, uniform concentration distributions in the lateral and vertical directions are assumed.

1. Instantaneous longitudinally distributed source of variable strength (weight per unit length), $S(\xi)$:

$$\phi(x, t) = \frac{1}{Bd}\int_0^s S(\xi) f_t(x-\xi, t)\, d\xi \qquad (20)$$

where

ξ = the distance downstream from $x=0$ along which the source is distributed over length s at time $t=0$, $(0 \le \xi \le s)$

$f_t(x-\xi, t)$ = the instantaneous plane source density function, $f_t(x)$ (eq 10), with x replaced by $x-\xi$.

2. Continuous plane source at $x=0$, discharging at a variable rate (weight per unit time), $S(\tau)$:

$$\phi(x, t) = \frac{1}{Bd}\int_0^{t_1} S(\tau) f_t(x, t-\tau)\, d\tau \qquad (21)$$

where

τ = the time after $t=0$ during which the source is discharging, $(0 \le \tau \le t_1)$

$f_t(x, t-\tau)$ = the instantaneous plane source density function (eq 10) with t replaced by $t-\tau$.

3. Continuous longitudinally distributed source of variable strength (weight per unit length), discharging at a variable rate (weight per unit time), $S(\xi, \tau)$:

$$\phi(x, t)=\frac{1}{Bd}\int_0^{t_1}\int_0^{s} S(\xi, \tau)f_t(x-\xi, t-\tau)d\xi d\tau \qquad (22)$$

where

$f_t(x-\xi, t-\tau)$ = the instantaneous plane source density function (eq 10) with x replaced by $x-\xi$, and t replaced by $t-\tau$.

By integrations such as these, an infinite variety of real situations can be approximated. In addition to longitudinal concentration-distribution curves, the instantaneous plane source density functions can be used, for example, to construct concentration-time curves, longitudinal discharge-distribution and discharge-time curves, and concentration- and discharge-growth and decay curves. The theoretical distribution functions also provide a means for making estimates such as the time of travel and reduction of maximum concentration of a slug of contaminated bed material as it travels from one location to another location farther downstream, the duration of contamination in excess of some specified level at a particular site, and the time required for the concentration of contaminated particles released from a continuous source to reach equilibrium as well as the equilibrium concentration.

One significant assumption in the development of the theoretical function was that a stream can be represented as a homogeneous probability field in space and time. Such an assumption will not be justified in many cases. However, by use of available knowledge of stream characteristics and flow patterns, it should be possible to break up most streams into reaches in which the assumption of homogeneity is an acceptable approximation for limited periods of time. This would be analogous to the procedure commonly used in calculating backwater curves in, or routing floods through, nonuniform channels.

Also, in the development of the theory, the effects of exchange of radionuclides among various phases of the transporting media were not considered. It was assumed that once a particle became contaminated by radionuclides it would remain so. However, use of the mathematical device of secondary sources and sinks should enable allowance for the effects of the exchange of radionuclides between the sediment, solution, or biota.

If it is assumed that the mathematical model on which the theoretical distribution functions are based approximates reality acceptably, the validity of any predictions based thereupon depends on the accuracy with which the different independent variables in the theoretical distribution functions can be estimated. In most practical situations, the amount and initial distribution of contaminated particles, the width of the stream, and the bulk specific gravity of the bed material can be determined readily. However, three other variables—the depth of the zone of particle movement (d) and the constants k_1 and k_2—need to be known.

When the bed configuration consists of dunes or ripples, the depth of the zone of particle movement, d, can be estimated from depth-sounding data. For this purpose continuous longitudinal profiles of the bed surface are required. The method for estimating d is illustrated in figure 41 and corresponds to the method presented by Hubbell (1964). The length of the reach for which d is to be determined is divided into sections. Starting from the upstream end, each section of length l_i extends from the dune trough at which the section begins to the first trough downstream that is deeper. After sectioning, a mean depth for each section, d_i, is determined, and the d for the total reach length, L, is computed as the weighted average of the d_i's for each section. Expressed mathematically (see fig. 41),

$$d=\frac{1}{L}\sum_{i=1}^{n} l_i d_i.$$

The reasoning behind this procedure is based upon the assumption that although the individual bed forms may change shape as they progress downstream, a statistical constancy of form exists over a long reach. Hence, quantitatively the particles subject to movement are those that would move if the entire profile were to progress downstream without changing form, and the depth of particle movement is defined by lines that are parallel to the mean bed surface and extend downstream from the deepest trough as illustrated.

On the basis of depth-sounding records obtained in the upstream half of the test reach during 10 of the runs, d was computed to be 1.41 feet. Because the tracer particles were tagged in the experiment, two additional independent estimates of d could be made. From the core-sample data in figures 25–29, the average depth beneath the bed surface to which the tracer particles were distributed was computed as 1.45 feet. From

$$d=\frac{W}{BA}$$

the average depth was computed as 1.46 feet for $W=40$ pounds, $B=50$ feet, and $A=250$ g per sq ft.

As previously mentioned, the constants k_1 and k_2 cannot be predicted until their relations to pertinent hydraulic and sediment parameters are established by further experiments. However, they can be determined

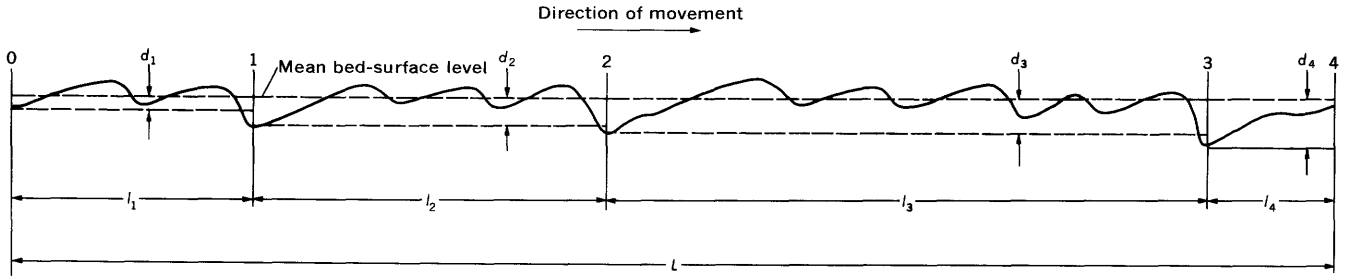

FIGURE 41.—Method for estimating average depth of zone of particle movement. $d=\frac{1}{L}\sum_{i=1}^{n} l_i d_i$.

individually by experiments as was done in this study, and k_2/k_1 can be determined from

$$\frac{k_2}{k_1}=\frac{\bar{x}}{t}.$$

The ratio $\bar{x}/t$ can be computed from any single longitudinal concentration-distribution curve for time t following release from an instantaneous vertical plane source. In addition, the ratio can be computed from a known or independently computed bed-material discharge by using equation 19 if the stream width and the depth of particle movement also are known. Once k_2/k_1 and $\bar{x}$ are determined, k_1 can be estimated from the variance of the concentration-distribution curve, σ_x^2, by the formula

$$k_1=\frac{2\bar{x}}{\sigma_x^2}.$$

Unfortunately, there is no theory available at the present time for predicting σ_x^2 quantitatively for a given set of conditions.

CONCLUSIONS

1. Application of radioactive-tracer techniques to the study of the dispersion and transport of contaminated bed-material particles is both experimentally feasible and safe.
2. The longitudinal distribution of contaminated particles that are released instantaneously from a line source that extends across the channel is skewed in the upstream direction. The distribution is highly skewed initially and becomes progressively more uniform and symmetrical as the dispersion time increases.
3. When the streambed is composed of dunes and contaminated bed-material particles are transported by the flow, some of the contaminated particles will be deposited in deep troughs and become buried. The contaminated deposits may remain buried for long periods of time and then be reexposed when another deep trough passes by.
4. The lateral distribution of contaminated particles that are nonuniformly distributed in the lateral direction at some cross section at some initial time tends to become uniform as the distance from the cross section and (or) the dispersion time increases.
5. The vertical distribution of contaminated particles in a streambed that consists of dunes varies considerably from place to place and follows no regular discernible pattern.
6. If contaminated particles having identical transport characteristics are released instantaneously from a uniformly distributed plane source that extends laterally across the channel and vertically from the surface of the bed to the lower limit of the zone of particle movement, and if the conditions within the zone of particle movement that govern the transport of bed-material particles are statistically steady and homogeneous, probability theory provides a mathematical model for the derivation of a concentration-distribution function that gives the concentration of contaminated particles in the bed at any time and place. The theoretical distribution function contains two constants that are related to step lengths and rest periods of particles.
7. According to the theoretical concentration-distribution function, the mean displacement from the source of the contaminated bed-material particles and the variance of the distribution are directly proportional to the dispersion time. The change in displacement of the mode is also proportional to the dispersion time except for short dispersion times. Also, at large dispersion times the rate of decrease of the maximum concentration varies inversely with the square root of the dispersion time, and at small or intermediate dispersion times the attenuation is more rapid.
8. The two constants in the theoretical concentration-distribution function can be determined by equating the time rate of displacement of the mode and the rate of attenuation of the peak concentration for the theoretical function to the corresponding rates determined for the observed distributions.
9. The theoretical and observed concentration-distribution curves for equal dispersion times agree well and exhibit the same characteristics except

at the origin and at the downstream tails. The differences apparently resulted from discrepancies between certain physical features of the experiment and some of the corresponding assumptions by which the theoretical distribution function is restricted. For example, whereas the theoretical distribution function is restricted to contaminated particles having identical transport characteristics that are released from a vertical plane source, the tracer particles actually used in the experiment had a range of transport characteristics and were released from a line source at the surface of the bed.

10. Probability theory also provides a mathematical model for the derivation of a discharge-distribution function that expresses the discharge of contaminated bed-material particles past any cross section at any given time; the function is similar in form to the concentration-distribution function and involves the same assumptions, variables, and constants.
11. The discharge of any fraction of the bed material that is simulated by tracer particles can be computed by a continuity-type equation, which states that the discharge is proportional to the product of the cross-sectional area of the bed through which the particles move and the mean velocity of the particles. The cross-sectional area can be determined either from longitudinal profiles of the bed surface, the area under the concentration-distribution curve, or core-sampling measurements, which define the depth of penetration of the tracer particles. The mean velocity is defined by the rate at which the mean displacement of tracer particles from the source varies with time.
12. The discharge computed with the continuity-type equation for the part of the bed material represented by the tracer particles compares favorably with the discharge computed by the modified Einstein procedure (Colby and Hembree, 1955) for approximately the same part.
13. The theoretical concentration- and discharge-distribution functions, which apply to the initial condition of an instantaneous vertical plane source, can be extended by means of the mathematical superposition principle to describe a variety of practical situations that involve more complex initial conditions. This is done by introducing functions that define the source strength as functions of space and (or) time and performing the appropriate integrations. By such devices, the theoretical distribution functions can be used, for example, to estimate concentration and and discharge growth and decay curves, times of travel and reduction in maximum concentration of slugs of contaminated bed material, the duration of contamination in excess of some specified level at a particular site, and the level of and length of time required to reach an equilibrium concentration of contaminated particles released from a continuous source.
14. For application of the theoretical functions to real situations, usually all the required variables except for two constants will either be known or can readily be estimated. Until the relations between the two constants and the pertinent hydraulic and sediment parameters are defined, the constants can be determined only by experiment.

SUPPLEMENTARY DATA—POINT-SOURCE METHOD FOR DETERMINING DETECTION-SYSTEM SENSITIVITY

During the course of the study a method was developed for estimating the overall sensitivity of a radiation-detection system to a source that is uniformly distributed throughout a volume of submerged sand. The method is useful for predetermining the amount of radioactivity required in experiments in which radioactive tracer particles become distributed throughout the bed of an alluvial channel, and undoubtedly it has other applications. In the method, the only activity required is a single-point source having a strength of from 1 to 10 μc (microcuries), which is a license-exempt quantity for most radionuclides.

The required experimental data are obtained by measuring the counting rates from the point source, which is buried at different locations relative to the detector in a tank of submerged sand (fig. 42). In the

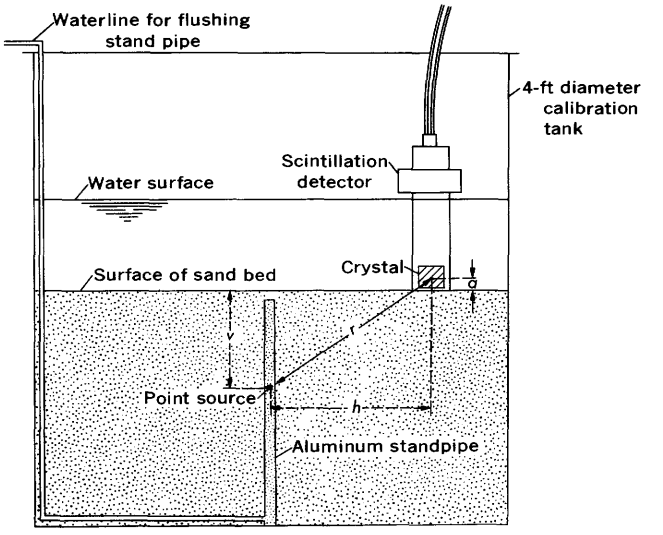

FIGURE 42.—Schematic sketch of arrangement of equipment for point-source sensitivity calibration.

tank, the vertical source-detector distance, v, is varied by moving the source vertically in the standpipe; and the horizontal distance, h, is varied by moving the detector laterally. Readings, corrected for background, are obtained at about 80 different source-detector positions. Because it usually increases toward the wall of the tank, the level of background radiation is measured at several different lateral positions.

The measured counting rates from each different source-detector position are used to define loci of equal counting rate (isocounts) about the center of the detector crystal. Isocounts obtained for a 7-μc iridium 192 source are shown in figure 43; isocounts for gold 198 and cesium 137 are similar in appearance. In figure 43, the isocounts are closely approximated by arcs of circles with centers located at the center of the detector crystal. Because the approximations are sufficiently close, the circular arcs are used to represent the isocounts. Figure 44, which is defined from the approximate isocounts in figure 43, is a plot of counting rate per microcurie against radial distance from the center of the detector crystal. The curves in figure 44 define attenuation functions that reflect the combined effects of radiation absorption and scatter in the submerged sand and of source-detector geometry. The relative penetrating ability of the radiation from the different radionuclides is shown by the slopes of the curves.

Each attenuation function provides a basis for estimating the counting rate, R_{r_o}, of a particular detection system due to a source that is uniformly distributed throughout the volume of submerged sand within a radius, r_o, of the center of the crystal. The estimated counting rate (see fig. 45) is

$$R_{r_o} = m\int_a^{r_o} f(r)\,dV \qquad (23)$$

where

m = the activity per unit volume (specific activity) in the submerged sand

$V \approx 2/3\pi r^3 - a\pi r^2$

$dV \approx 2\pi(r^2 - ar)\,dr$

$f(r)$ = the counting rate per microcurie from a point source of radioactivity located at a distance r from the center of the crystal. $f(r)$ plotted against r (fig. 44) defines the attenuation function

a = the vertical distance from the surface of the sand to the center of the crystal. (For a 2×2-in. crystal, a = 1 in.)

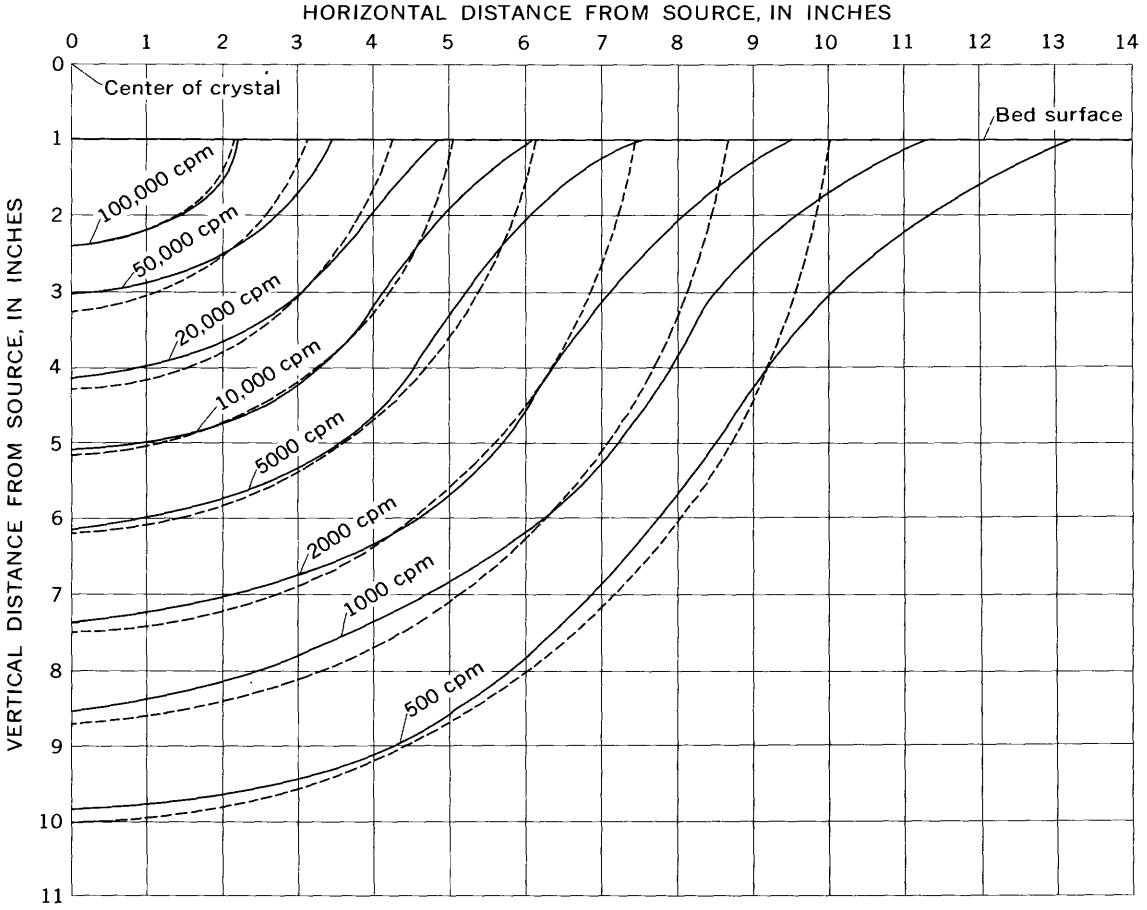

FIGURE 43.—Isocounts for a 7-μc iridium 192 point source in submerged sand. Solid line indicate observed isocounts. Dashed line indicates circular arcs with origin at center of crystal.

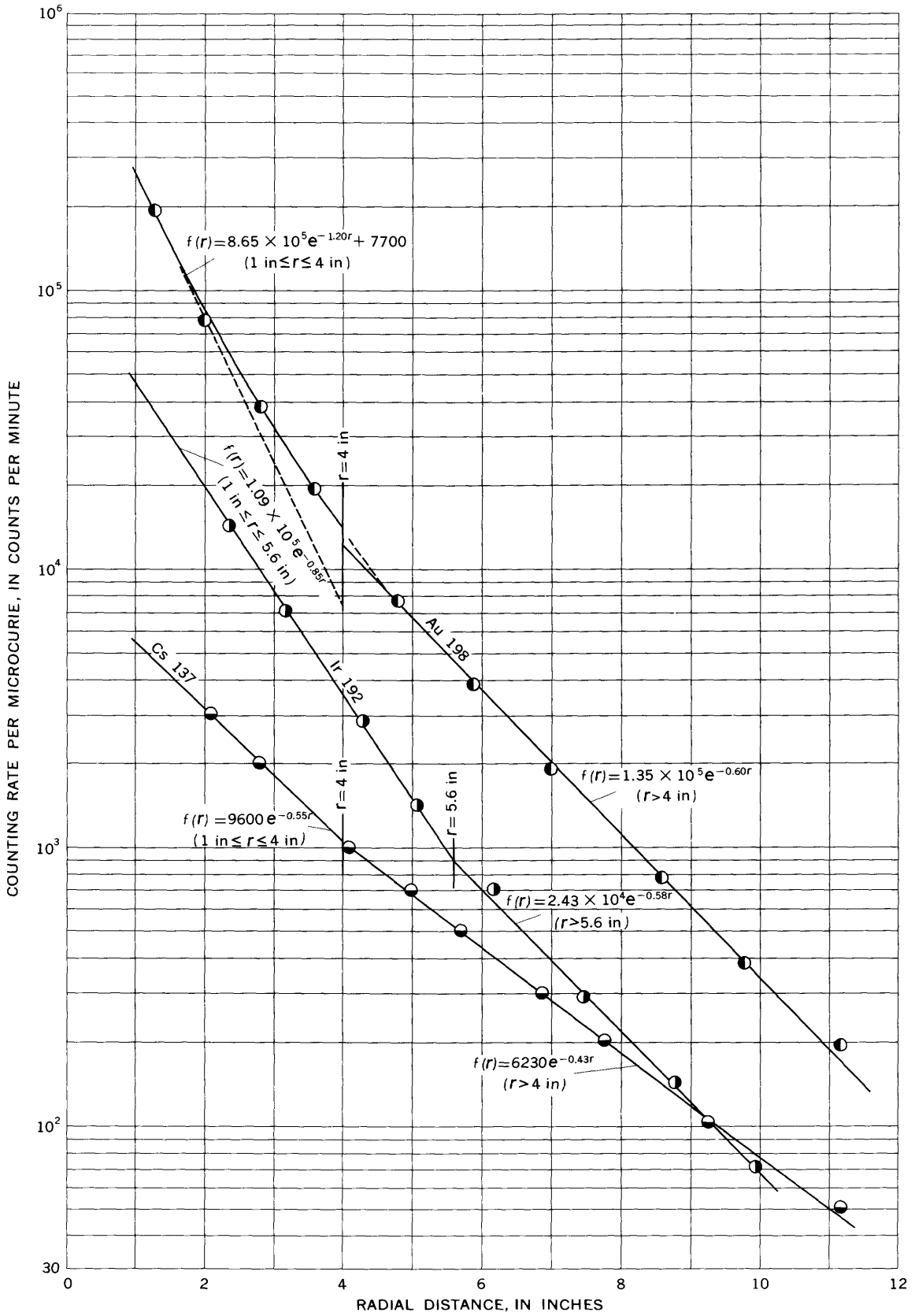

FIGURE 44.—Counting rates per microcurie from point sources located in submerged sand at various radial distances from the center of the detector crystal.

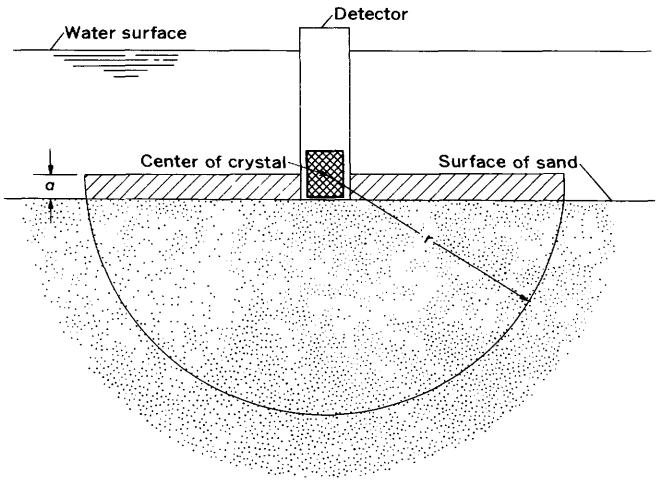

FIGURE 45.—Definition sketch for calculation of sensitivity from point-source calibration.

By substitution,

$$R_{r_o} \approx 2\pi m \int_a^{r_o} f(r)(r^2 - ar)\,dr. \tag{24}$$

If the sensitivity, S, is defined as the ratio of R_∞, which is the counting rate due to a source uniformly distributed throughout an infinite volume, to the specific activity, m, then

$$S = \frac{R^\infty}{m} \approx 2\pi \int_a^\infty f(r)(r^2 - ar)\,dr. \tag{25}$$

For example, consider the counting rate from an infinitely large uniformly distributed source of iridium 192 as measured with the equipment that was used to define figure 43. For iridium 192 (see fig. 44),

$$f_1(r) = C_1 e^{-\alpha_1 r}, \qquad 1 \text{ in.} \leq r \leq 5.6 \text{ in.}$$
$$f_2(r) = C_2 e^{-\alpha_2 r}, \qquad r > 5.6 \text{ in.}$$

where

$C_1 = 1.09 \times 10^5$ cpm per μc, $\alpha_1 = 0.85$
$C_2 = 2.43 \times 10^4$ cpm per μc, $\alpha_2 = 0.58$.

By substituting these attenuation functions and the appropriate constants into equation 25,

$$S \approx 2\pi \left[\int_1^{5.6} C_1 e^{-\alpha_1 r}(r^2 - r)\,dr + \int_{5.6}^\infty C_2 e^{-\alpha_2 r}(r^2 - r)\,dr \right]$$
$$= 2\pi \left\{ \frac{C_1}{\alpha_1^3} \left[-e^{-\alpha_1 r}(\alpha_1^2 r^2 + 2\alpha_1 r + 2) + \alpha_1 e^{-\alpha_1 r}(\alpha_1 r + 1) \right]_1^{5.6} \right.$$
$$\left. + \frac{C_2}{\alpha_2^3} \left[-e^{-\alpha_2 r}(\alpha_2^2 r^2 + 2\alpha_2 r + 2) + \alpha_2 e^{-\alpha_2 r}(\alpha_2 r + 1) \right]_{5.6}^\infty \right\}$$
$$= 1.58 \times 10^6 \text{ cpm per } \mu\text{c per cu in.} = 9.15 \times 10^5 \text{ cpm per mc per cu ft.}$$

Sensitivities that were computed for gold 198 and cesium 137 from their respective attenuation functions are listed in table 5, together with the sensitivity for iridium 192. Also included in the table are the principal gamma-ray energies for these three radionuclides and the energy-range setting of the pulse-height

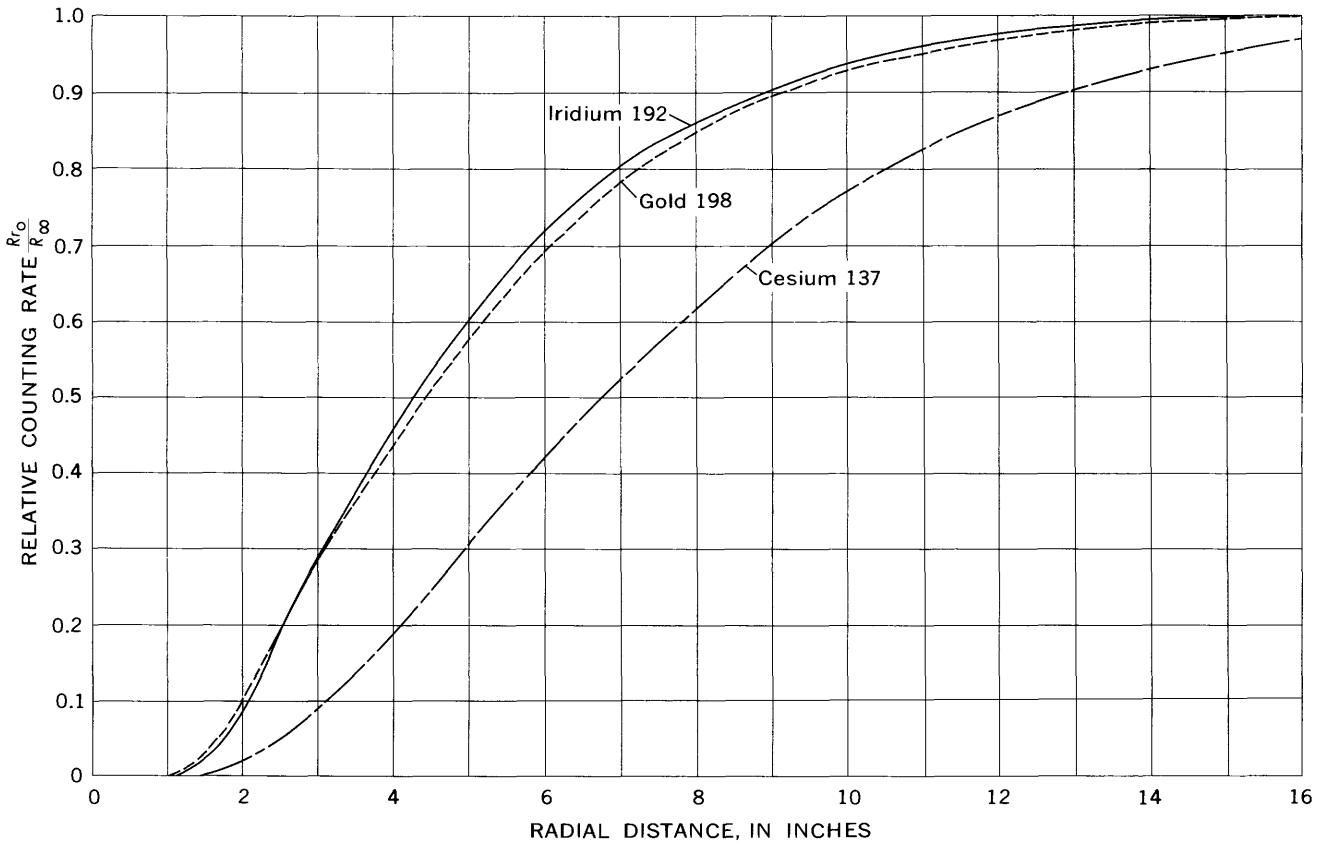

FIGURE 46.—Relative counting rate from sources uniformly distributed throughout the volume of submerged sand within various radial distances of the center of the detector crystal.

analyzer that was used for measuring the counting rates.

TABLE 5.—*Sensitivities of three radionuclides*

Radionuclide	*Principal gamma-ray energies* [1] *(Mev)*	*Measured energy range (Mev)*	*Sensitivity (cpm per mc per cu ft)*
Iridium 192	0.315, 0.470, 0.605	0.40–0.74	9.15×10^5
Gold 198	.411	.31–0.51	3.86×10^6
Cesium 137	.662	.56–0.76	4.56×10^5

[1] From Heath (1957).

Figure 46 indicates the variation of R_{r_o}/R_∞, the relative counting rate, with r_o. The figure shows that if iridium 192 were uniformly distributed throughout an infinite volume of submerged sand, 50 percent of the counts would be contributed by activity within 4.4 inches of the detector and 95 percent would be contributed by activity within 9.2 inches of the detector. The figure also shows that the attenuation of radiation from cesium 137 is considerably less than that from iridium 192 or gold 198.

LITERATURE CITED

Colby, B. R., and Hembree, C. H., 1955, Computations of total sediment discharge, Niobrara River near Cody, Nebraska: U.S. Geol. Survey Water-Supply Paper 1357, 187 p.

Einstein, H. A., 1937, Der Geschiebetrieb als Wahrscheinlichkeitsproblem [Bed-load transport as a probability problem]: Zurich, Verlag Rascher, 110 p.

——— 1950, The bed-load function for sediment transportation in open channel flows: U.S. Dept. Agriculture Tech. Bull. 1026, 70 p. [1951].

Heath, R. L., 1957, Scintillation spectrometry gamma-ray spectrum catalogue: Idaho Falls, Idaho, Phillips Petroleum Co., Atomic Energy Div.

Hours, R., and Jaffry, P., 1959, Application des isotopes radioactifs á l'étude des mouvements sédiments et des galets dans les cours d'eau et en mer [The application of radioactive isotopes to the study of motion of silt and pebbles in the rivers and in the sea]: La Houille Blanche, v. 14, no. 3, p. 318–347.

Hubbell, D. W., 1964, Apparatus and techniques for measuring bedload: U.S. Geol. Survey Water-Supply Paper 1748, 74 p.

Hubbell, D. W., and Haushild, W. L., 1962, Discussion of "Dual channel stream monitor": Am. Soc. Civil Engineers Proc., v. 88, no. HY 4, p. 287–291.

Hubbell, D. W., and Matejka, D. Q., 1959, Investigations of sediment transportation, Middle Loup River at Dunning, Nebraska: U.S. Geol. Survey Water-Supply Paper 1476, 123 p.

Karaki, S. S., Gray, E. E., and Collins, Jack, 1961, Dual channel stream monitor: Am. Soc. Civil Engineers Proc., v. 87, no. HY 6, p. 1–16.

Kennedy, V. C., 1963, Mineralogy and exchange capacity of modern fluvial sediments, *in* U.S. Atomic Energy Comm., Transport of radionuclides in fresh water systems: U.S. Atomic Energy Comm. Rept. TID–7664, p. 71–81.

Korn, G. A., and Korn, T. M., 1961, Mathematical handbook for scientists and engineers: New York, McGraw-Hill Book Co., 943 p.

Krone, R. B., 1957, First annual progress report on the silt transport studies utilizing radioisotopes: Berkeley, California Univ. Inst. Eng. Research, 118 p.

Lean, G. H., and Crickmore, M. J., 1960, The laboratory measurement of sand transport using radioactive tracers: Wallingford, England, Dept. Sci. and Indus. Research, Hydraulics Research Sta., 26 p.

Nace, R. L., 1959, Activities of the United States Geological Survey in problems of radioactive-waste disposal—Hearings before the special subcommittee on radiation of the Joint Committee on Atomic Energy: U.S. 86th Cong., 1st sess. on industrial radioactive waste disposal, v. 4, p. 2580–2645.

Parzen, Emanuel, 1960, Modern probability theory and its applications: New York, John Wiley & Sons, 464 p.

Robeck, G. C., Henderson, C., and Palange, R. C., 1954, Water quality studies on the Columbia River: Cincinnati, U.S. Dept. Health, Education, Welfare, Robert A. Taft Sanitary Eng. Center, 99 p.

Sayre, W. W., Guy, H. P., and Chamberlain, A. R., 1963, Uptake and transport of radionuclides by stream sediments: U.S. Geol. Survey Prof. Paper 433–A, 35 p.

U.S. Department of Commerce, 1959, Maximum permissible body burdens and maximum permissible concentrations of radionuclides in air and in water for occupational exposure: Natl. Bur. Standards Handb. 69, 95 p.

U.S. GOVERNMENT PRINTING OFFICE: 1965 O—761–353